universität wien

DISSERTATION

Titel der Dissertation

„Preparation and first preclinical evaluation of
[^{11}C]SNAP-7941 and [^{18}F]FE@SNAP:
two novel PET-tracer for the melanin-concentrating hormone receptor 1 (MCHR1)“

Verfasserin

Mag. pharm. Cécile Philippe

angestrebter akademischer Grad

Doktorin der Naturwissenschaften (Dr. rer. nat.)

Wien, 2013

Studienkennzahl lt. Studienblatt:	A 091 449
Dissertationsgebiet lt. Studienblatt:	Pharmazie
Betreuerin / Betreuer:	o. Univ. Prof. Mag. Dr. Helmut Viernstein

„Ein guter Forscher muß nach der Wahrheit streben und wissen,
daß er ihr immer nur nahe kommen kann. Er muß Tatsachen anerkennen,
gleichgültig, ob diese seinem Denken und seinen Wünschen entgegenkommen
oder nicht, das heißt, er muß selbstlos sein. Und er muß die Fähigkeit haben,
sich über das Naturgeschehen zu wundern und es zu bewundern.“

Lise Meitner (1878 – 1968)

DANKSAGUNG

„Bei jeder wissenschaftlichen Produktion ist der Einfluß des Milieus, in dem man arbeitet, sehr erheblich, und ein Teil der Ergebnisse ist diesem Einfluß zuzuschreiben.“

Pierre Curie (1859 – 1906)

Ich bedanke mich bei meinem Betreuer o. Univ. Prof. Mag. Dr. Helmut Viernstein für die Aufnahme am Departement für Pharmazeutische Technologie und Biopharmazie und für den gegebenen Freiraum bei der Durchführung meiner Dissertation.

Mein besonderer Dank gilt Priv.-Doz. Mag. Dr. Markus Mitterhauser und assoc. Prof. Mag. Dr. Wolfgang Wadsak für die Aufnahme in ihrem Team (Radiochemistry and Biomarker Development Unit) und die immerwährende Unterstützung vor und während meiner Dissertation.

Mag. Dr. Daniela Häusler möchte ich für die Hilfe bei jeglichen Fragen und die intensive Zusammenarbeit bei sämtlichen Experimenten danken.

Bei Mag. Dr. Johanna Ungersböck bedanke ich mich für die Unterstützung, Ermutigung und ihren fachlichen Rat bei den Radiosynthesen.

Mag. Dr. Lukas Nics danke ich für die Zusammenarbeit bei den metabolischen Stabilitätstests und seine Hilfsbereitschaft bei allen technischen Problemen.

Markus Zeilinger, MS danke ich für die gute Zusammenarbeit bei den Zellbindungsstudien und sein mathematisches Verständnis.

Bei Christina Mark, MS möchte ich mich für ihre Flexibilität und Spontanität bei der Unterstützung kritischer Synthesen bedanken.

Weites bedanke ich mich bei dem gesamten Team der “Radiochemistry and Biomarker Development Unit” für die gute Gruppenatmosphäre und gegenseitige Unterstützung.

Meinem Ehemann Mag. Johannes Mattes danke ich für die Ermutigung zum Pharmaziestudium und zur Dissertation. Danke für die mentale Unterstützung und das Verständnis während der vergangenen zehn Jahre.

ABSTRACT

The melanin concentrating hormone receptor 1 (MCHR1) is discussed to be involved in a variety of pathologies, such as obesity, diabetes, depression or gut inflammation – all lifestyle diseases of our days. Therefore, MCHR1 has become a very interesting pharmacological target since its discovery in 1999. MCHR1 is predominantly expressed in the brain; besides, it is also found in peripheral tissues, such as adipocytes, colonic epithelial cells and beta-cells of the pancreas.

Several MCHR1 antagonists were presented in the last decade; some of them have entered clinical trials for the treatment of obesity, while some are in discussion of becoming anti-diabetic drugs. However, to enable confidence in preclinical to clinical translation of MCHR1 pharmacology, a suitable positron emission tomography (PET) tracer needs to be developed. PET is a non-invasive technique, which permits *in vivo* visualization and quantification of receptors (amongst others) at a molecular level.

On the basis of the highly potent MCHR1 antagonist SNAP-7941, two PET-tracers were developed and evaluated in this thesis. [^{11}C]SNAP-7941, the radioactive counterpart of SNAP-7941, was developed first. The second tracer was the [^{18}F]fluoroethylated analogue [^{18}F]FE@SNAP, which has the advantage of the longer half-life of fluorine-18 ($t_{1/2}$ = 109.7min) compared to carbon-11 ($t_{1/2}$ = 20.4min).

For both tracers, a suitable radiosynthesis method had to be developed. [^{11}C]SNAP-7941 could be synthesized via [^{11}C]methyl trifalte starting from the precursor "SNAP-acid". The synthesis of [^{18}F]FE@SNAP was only possible via a microfluidic device by direct [^{18}F]fluorination of a tosylated precursor (Tos@SNAP). Both tracers could be synthesized in a reliable and feasible manner. Preclinical *in vitro* evaluation included binding affinity studies on CHO-cell expressing the human MCHR1, plasma stability testing and determination of the plasma free fraction, stability testing against liver microsomes and carboxylesterases, determination of the lipohilicity via log$D$ and immobilized artificial membrane (IAM) chromatography and autoradiography on rat brain and human brain tissues.

Additionally, [^{11}C]SNAP-7941 was also preclinically evaluated *in vivo*. Biodistribution and small animal PET experiments with rats were conducted.

Both tracers had a high binding affinity to the MCHR1 in a low nanomolar range. They showed high stability in human plasma and against liver microsomes and carboxylesterase. The plasma free fraction was high enough for potential brain imaging. The log*D* values and IAM chromatography results let expect (considering only the passive diffusion) a penetration through the blood brain barrier. Autoradiographic experiments showed the high potency of both tracers compared with a commercially available MCHR1 ligand. Small-animal PET revealed that [^{11}C]SNAP-7941 is a P-gp/BCRP substrate in rats.

ZUSAMMENFASSUNG

Der Melanin-konzentrierendes Hormon Rezeptor 1 (MCHR1) steht im Zusammenhang mit mehreren Erkrankungen wie Adipositas, Diabetes, Depression oder Darmentzündungen. Da diese Erkrankungen hauptsächlich auf den Lebensstil der heutigen Zeit zurückzuführen sind, ist der MCHR1 ein überaus interessantes pharmakologisches Target seit seiner Entdeckung im Jahre 1999 geworden. Der MCHR1 wird überwiegend im Gehirn exprimiert. Weites findet man ihn auch in peripheren Geweben, wie Adipozyten, Dickdarmmukosa säumenden Epithelzellen oder Beta-Zellen des Pankreas.

Mehrere MCHR1 Antagonisten wurden während des vergangenen Jahrzehnts entwickelt; einige davon werden in klinischen Studien für die Behandlung von Adipositas getestet, andere sind in Diskussion als Pharmaka gegen Diabetes.

Um Konfidenz über die Umsetzung der MCHR1 Pharmakologie von Präklinik zu Klinik zu gewinnen, sollte ein geeigneter Positronen Emissions Tomographie (PET) Tracer entwickelt werden.
Die PET ist eine nicht invasive Technik, welche eine *in vivo* Visualisierung und Quantifizierung von (unter anderen) Rezeptoren auf molekularer Ebene ermöglicht.

Auf Grundlage des stark wirksamen MCHR1 Antagonisten SNAP-7941, wurden zwei PET-Tracer in dieser Dissertation entwickelt und evaluiert. [^{11}C]SNAP-7941, das radioaktive Pendant von SNAP-7941, wurde als erstes synthetisiert. Der zweite Tracer war das [^{18}F]fluorethylierte Analogon [^{18}F]FE@SNAP, welches den Vorteil der längeren Halbwertszeit des Fluor-18 ($t_{1/2}$ = 109.7min) gegenüber dem Kohlenstoff-11 ($t_{1/2}$ = 20.4min) hat.

Für beide Tracer musste ein geeigneter Syntheseweg gefunden werden. [^{11}C]SNAP-7941 konnte über Methylierung der "SNAP-säure" mittels [^{11}C]Methyltriflat hergestellt werden. Die Synthese von [^{18}F]FE@SNAP gelang nur mittels einer direkten [^{18}F]Fluorierung eines tosylierten Präkursors (Tos@SNAP) in einem Mikrofluidsystem. Beide Tracer konnten erfolgreich und reproduzierbar hergestellt werden.

Die präklinische *in vitro* Evaluierung umfasste Bindungsstudien an humanen MCHR1 exprimierenden CHO-Zellen, Plasmastabilitätstests und Messung des freien Plasma Anteils, Stabilitätstests gegenüber Lebermikrosomen und Carboxylesterase, Messung der Lipophilie über log*D* Bestimmung und IAM (immobilisierte artifizielle Membran) Chromatographie, sowie Autoradiographie auf Rattenhirnschnitten und humanen Hirnteilen. [^{11}C]SNAP-7941 wurde überdies noch an Ratten mittels Biodistribution und Kleintier-PET in vivo evaluiert.

Beide Tracer zeigten eine hohe Affinität im niedrigen nanomolaren Bereich zum MCHR1. Weiters waren beide äußerst stabil im humanen Plasma und gegenüber Lebermikrosomen und Carboxylesterase. Der freie Plasmaanteil wäre für eine Bildgebung im Gehirn groß genug. Die log*D* und IAM Werte lassen auf eine zumindest passive Diffusion über die Bluthirnschranke schließen. Die aus der Autoradiographie gewonnenen Daten unterstreichen nochmals die hohe Affinität der beiden Tracer im Vergleich zu kommerziel verfügbaren MCHR1 Liganden. Die Experimente im Kleintier-PET zeigten, dass [^{11}C]SNAP-7941 in der Ratte ein P-gp/BCRP Substrat ist.

RÉSUMÉ

Le récepteur 1 de l'hormone de mélano-concentration (MCHR1) est involvé dans de nombreuse pathologies, comme l'obésité, le diabète, la dépression ou les inflammations intestinales. Ce sont ces maladies liées au style de vie de nos jours, qui rendent ce récepteur particulièrement intéressant come cible pharmacologique depuis sa découverte en 1999. Le MCHR1 est exrimé en majorité dans le cerveau; de plus on le trouve dans des tissus péripheriques comme les adipocytes, les cellules épithéliales couvrant la muqueuse du côlon et les cellules bêta du pancréas.

Plusieurs antagonistes du MCHR1 ont été dévloppés durant la dernière décennie; quelques-uns sont téstés dans le cadre d'études cliniques pour le traitment de l'adipose, autres sont en discussion de devenir des médicaments anti-diabetiques.

Néanmoins, pour obtenir confiance sur le passage du développement préclinique au développement clinique de la pharmacologie du MCHR1, un traceur pour la tomographie par émission de positons (TEP) serait l'idéal. TEP est une téchnique d'imagerie médicale non-invasive, qui permet une visualisation et quantification de recepteurs (entre autres) à l'échelle moleculaire *in vivo*.

A base de SNAP-7941, un antagoniste puissant du MCHR1, deux traceurs pour TEP ont été devloppés et évalués dans cette thèse. [^{11}C]SNAP-7941, qui est l'equivalent radioactive de SNAP-7941, a été synthétisé en permier. En ajoutant un groupe éthyle avec un fluor-18, le deuxième traceur, [^{18}F]FE@SNAP, a été créé avec l'avantage de la demi-vie plus longue du fluor-18 ($t_{1/2}$ = 109.7min) comparé au carbone-11 ($t_{1/2}$ = 20.4min).

Pour les deux traceurs un procédé de synthèse a du être trouvé. [^{11}C]SNAP-7941 a pu être synthetisé a partir du précurseur «acide de SNAP» en untilisant le triflate de [^{11}C]méthyle. La sythèse de [^{18}F]FE@SNAP etait uniquement possible par [^{18}F]fluoration directe d'un précurseur tosylé (Tos@SNAP) dans un système microfluidique. Les deux traceurs ont pu être préparés avec succès et de manière reproductible. L'évaluation préclinique *in vitro* contenait des essais d'affinité de liason (en utilisant des cellules CHO expriment le MCHR1 humain), de stabilité dans le plasma et envers des microsomes du foie et de la caboxylésterase, la

détermination de la fraction libre dans le plasma et de la lipophilie (par log*D* et chromatographie avec membrane artificielle immobilisé (MAI)) et l'autoradiographie sur des tranches de cerveau de rat et des parties de cerveau humain. De plus, [^{11}C]SNAP-7941 a aussi été evalué *in vivo* par distribution biologique et TEP pour rats.

Les deux traceurs ont une haute affinité pour le MCHR1 et sont extrèmement stable dans le plasma humain et envers le microsomes du foie et la carboxylésterase. La fraction libre dans le plasma est assez haute pour une imagerie du cerveau. La valeur du log*D* et les résultats de la chromatographie MAI suggèrent une pénétration passive à travers la barrière hémato-encéphalique. L'autoradiographie a montré l'efficacité des deux traceurs en comparaison avec des ligands du MCHR1 comercielles. Les résultats de la TEP ont montré que [^{11}C]SNAP-7941 est un substrat du P-gp/BCRP dans le rat.

TABLE OF CONTENTS

FIGURES

TABLES

LIST OF ABBREVIATIONS

β^+	positron
µl	microliter
µm	micrometer
µmol	micromole
AC	adenylate cylase
AGRP	agouti-related protein
ATP	adenosine triphosphate
BAT	brown adipose tissue
BBB	blood-brain barrier
BCRP	breast cancer resistance protein
B_{max}	maximum concentrations of binding sites
cAMP	cyclic adenosine monophosphate
CNS	central nervous system
DAG	diacylglycerol
DIO	diet-induced obesity
DMF	*N,N*-dimethylformamide
DMSO	dimethyl sulfoxide
DPPIV	dipeptidyl peptidase-4
e^-	electron
EOB	end of bombardment
EOS	end of synthesis
ERK	extracellular-signal-regulated kinase
EU	Endotoxin Units
f_1	plasma free fraction
GBq	gigabecquerel
GIRK	G protein-coupled inward rectifying K^+ channel
hERG	human *ether-a-go-go* gene
HI	hydroiodic acid
IAM	immobilized artificial membrane
i.c.v.	intra-cerebroventricular
Ins(1,4,5)P_3	inositol (1,4,5)-triphosphate

i.p.	intraperintoneal
i.v.	intravenously
keV	kiloelectron-volt
K_d	equilibrium dissociation constant
kg	kiligramm
K_i	equilibrium inhibition constant
K_m	Michaelis constant
LAH	lithium aluminium hydride
MCH	melanin-concentrating hormone
MCHR1	melanin-concentrating hormone receptor 1
MCHR2	melanin-concentrating hormone receptor 2
MeV	megaelectron-volt
min	minutes
ml	milliliter
mm	millimeter
MMK	Michaelis-Menten kinetics
mosm	milliosmole
MSH	melanocyte-stimulating hormone
n.c.a.	no carrier added
NEI	neuropeptide-glutamic acid-isoleucine
NGE	neuropeptide-glycine-glutamic acid
nM	nanomolar
NPY	neuropeptide Y
PET	positron emission tomography
P-gp	P-glycoprotein
P_m	permeability through the membrane
PLC	phospholipase C
Pmch	gene encoding MCH
POMC	proopiomelanocortin
ppMCH	pre-pro Melanin-concentrating hormone
PtdIns(4,5)P_2	phosphatidylinositol (4,5)-bisphosphate
QSAR	quantitative structure-activity relationship
ROI	region of interest

SLC-1	somatostatin-like clone 1
SUV	standardized uptake value
TdP	torsade de pointes
THF	tetrahydrofuran
TQD	Tariquidar
VGCC	voltage-gated Ca^{2+} channel
V_{max}	maximum velocity

1.1. The melanin-concentrating hormone system

1.1.1. Melanin-concentrating hormone

Melanin-concentrating hormone (MCH) was first referenced as "melanophore-concentrating hormone" in studies examining the possible origin of a factor leading to lightning of fish skin color in 1955 [1]. Although speculations regarding the existence of such a factor date back to the 1930s - when studies of pigmentation changes in amphibians were performed [2] - the isolation of MCH succeeded only in 1983 [3]. It was gained from the pituitary gland of the salmon and characterized as a cyclic 17-amino acid polypeptide with a cysteine – cysteine disulfide bond [3]. In teleost fish, MCH is synthesized as a preprohormone in the pituitary gland and is secreted into the circulation, where it acts as the opponent of melanocyte-stimulating hormone (α-MSH) by lightning the skin color in response of the environmental background. This effect is due to the aggregation of pigment granules within melanophores [4, 5].

Several years after the discovery in fish, MCH was identified in mammalian brain, too. It was first isolated from rat hypothalamic fragments and characterized as a 19-amino acid peptide [6], which was found to be identical to human MCH (hMCH) [7] (Figure 1). Generally, MCH is present in all groups of vertebrates from lampreys to humans and exhibits considerable structural coherence among different species [8].

Asp-Phe-Asp-Met-Leu-Arg-Cys-Met-Leu-Gly-Arg-Val-Tyr-Arg-Pro-Cys-Trp-Gln-Val

Figure 1: Human MCH amino acid sequence.

MCH is derived by posttranslational cleavage from the C terminus of a 165 amino-acid precursor, pre-proMCH (ppMCH). The preprohormone is also generating two additional peptides, neuropeptide-glutamic acid-isoleucine (NEI) and neuropeptide-glycine-glutamic acid (NGE). The gene encoding MCH is called *Pmch* [7].

In mammals, MCH is predominantly expressed in the lateral hypothalamus and zona incerta and projects broadly throughout the central nervous system (CNS) [9, 10]. Furthermore, it is also found in peripheral tissues, such as colonic epithelial cells [11], adipocytes [12] or beta-cells of the islets of Langerhans [13]. Although it is expressed in human melanocytes too, it has not been shown to affect human pigmentation [14]. In mammals, MCH operates as a neuropeptide, playing a key role in energy homeostasis, e.g. the control of food intake, body weight and metabolism [15, 16].

1.1.2. MCH receptors

Initial efforts to identify a MCH receptor were based on binding assays by using radiolabeled MCH. MCH binding sites were detected in a variety of cells and in rat brain [17, 18]. However, the existence of the MCH receptor remained obscure until 1999, when it was found to be identical to the previously cloned orphan G protein-coupled receptor SLC-1 (somatostatin-like clone 1), which exhibited about 40% homology to the five somatostatin receptors in its hydrophobic domains [19]. The first MCH receptor (MCHR1) was identified simultaneously by several groups using different pharmacological approaches [20-24]. MCHR1 is 353 amino acids long and has all hallmark features of the G protein-coupled receptors, including seven transmembrane helices, a DRY motif at the end of the third intracellular loop and three potential glycosylation sites at the N-terminus [25].

Comparison of the human and the rodent receptors shows a high degree of conservation between species (human – rat 96% identity; human – mouse 95% identity), which is not unexpected knowing that the ligand structure is identical in human, rat and mouse [25, 26].

Activation of MCHR1, which couples to multiple G proteins (G_i, G_o and $G_{q)}$, leads to an increase in intracellular Ca^{2+} accumulation via stimulation of phospholipase C (PLC), lowered cyclic adenosine monophosphate (cAMP) levels via inhibition of adenylate cylase (AC) and stimulation of extracellular-signal-regulated kinase (ERK) [27]. In the CNS, activation of these signaling pathways has diverse effects, ranging from changes in gene expression to modulation of ion channel activity [28]. Additionally, several ion channels are direct effectors of activated G proteins, like the voltage-gated Ca^{2+} channel (VGCC) and the G protein-coupled inward rectifying

K^+ channel (GIRK) [29, 30]. A scheme of the signaling pathways is presented in Figure 2.

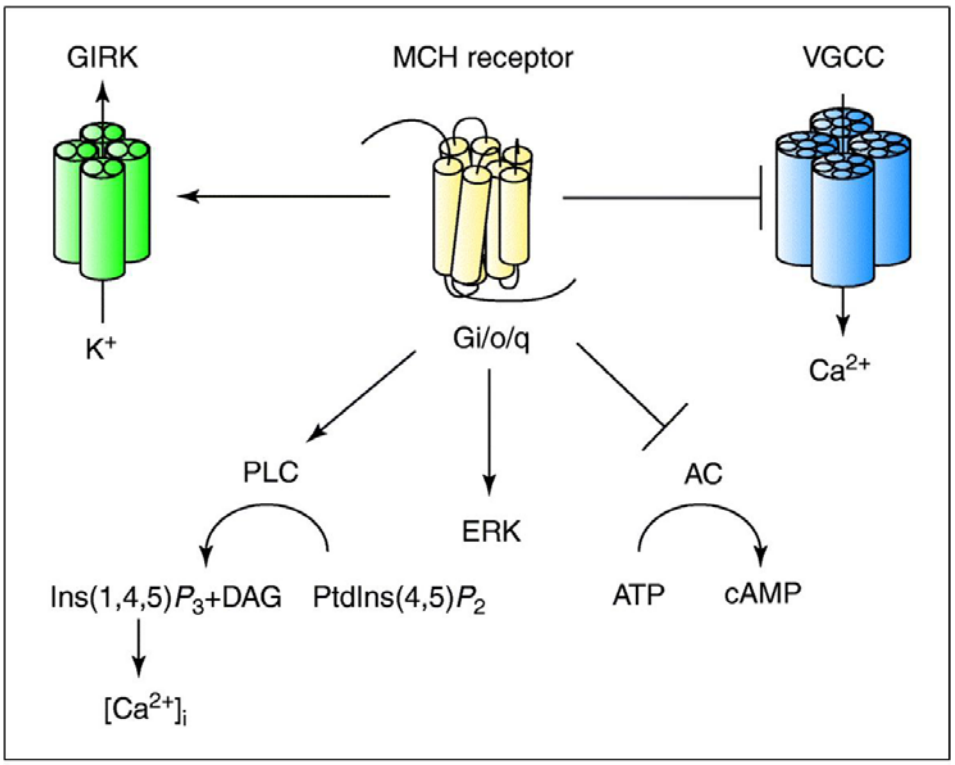

Figure 2: Activation of signaling pathways by MCH receptors.
Through coupling to multiple G proteins, MCH receptors activate phospholipase C (**PLC**), which catalyzes [from phosphatidylinositol (4,5)-bisphosphate (**PtdIns(4,5)P_2**)] the production of diacylglycerol (**DAG**) and inositol (1,4,5)-triphosphate (**Ins(1,4,5)P_3**). Ins(1,4,5)P_3, in turn, causes an increase in intracellular calcium (**$[Ca^{2+}]_i$**). Inhibition of adenylate cyclase (**AC**) decreases the production of cyclic adenosine monophosphate (**cAMP**) from adenosine triphosphate (**ATP**). Extracellular-signal-regulating kinase (**ERK**) is also activated. Important effectors in the CNS include inhibition of voltage-gated Ca^{2+} channel (**VGCC**) and activation of G protein-coupled inward rectifying K^+ channel (**GIRK**) [31].

MCHR1 is predominately expressed in the brain; besides it is also found in moderate to weak concentration in other tissues. An overview of the widespread MCHR1 distribution is given in Table 1.

Brain region	Rat		Human	
Hypothalamus	++	[23]	+++	[32]
Thalamus	+++	[33]	++	[32]
Hippocampus	+++	[23]	++	[34]
Amygdala	++	[23]	+	[34]
Pons	+	[22]	++	[32]
Medulla oblongata	?		++	[32]
Substantia nigra	++	[23]	++	[35]
Nucleus accumbens	+++	[23]	++	[36]
Locus coeruleus	++	[23]	?	
Olfactory system	+++	[23]	?	
Cerebral cortex	++	[22]	+	[32]
Cerebellum	++	[37]	+	[32]
Peripheral tissues	Rat		Human	
Pituarity	+	[23]	++	[36]
Eye	++	[23]	?	
Tongue	+	[23]	?	
Sceletal muscle	++	[23]	-	[35]
Adipose tissue	+	[23]	+	[36]
Liver	-	[23]	+	[35]
Heart	-	[23]	-	[35]
Thymus	?		-	[35]
Spleen	?		-	[35]
Kidney	-	[23]	-	[35]
Adrenal	+	[38]	+	[34]
Testis	+	[39]	+	[35]
Ovary	++	[39]	++	[35]
Placenta	?		-	[35]
Prostate	?		-	[35]
Stomach	?		-	[36]
Pancreas	+	[40]	+	[13]
Colonic epithelial cells	?		+	[11]

Table 1: Binding sites of MCH / MCHR1 mRNA distribution pattern (+++ high abundance, ++ moderate abundance, + low abundance, - not detectable, ? not investigated).

In 2001, a second MCH receptor (MCHR2) was identified with 340 amino acids of length [35, 36, 41-43]. The overall homology between the two MCH receptors is quite low; they share only 38% identical amino acids. It also seems that the signal transduction mechanism of MCHR2 is limited to the G_q protein, resulting in increased intracellular Ca^{2+} levels. Its expression profile is similar to MCHR1, with the highest expression in the brain, notably in the frontal cortex, amygdala, hippocampus, nucleus accumbens and putamen [42]. Low levels were found in the thalamus, hypothalamus, medulla oblongata and no expression was found in the cerebellum. Peripheral expression was shown in adipocytes, pancreas, prostate and intestine [41]. MCHR2 is found to be a pseudogene in rodent species, but – interestingly – is known to be functional only in dogs, ferrets, rhesus monkeys and humans [44]. Due to the lack of appropriate animal models, the physiological importance of MCHR2 remains unknown until today.

1.1.3. Physiological function of MCH

MCH plays a major role in energy homeostasis, e.g. the control of food intake, body weight and metabolism [15, 16]. It has been shown that MCH deficient (MCH-KO) mice are leaner than wild-type mice and their body weight deficit is about 25% at 4 months of age. The decrease in body weight is the result of reduced food intake and a slight increase in energy expenditure. Leptin levels are low, as would be expected in a lean mouse model. Otherwise, the mice appear to be normal, with normal levels of activity and normal fertility [45]. In contrast, MCH overexpressing (MCH-OE) mice developed – when placed on a high-fat diet – excessive obesity compared with wild-type mice. The reason therefore is that MCH-OE mice are hyperphagic. Furthermore, these animals had elevated blood glucose levels, significant hyperinsulinemia and islet cell hyperplasia [46]. Chronic infusion of MCH in mice reproduced the hyperphagic obese phenotype seen in the transgenic mice (MCH-OE mice) [16]. Considering the receptor, MCHR1 knockout (MCHR1-KO) mice are – when maintained at regular feed – lean and have a reduced fat mass. The leanness is due to hyperactivity, increased energy expenditure and altered metabolism. Paradoxally, they were found to be hyperphagic compared to wild-type mice. This effect was interpreted as a compensatory response. When placed on a high-fat diet

they gain significantly less weight and are less susceptible to diet-induced obesity (DIO). Chronic infusion of MCH did not show any effects in MCHR1-KO mice [15]. Moreover, MCH plays an important role in mediating the effects of leptin on energy homeostasis. Leptin is predominantly secreted from adipocytes and is referred as "adiposity signal", circulating in proportion to body-fat content [47]. Leptin deficient (ob/ob) mice are obese, hyperphagic, insulin resistant and had significantly increased MCH expression [48]. Crossing the ob/ob mice to the MCH-KO mice caused a significant reduction in body weight with increased energy expenditure, thermogenesis and locomotor activity. Further, they showed improved glucose homeostasis [49]. In MCHR1-KO mice, which were crossed with the ob/ob mice, body-fat mass decreased and locomotor activity increased. No differences in body weight, food intake or energy expenditure could be observed compared to the ob/ob mice. Despite being obese, MCHR1-KO ob/ob mice had improved insulin sensitivity [50].

All these findings illustrate the central role of MCH in regulating energy homeostasis. MCH neurons are implicated as downstream mediators of feeding response initiated by arcuate nucleus neurons (Figure 3).

Since both, MCH and MCHR1, are expressed in islets and clonal beta-cell lines [13], some peripheral effects of MCH were also observed. MCH has a direct effect on islet signaling pathways, insulin secretion and insulin sensitivity [13]. As mentioned above, MCH-OE mice have substantial hyperinsulinemia and islet hyperplasia that is out of proportion with their degree of obesity [46]. In contrast, MCH-KO mice have normal or improved glucose tolerance, despite having less insulin release in response to a glucose load [52]. Furthermore, MCH stimulates leptin production in adipocytes, where the MCHR1 is present too [12]. MCH was also found to be a mediator of intestinal inflammation. MCH and MCHR1 mRNA expression are increased in human colitis. MCH-KO mice had a significant protection from induced colitis, suggesting that MCH has a pro-inflammatory role in the development of colitis [11]. *Pmch* and MCHR1 were also found in human immune cells. This may provide a link between allergic inflammation, asthma and obesity [53, 54].

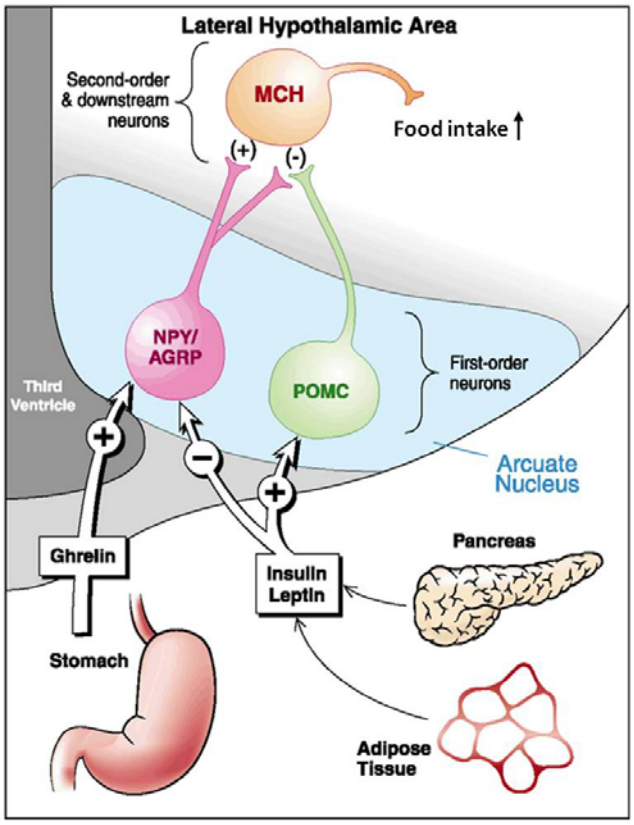

Figure 3: Schematic representation of MCH regulation.

MCH neurons are downstreamed of proopiomelanocortin (**POMC**) and neuropeptide Y (**NPY**) / agouti-related protein (**AGRP**) neurons. Leptin and insulin activate POMC neurons while inhibiting NPY/AGRP neurons and, therefore, promoting weight loss. In contrast, the gastric hormone ghrelin stimulates NPY/AGRP neurons and promotes weight gain. Input from POMC neurons inhibits MCH neurons, whereas input from NPY/AGRP neurons has the opposite effect [51].

1.1.4. MCHR1 antagonists

Due to elevated grehlin and reduced insulin and leptin levels during fasting, MCH neurons are activated via arcuate nucleus response. This pathway can be disrupted by pharmacological antagonism of the MCHR1. Several MCHR1 antagonists were developed in the last 13 years. The first functional, competitive antagonist was the $_{D}$-Ala^{11} analog of hMCH [55]. Subsequently, a series of analogs with antagonist activity were generated, such as Ac-(Ava$^{9-10}$, Ava$^{14-15}$)-hMCH(6-16)-NH2 (also known as PMC-3881-PI) [56]. However, peptide MCHR1 antagonists are not able to cross the blood-brain barrier (BBB) and interact with the MCHR1 in the CNS. Therefore, small molecule MCHR1 antagonists were developed. The first non-

peptide antagonist was T-226296 (Takeda), an orally active compound that demonstrated high affinity and selectivity to the MCHR1 (K_i = 5.5nM) [57].

Screening of a G protein-coupled receptor based compound library against the human MCHR1 in a functional assay measuring intracellular Ca^{2+} mobilization resulted in the discovery of a second non-peptide antagonist, SNAP-7941 ((+)-methyl (4S)-3-{[(3-{4-[3-(acetylamino)phenyl]-1-piperidinyl}propyl)amino]carbonyl}-4-(3,4-difluorophenyl)-6-(methoxymethyl)-2-oxo-1,2,3,4-tetrahydro-5-pyrimidine carboxylate hydrochloride) (Synaptic/Lundbeck, Figure 4) [58]. SNAP-7941 has an excellent binding affinity (K_d = 0.18nM) and selectivity (over 1000-fold) to the MCHR1. In rat brain sections, binding of radiolabeled SNAP-7941 ([^{3}H]SNAP-7941) was detected in the cerebral cortex, olfactory tubercle, claustrum, piriform cortex, hippocampus, amygdala, caudate-putamen, accumbens nucleus, hypothalamus, dorsal raphe and locus coerulus [58]. This distribution pattern parallels the widespread MCHR1 expression in the brain [33]. Further, systemic pre-treatment with SNAP-7941 (10mg/kg, intraperintoneal (i.p.)) inhibited the increase in food intake induced by intra-cerebroventricular (i.c.v.) injection of MCH (3nmol). Rats treated with SNAP-7941 (10mg/kg, i.p.) twice a day for seven days gained 26% less weight compared to their littermates. SNAP-7941 was also capable to decrease milk consumption in satiated rats: 13% less milk consumption in rats treated with 3mg/kg (i.p.), 41% with 10mg/kg (i.p.) and 59% with 30mg/kg (i.p.) compared to vehicle-treated rats. These results suggest that SNAP-7941 acts as an anorectic agent. To rule out that this anorectic effect was due to malaise, a taste aversion study was performed, which confirmed that the anorectic effect of SNAP-7941 is not a result of malaise. In DIO rats, SNAP-7941 (10mg/kg, i.p., twice daily over four weeks) produced a sustained and consistent decrease in food consumption and body weight. This effect was reversible insofar as two weeks after the termination of the treatment, DIO rats previously treated with SNAP-7941 showed an increase in body weight and food consumption. A toxic effect of SNAP-7941 as a causal role for reduction in food intake and weight gain was ruled out by blood tests of the hepatic and renal function of the drug treated rats [58]. All these findings render the MCHR1 a viable target for the treatment of obesity. Additionally to the reported anorectic effects, SNAP-7941 evinced antidepressant and anxiolytic properties. A

single oral dose of SNAP-7941 (3, 10 and 30mg/kg) significantly decreased the duration of immobility and increased the swimming time of rats in the forced-swim test. Unfamiliar male rats showed increased social interaction time after acute treatment with SNAP-7941. Finally, the high frequency vocalizations emitted from guinea pig pups separated from their mothers were significantly reduced after treatment with SNAP-7941 [58]. These anxiolytic effects were not supported by another group [59].

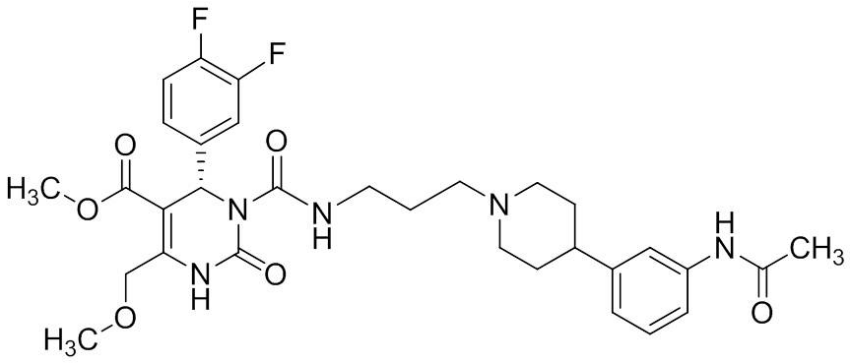

Figure 4: Chemical structure of SNAP-7941.

Several other small molecule antagonists were developed from pharmaceutical companies, e.g. ATC0065 and ATC0175 (Arena/Taisho collaboration) [60, 61], GW803430 (GlaxoSmithKline) [62], SNAP 94847 (Synaptic/Lundbeck) [63], AMG-076 (Amgen) [64] and NGD-4715 (Neurogen) [65]. All these drugs are BBB penetrating compounds, which is mandatory to reduce body weight [66]. Due to medical need for oral anti-diabetics that give weight loss, a dual MCHR1 antagonist/dipeptidyl peptidase-4 (DPPIV) inhibitor had been developed recently [67].

Unfortunately, a significant number of MCHR1 antagonists showed a cardiovascular risk involving human *ether-a-go-go* gene (hERG) potassium channel inhibition and QT prolongation. hERG blockers are associated with lethal arrhythmias known as torsade de pointes (TdP). Structural requirements, such as a positively charged group and at least one distal aromatic/hydrophobic region, for MCHR1 potency correlate with hERG inhibition. Efforts in designing MCHR1 antagonists with improved selectivity over hERG are undertaken by several

pharmaceutical companies; a few candidates have progressed to clinical development [68]. Amongst these compounds, BMS-830216 (prodrug of BMS-819881, Bristol-Myers Squibb) [69] has completed a randomized, double-blind, placebo-controlled, ascending multiple-dose and parallel arm study to evaluate its safety, pharmacokinetics and pharmacodynamics in obese subjects [70].

.

1.2. PET-tracer development

Positron emission tomography (PET) is a non-invasive molecular imaging technique for *in vivo* visualization and quantification of e.g. receptors and transporters. It is not only a useful technique in oncology, neurology and cardiology, but also in drug development and clinical studies for understanding biochemical processes. Central to molecular imaging with PET is the development of appropriate radiopharmaceuticals, also called PET-tracers. This process starts with the definition of a target and the idea of a molecule (based on literature or through QSAR modeling) with high binding affinity and selectivity to the desired target. For radiolabeling of the selected molecule, a suitable precursor has to be synthesized and labeling strategies have to be identified. After successful radiosynthesis, the molecule has to be evaluated regarding its parameters in various preclinical experiment settings. These are primarily *in vitro* studies, comprising metabolic stability testing, determination of lipophilicity and plasma free fraction, and autoradiography. If the radiotracer appears promising, subsequently preclinical *in vivo* evaluation is performed via small-animal PET, biodistribution and, again, metabolic stability testing. Before human application, a limited toxicity test needs to be performed. The final phase of development is the clinical evaluation and validation of the designed radiotracer [71, 72].

1.2.1. PET methodology

The radiopharmaceutical is injected (usually intravenously (i.v.)) into the living subject. It is transported through the blood stream to the target sites and binds there according to its affinity. PET-tracers are radiolabeld with positron-emitting radionuclides, which decay by the emission of a positron (β^+). After being emitted from the nucleus, the positron travels a short distance until it annihilates with an electron (e^-). The distance traveled by the positron before annihilation depends on the energy emitted by the positron and is different for each positron-emitting radionuclide (Table 2). Annihilation produces two 511keV γ-rays, which are emitted simultaneously in opposite directions (angle: nearly 180°) and can then be detected by the detectors of the PET-scanner in coincidence (Figure 5). A detector pair gives a line of response and through a large number of coincidences the source of

annihilation can be reconstructed. Finally, an image with information on the spatial distribution of radioactivity as a function of time is obtained [72].

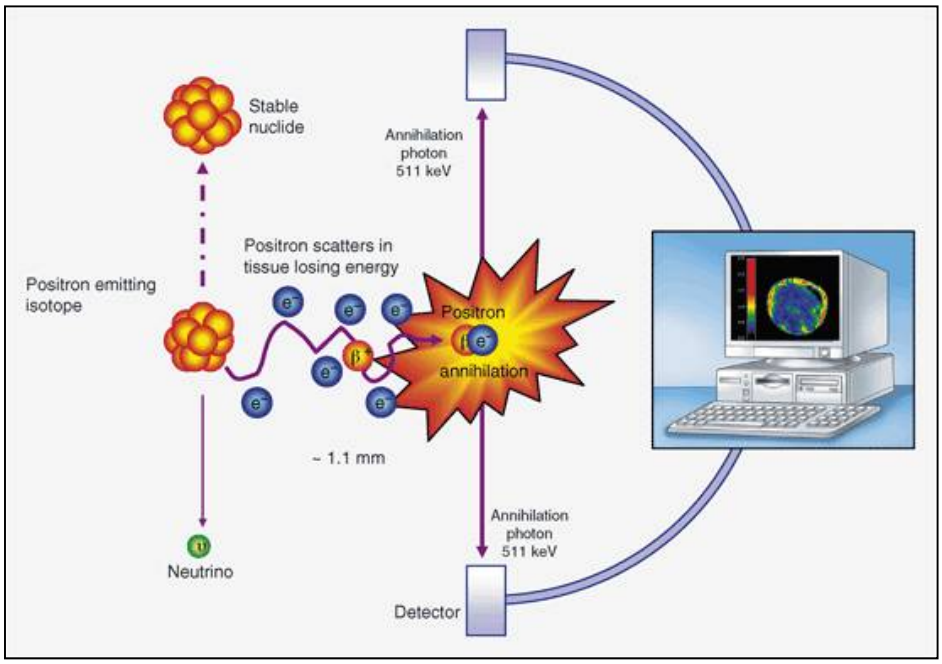

Figure 5: Principle of PET (β^+ positron, e^- electron) [73].

1.2.2. Radiochemistry

A PET radiopharmaceutical consists of two components: a molecular structure (which interacts with the target) and a positron emitting radionuclide (for the visualization of the target). The most important radionuclides for PET are summarized in Table 2. The choice of the adequate radionuclide is a compromise between availability of the radionuclide and authenticity of the resulting tracer. Carbon-11 labeled molecules are able to directly represent the authentic molecule but for the production of carbon-11 a cyclotron is indispensible. Gallium-68 is readily available through a radionuclide-generator system but leads to a high degree of unpredictability in the *in vivo* behavior of ^{68}Ga-labeled compounds. Further, the half-life of the radionuclide should be long enough for successful radiolabeling, accumulation at the target region and imaging procedure [74]. The most widely used PET radionuclides are carbon-11 and fluorine-18 and this thesis focusses upon these two nuclides.

Radio nuclide	Production	Target material	Half-life	$E_{\beta+,max}$ (MeV)
O-15	$^{14}N(d,n)^{15}O$	N_2 gas	2.03min	1.74
N-13	^{16}O (p,α)^{13}N	H_2O	9.98min	1.19
C-11 (CO_2)	$^{14}N(p,\alpha)^{11}C$	N_2 gas + <1% O_2 gas	20.4min	0.96
C-11 (CH_4)		N_2 gas + 5-10% H_2 gas		
F-18 (F^-)	$^{18}O(p,n)^{18}F$	$[^{18}O]H_2O$	109.7min	0.63
F-18 (F_2)	^{20}Ne (d,α)^{18}F	Ne gas + 0.1-0.2% F_2 gas		
Ga-68	$^{68}Ge/^{68}Ga$-Generator		67.6min	1.83

Table 2: Important positron-emmiting radionuclides [75].

Carbon-11 chemistry

A variety of carbon-11 labeling compounds can be produced (Figure 6). Two primary compounds can be produced in the cyclotron: [^{11}C]carbon dioxide ([^{11}C]CO_2) is obtained by addition of oxygen (<1%) to the nitrogen gas; [^{11}C]methane ([^{11}C]CH_4) is obtained by addition of hydrogen gas (5-10%) (Table 2). [^{11}C]CO_2 can be used directly for the synthesis of carboxyls and carbonyls via corresponding Grignard reactions [76].

The vast majority of the carbon-11 labeled radiotracers are synthesized by ^{11}C-methylation at heteroatoms of the precursor molecules. The two most important ^{11}C-methylation agents are [^{11}C]methyl iodide ([^{11}C]CH_3I) and [^{11}C]methyl triflate ([^{11}C]CH_3OTf). [^{11}C]CH_3I can be obtained either by trapping [^{11}C]CO_2 in a solution of the reduction agent lithium aluminium hydride (LAH) in tetrahydrofuran (THF) followed by the treatment of the resulted [^{11}C]CH_3OH with hydroiodic acid (HI) [77], or by gas-phase free radical iodination of [^{11}C]CH_4 at 720°C [78]. This method is commonly used nowadays. It is less labor intensive than the wet-chemistry method and results in higher specific radioactivity of the alkylating agents due to the avoidance of the use of LAH (a source of cold CO_2). [^{11}C]CH_3OTf is a more reactive ^{11}C-methylation agent and, therefore, is used for the ^{11}C-alkylation of nucleophiles

with a low reactivity. It is produced by online by passing [^{11}C]CH_3I through an heated (190°C) column loaded with silver-triflate coated material [79].
Other reactive ^{11}C-radiolabelling agents are [^{11}C]phosgene ([^{11}C]$COCl_2$), [^{11}C]cyanide ([^{11}C]HCN) and [^{11}C]carbon monoxide ([^{11}C]CO) [76].

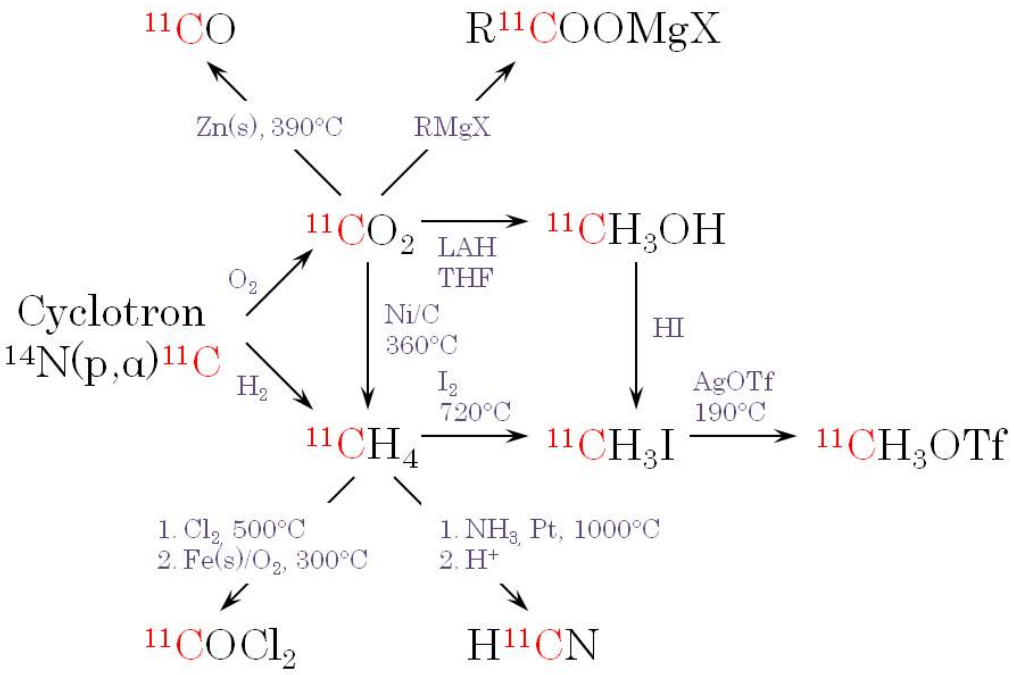

Figure 6: Carbon-11 labeling synthons.

Fluorine-18 chemistry

Fluorine-18 labeled radiotracers have the advantage of the longer physical half-life (109.7min) compared to carbon-11 (20.4min), which allows multistep radiosytheses, longer *in vivo* investigations and commercial distribution to other clinical PET centers that lack a cyclotron. However, in contrast to carbon-11 labeled molecules (where carbon-11 replaces a carbon-12 atom and, therefore, no changes in the structure per se of the labeled molecule compared to the unlabeled molecule can be observed), the introduction of fluorine-18 into the molecule alters the chemical properties and biological behavior of the molecule, since the original structure often does not bear a fluorine atom at first. This could, on the one hand, reduce the affinity, stability or selectivity of the molecule or, on the other hand, even ameliorate the in vivo behavior [74].

The most prominent example of a changed metabolic behavior, which had a positive effect on the imaging properties, is [^{18}F]FDG (2-deoxy-2-[^{18}F]fluoro-D-glucose) [80]. [^{18}F]FDG is a derivative of glucose, with a [^{18}F]fluorine atom instead of the hydroxyl moiety at the C-2 position. Like glucose it is transported into the cells and phosphorylated by hexokinase. The enzyme of the second step of the glucose metabolism, the phosphohexose isomerase, requires the hydroxyl moiety at the C-2 position for further glycolysis. Since [^{18}F]FDG is lacking this hydroxyl moiety, it cannot be further metabolized and is "trapped" in the cell. Thereby, the cells with high glucose metabolism (e.g. tumor cells) are able to be imaged with high contrast [81].

In general, there are two methods to introduce a fluorine-18 label into a molecule: electrophilic and nucleophilic radiofluorination. For electrophilic fluorination, elemental ^{18}F-labeled fluorine ([^{18}F]F_2) is needed. It can be produced through the ^{20}Ne(d,α)^{18}F nuclear reaction in the cyclotron (Table 2). 0.1-0.2% non-radioactive F_2 gas (carrier) have to be added to the ^{20}Ne gas in order to avoid sticking of [^{18}F]fluorine on target walls and transport lines. Through this addition, only low specific radioactivities can be achieved using the electrophilic fluorination method. For PET studies requiring high specific radioactivities, the no carrier added (n.c.a.) nucleophilic fluorination is more suitable. Nca ^{18}F-fluoride ([^{18}F]F^-) is produced by irradiation of oxygen-18 enriched water ([^{18}O]H_2O) via the ^{18}O(p,n)^{18}F nuclear reaction. In this aqueous medium fluoride is strongly hydrated and a poor nucleophile. Nucleophilic fluorine-18 labeling is only possible in total absence of water. Therefore, the fluoride-18 aqueous solution is pushed over an anion exchange cartridge, where [^{18}F]F^- is retained. To elute [^{18}F]F^- from the cartridge, a mixture of acetonitrile and 1) a cryptand (e.g. Kryptofix 2.2.2, 4,7,13,16,21,24-hexaoxa-1,10-diaza-bi-cyclo[8.8.8]hexacosane) in combination with alkali salts (e.g. potassium carbonate) or 2) a large soluble cation (e.g. tetrabutylammonium ion) is used. To facilitate elution, small quantities of water are added, which are removed by drying of the eluate. Since acetonitrile forms an azeotrope with water, a more efficiently evaporation of residual water is possible. After that azeotropic drying process, [^{18}F]F^- is present as a highly nucleophilic fluoride ion and can be dissolved in dipolar aprotic solvents, like acetonitrile itself, dimethyl sulfoxide (DMSO) and *N,N*-dimethylformamide (DMF). Nucleophilic radiofluorination can be achieved via

direct labeling of a suitable precursor compound or by a two-step reaction, first creating a small and simple ^{18}F-labeled molecule (prosthetic groups) as labeling agent [72, 76].

Direct ^{18}F-fluorination: For labeling of aliphatic moieties the reaction mechanism proceeds via an S_N2 reaction, where a nucleophile attacks the electrophilic substrate and bonds to it, expelling the so called leaving group. Precursors bearing bromo, iodo, tosylate, triflate, nosylate and mesylate as leaving groups are employed. Aromatic nucleophilic substitution is only feasible through the S_NAr mechanism. Strong electron-withdrawing groups in *ortho* or *para* position activate the leaving groups (e.g. nitro and trimethylammonium salts) so that the fluorine-18 label can be directly introduced into the aromatic ring [72, 76].

^{18}F-radiolabeling via prosthetic groups: If the precursor molecule does not imply a suitable leaving group, ^{18}F-fluoroalkylation agents have to be synthesized in a first step. Most common are small moieties, like [^{18}F]fluoroethyl bromide, [^{18}F]fluoromethyl bromide, [^{18}F]fluoroethyl tosylate, [^{18}F]fluoromethyl tosylate, [^{18}F]fluoroethyl triflate and [^{18}F]fluoromethyl triflate. In a second step, these small molecules are attached to the precursor molecule [72, 76].

Recently, the so called “click chemistry” (where prosthetic groups are used for labeling peptides, proteins and also small molecules) has been applied to prepare ^{18}F-labeled compounds. [72, 76].

Instrumentation

Automation of the radiosynthesis is required in order to reduce the manual steps and in consequence reduce exposure to radiation. Further advantages are reproducibility, high reliability and reduced time consumption.

A huge variety of conventional radiosynthesis modules is commercially available. Whereas some are designed for the preparation of only one tracer, others are more flexible and several tracers can be produced via these modules.

Within this thesis two commercially available conventional synthesis modules were used: the TRACERlab FX C Pro (Figure 7) and the Nuclear Interface® synthesizer (both GE Healthcare, Uppsala, Sweden).

The TRACERlab FX C Pro synthesizer is equipped with a unit to form [^{11}C]CH_3I, a heated column for the production of [^{11}C]CH_3OTf and a preparative HPLC system [82]. It was used for the preparation of the carbon-11 labeled MCHR1 ligand, [^{11}C]SNAP-7941.

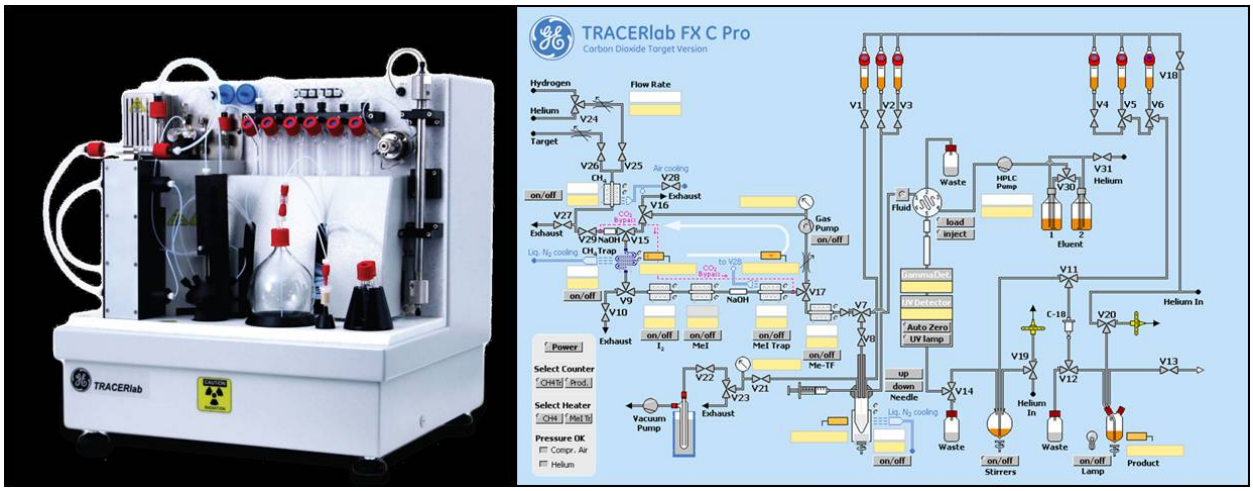

Figure 7: TRACERlab FX C Pro synthesis module (left) with scheme (right) [82].

The Nuclear Interface® synthesizer is able to produce [^{11}C]CH_3OTf but not [^{11}C]CH_3I itself. It is also equipped with a preparative HPLC system. Within this thesis, the Nuclear Interface® module was not used for carbon-11 chemistry but for purification of the fluorine-18 labeled MCHR1 ligand, [^{18}F]FE@SNAP.

A relatively new concept for radiosynthesis is the microfluidic preparation. Microfluidic devices consist of a network of micro-sized channels/capillaries (10-300 µm diameter), microreactors, liquid storage loops/chambers and micro-scale pumps and syringes. The principle of microfluidic chemistry is the downscale of chemical reactions from the macroscopic (ml) to the microscopic scale (µl) with numerous advantages:

- due to small reactor volumes, minimal amounts of material are used;
- the short residence in the microreactor leads to improved selectivity, reduction of side reactions and higher radiolabelling yields and
- the capillaries allow a high specific phase interface and a high surface to volume ratio.

In addition, the pushing of the solvents through the capillaries causes a back-pressure and solvents might be heated to temperatures above their boiling point at normal pressure [83]. Microfluidic devices might also enable conversions that would not occur under the conditions in conventional synthesis modules. This was the case for the radiosynthesis of [^{18}F]FE@SNAP, which was only successful in the Advion NanoTek® mircrofluidic device (Ithaca, NY, USA) (Figure 8).
Despite the multiple advantages of microfluidic devices, they have not been used for routine productions in the clinical set-up yet.

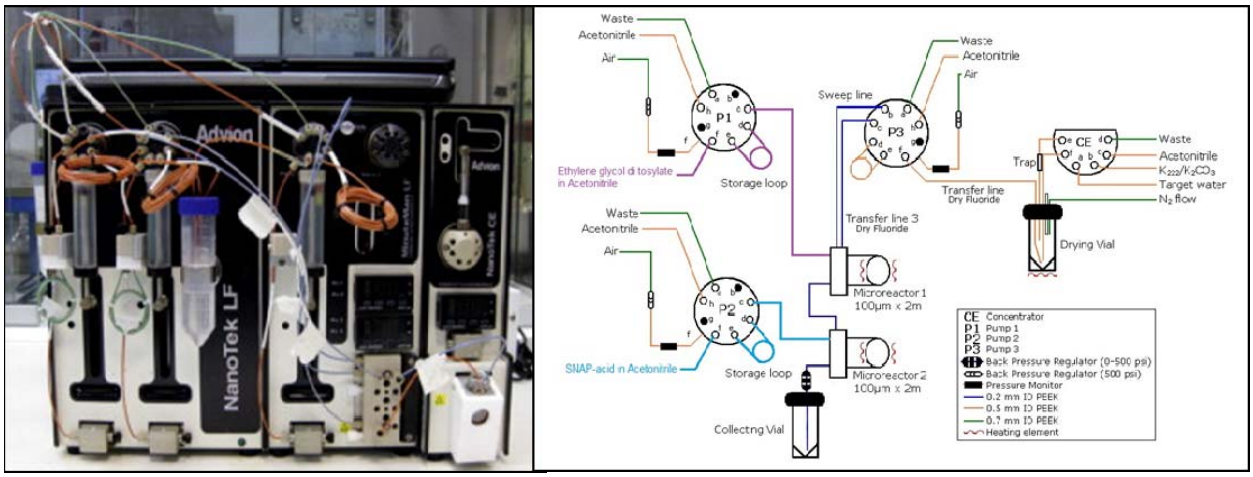

Figure 8: Advion NanoTek® synthesis module (left) with scheme (right).

1.2.3. Quality control of PET radiopharmaceuticals

All radiopharmaceuticals must be tested to assure acceptable quality prior to administration to human subjects. The European Pharmacopeia describes the guidelines for the quality assurance of radiopharmaceuticals and the final product must meet all the criteria required to assure safety and efficacy [84].

Main quality control parameters:

- Radiochemical identity and purity

Both, identity and purity are analyzed via chromatography. Radiochemical identity is given when the retention time of the radiolabeled product corresponds to the retention time of the non-radiolabeled product. Radiochemical purity is defined as the percentage of the desired radiolabeled product in relation to the total

radioactivity of the final drug formulation. The percentage should be ≥ 95% for the product. All other single radiochemical impurities should not exceed 3%.

- Chemical purity

Chemical purity is analyzed via high performance liquid chromatography (HPLC) and is defined as the absence of any undesirable chemical species in the final drug formulation.

- Specific radioactivity

Specific radioactivity is one of the most important quality control criteria for radiopharmaceuticals. It refers to the amount of radioactivity per unit mass of the radiolabeled compound and is usually expressed as GBq/μmol. For *in vivo* brain imaging it is important that radiopharmaceuticals are prepared in high specific radioactivities to avoid a deterioration of signal-to-noise ratios.

- Radionuclidic identity and purity

Radionuclidic identity and purity are determined by recording a gamma-spectrum and, additionally, by measuring the half-life of the radioactivity of the final drug formulation.

- Residual solvents

Since organic solvents are used during the synthesis and purification process of the radiopharmaceutical, the final drug solution may contain small amounts of organic solvents, known as residual solvents. Gas chromatography is the most common technique for the determination of the residual solvent concentration. For each organic solvent limits are defined in the European Pharmacopoeia.

- pH

The pH value of radiopharmaceutical formulation intended for intravenous administration should be close to the pH of blood. In general, pH values in the range of 4.5-8.5 are quite acceptable since blood has a very good buffering capacity.

- Osmolality

The final drug formulation intended for intravenous administration must be isotonic. Osmolality is expressed as mosm/kg and is measured in an osmometer. The limits of the osmolality are set to be 190-370mosm/kg.

- Microbiological testing

For radiopharmaceuticals intended for injection, sterility and endotoxin tests have to be conducted. Sterility tests are designed to determine the presence of mesophilic

bacteria and fungi. They have to be conducted in an aseptic environment and last several days. Endotoxins can be detected readily by a *gel-clot technique* based on Limulus amebocyte lysate. Radiopharmaceuticals for parenteral injection must be sterile and the endotoxin concentration must be < 1.0EU/ml.
Due to the short half-life of PET radiopharmaceuticals, it is allowed to release them for administration into human subjects prior to microbiological testing. Nevertheless, for validation of the preparation process, sterility and endotoxin tests must be conducted for each batch of radiopharmaceuticals.

1.2.4. Preclinical evaluation

Binding affinity & selectivity

The binding affinity can be expressed as K_d (equilibrium dissociation constant) or K_i (equilibrium inhibition constant) value. The K_d is evaluated within saturation experiments: increasing amounts of radioligand are added to a fixed concentration of the target protein (expressed on cells or cell membranes) and the amount of radiotracer bound is measured. A different approach is used for the measurement of the K_i: different concentrations of the ligand of interest and a defined amount of a reference radioligand are added to the cell preparations. The competitive effect of the ligand to the reference radioligand results in the K_i value [75].

Considering that the B_{max} (maximum concentrations of binding sites) for most brain receptors is rather low (nano- to femtomoles per milligram tissue), a high binding affinity in a low nanomolar range for brain imaging radiotracers is mandatory. However, a too high affinity can render the tracer unsuitable because its uptake may become blood flow dependent instead of being dependent on the rate of binding. The binding may be irreversible, and equilibrium studies may not be possible [72].
In addition to high affinity, a radiotracer should also be selective for the target. Selectivity is defined as the ratio of affinity of the ligand for the target of interest to the affinity for each of the other target subtypes [75]. Furthermore, the non-specific binding (insaturable binding to nontarget sites) has to be low in order to achieve a high target to background ratio [72].

Metabolic stability

Like all drugs, radiopharmaceuticals are metabolized by enzymes in the organism. These enzymes are found extracellularly (e.g. cholinesterases in blood plasma) or intracellularly (e.g. carboxylesterases and cytochromes P450 in hepatocytes). The initial *in vitro* investigations are typically performed in liver microsomes (containing the cytochrome P450) and in blood plasma. The enzymes are incubated with the radiotracer for a given period; the radiotracer is extracted with suitable solvents and analyzed by radiochromatography.

For *in vivo* measurements, the radiotracer is administered to the animal; blood samples are collected and the brain is removed after decapitation. The radiotracer is also extracted and analyzed by radiochromatography.

Since PET cannot discriminate between signals from parent radioligand and radiolabeled metabolites, it is essential that radiotracers do not undergo too rapid metabolism and potential radiolabeled metabolites of brain tracers do not cross the BBB. The position of the radiolabel in the molecule has to be considered carefully, since the loss of the radiolabel by metabolic degradation and the formation of BBB penetrating radiometabolites will limit the tracer's usefulness as a PET tracer [72, 85].

A prominent example therefore is the metabolism of the serotonin 5-HT_{1A} receptor antagonist [O-*methyl*-^{11}C]WAY-100635, which gives rise to a brain-penetrant and pharmacologically active radiometabolite ([O-*methyl*-^{11}C]WAY-100634) [86]. This metabolite attenuates an additional specific signal. As a consequence, a new position of the radiolabel was chosen, which resulted into [*carbonyl*-^{11}C]WAY-100635. There, [^{11}C]cyclohexanecarboxylic acid is formed as the major radiometabolite. Due to its almost complete ionization at physiological pH, it has low brain entry and neglectable affinity for the 5-HT_{1A} receptor [87].

However, radiotracer metabolism that occurs outside brain to produce non-brain-penetrating metabolites helps to eliminate parent radiotracer, which might be beneficial for observing brain radiotracer washout [88].

Enzyme kinetics, which describes the reaction rate of a chemical process that is catalyzed by enzymes, provides further information on the metabolic stability of the investigated tracer. One of the simplest and best-known models of enzyme kinetics

is the Michaelis-Menten kinetics (MMK) [89]. In the form of an equation, it describes the rate of enzymatic reactions by relating the reaction rate to the concentration of the substrate. The Michaelis constant (K_m) is the substrate concentration at which the reaction rate is half of V_{max} (maximum velocity, which means maximum reaction rate at saturating substrate concentrations).

Plasma protein binding

A low binding of the radiotracer to plasma proteins is essential since only the free fraction of the tracer in plasma is systemically bioavailable. The extent of plasma protein binding can be tested easily *in vitro* by mixing the tracer with plasma and by separating the protein through molecular weight filter. Total activity and activity of the filtrate can be measured in a Gamma Counter. For determination of the plasma free fraction (f_1), the ratio of filtrate (containing the unbound/free tracer) to the total activity is calculated [85].

Blood-brain barrier permeability

For tracers acting in the CNS, BBB permeability is mandatory. The BBB consists of tight junctions between the brain capillary endothelial cells and separates the CNS from the bloodstream in order to protect the brain from xenobiotics. The BBB is also well-equipped with efflux pumps (e.g. P-glycoprotein (P-gp)) and multi-drug resistance-associated proteins (e.g. breast cancer resistance protein (BCRP)). According to their molecular characteristics, drugs can pass the BBB by passive diffusion, transport proteins, transcytosis or paracellular pathways. However, more than 98% of all potential CNS-targeting drugs showed poor permeability across the BBB. Thus, the ability of compounds to cross the BBB remains challenging [90].
For estimation of BBB penetration of a tracer, log*P,* where *P* is the *n*-octanol/water partition coefficient of the unionized compound, is often used. It is an index of compound lipophilicity and describes the ratio of concentrations of a compound in the two immiscible solvents (*n*-octanol and water) at equilibrium. The corresponding distribution coefficient for unionized and ionized compounds at physiological pH is termed $D_{7.4}$. Log*P*/log$D_{7.4}$ values between 2 and 3.5 are generally considered optimal [88]. However, due to the complexity of the BBB, log*P* values are

rather poor predictors for BBB penetration [91]. The immobilized artificial membrane (IAM) chromatography offers a better prediction, since the IAM mimics the lipid environment of the BBB [92]. The permeability through the membrane (P_m) is obtained. Nevertheless, both log*P* and IAM chromatography only describe the compound's ability to cross the BBB via passive diffusion. To involve also the active transport mechanisms, more complex models using dedticated cells systems have to be applied [93].

Furthermore, it has to be assessed if the CNS imaging tracer is a substrate for brain efflux transporters, especially P-gp, which is highly prevalent at the BBB. In general, substrate behavior for P-gp is promoted by high lipophilicity, a molecular weight >400, multiple nitrogen and oxygen atoms and a positive charge at pH 7.4 [94]. The degree to which P-gp restricts brain entry varies across species: e.g. the two radioligands [*carbonyl*-^{11}C]WAY-100635 and [^{18}F]altanserin are P-gp substrates in rodents, but serve as routine brain tracers in human applications [95, 96]. Recently, it has been shown, that P-gp is more pronounced in rodent species [97].

Autoradiography

Autoradiography is a technique to produce an image of the tissue distribution of a radioactive substance. There are two general types of autoradiographic experiments: *in vitro* and *ex vivo* autoradiography.

In vitro autoradiography is performed by incubating a tissue slice expressing the target of interest (e.g. a brain tissue slice for CNS tracers) with the radioligand. In order to obtain quantitative values of the target of interest, additionally, selective blocking agents can be added.

For *ex vivo* autoradiography the radioligand is administered to animals, which are sacrificed thereafter and the organs of interest are sliced. For rodents even whole body autoradiography is possible.

In both methods, the slices are exposed to a film. The "imprint" given by the radioactivity on the film can be visualized via a Phosphor Imager. Autoradiography provides qualitative and quantitative information about the distribution of the target of interest and the binding characteristics (specific and non-specific binding) of the radioligand [98].

Biodistribution

A biodistribution experiment gives information about the *in vivo* distribution of the tracer in an animal model. Further, the tracer's way of excretion can be estimated. For a biodistribution experiment, the tracer is administered to the animal, which is sacrificed after a given period. The organs are removed and their activity is counted in a Gamma Counter. These experiments provide a first estimate for potential future dosimetric calculations.

Small-animal PET

Small-animal PET is used for the *in vivo* imaging of the radioligand in animals such as rats and mice. Like PET, it is a noninvasive technique, which provides a quantitative measure of the 3-dimensional distribution of the radioligand as a function of time in a living subject [99].

Due to the different physical size of human and rodent, small-animal PET scanners require a much higher resolution, ideally at submillimeter level, compared to clinical PET scanners (spatial resolution: 4-6mm). Usually, the volume resolution of small-animal PET is at the microliter level. Furthermore, in order to preserve a high signal-to-noise ratio, preclinical systems should have a much higher sensitivity compared to clinical systems. Since the sensitivity of small-animal PET scanners is still limited, significantly higher doses of radioactivity have to be administered to the animal to achieve a higher number of coincidences and to obtain similar count statistics to clinical PET studies. However, the requirement of higher injection doses is correlated with the injection of a significant mass of cold compound. This could lead to the deterioration of the signal-to-noise ratio due to high occupancy of the target protein [72, 99].

Another difference between human and small-animal PET is the requirement of anesthesia for small-animal PET. For PET data acquisition the subject has to remain still through the imaging session. Therefore, small animals must be anesthetized. However, anesthesia may have an influence on the tracer distribution [99].

For analysis of small-animal PET studies, regions of interest (ROIs) are drawn manually on the PET image. To facilitate comparison between animals, the

standardized uptake value (SUV) is used. SUV values normalize radioactivity concentrations for administered dose and subject body weight and, therefore, allow comparisons of radioactivity concentrations between tissues, subjects and species [88].

1.3. Aim of the present thesis

The aim of this PhD-thesis was the development and preclinical evaluation of the first PET-tracers for the MCHR1, which is widely expressed throughout the CNS and predominately involved in energy homeostasis.

The non-invasive technique PET permits the *in vivo* visualization and quantification of the receptor at a molecular level and will provide deeper information of MCHR1's role in physiological processes. Therefore, a suitable PET-tracer is required.

The first objective was the successful radiosynthesis of the MCHR1 radioligands [^{11}C]SNAP-7941 and [^{18}F]FE@SNAP (both analogues of the high affinity MCHR1 antagonist SNAP-7941) starting from suitable precursor molecules. In order to guarantee save and reliable availability of the tracers, the radiosynthetic procedures had to be automated.
The scientific manuscripts (1-3), included in this thesis, describe the radiosynthesis, automation and purification of [^{11}C]SNAP-7941 and [^{18}F]FE@SNAP.

The second objective was the *in vitro* evaluation of the two compounds regarding their binding affinity and selectivity, metabolic stability, plasma protein binding and lipophilicity. This is described in the manuscripts #3 and #4.
An autoradiographic investigation of SNAP-7941 and FE@SNAP compared to a commercially available MCHR1 ligand on rat brain slices and dedicated human brain tissue slices completed the *in vitro* evaluation. The results can be found in manuscript #5.

The third objective was the *in vivo* evaluation via biodistribution and small-animal PET studies.
In the course of this PhD-thesis, only [^{11}C]SNAP-7941 was evaluated *in vivo*, which is described in manuscript #4.

2.1. Author's contribution

I hereby declare to have significantly contributed to the realization of each of the five publications which are included in the present thesis.

Manuscript #1:

"Radiosynthesis of [^{11}C]SNAP-7941 – the first PET-tracer for the melanin concentrating hormone receptor 1 (MCHR1)"

Cécile Philippe, Eva Schirmer, Markus Mitterhauser, Karem Shanab, Rupert Lanzenberger, Georgios Karanikas, Helmut Spreitzer, Helmut Viernstein, Wolfgang Wadsak

Applied Radiation and Isotopes 2012; 70:2287-2294

I developed the radiosynthesis and the automation procedure. I performed all radiosyntheses, carried out data interpretation and wrote the manuscript.

Manuscript #2:

"[^{18}F]FE@SNAP - a new PET tracer for the melanin concentrating hormone receptor 1 (MCHR1): microfluidic and vessel-based approaches"

Cécile Philippe, Johanna Ungersboeck, Eva Schirmer, Milica Zdravkovic, Lukas Nics, Markus Zeilinger, Karem Shanab, Rupert Lanzenberger, Georgios Karanikas, Helmut Spreitzer, Helmut Viernstein; Markus Mitterhauser, Wolfgang Wadsak

Bioorganic & Medicinal Chemistry 2012; 20:5936-5940

I performed most of the microfluidic and all vessel-based experiments and participated in the analysis and interpretation of the data. I was mainly responsible in the writing of the manuscript.

Manuscript #3:

"Preparation and first preclinical evaluation of [^{18}F]FE@SNAP:
a potential PET tracer for the melanin concentrating hormone receptor 1 (MCHR1)"

Cécile Philippe, Lukas Nics, Markus Zeilinger, Eva Schirmer, Helmut Spreitzer, Georgios Karanikas, Rupert Lanzenberger, Helmut Viernstein, Wolfgang Wadsak, Markus Mitterhauser

Scientia Pharmaceutica 2013, in press (doi:10.3797/scipharm.1306-02)

I performed all radiosyntheses and developed the automation procedure. I participated in the determination and data interpretation of the binding affinity, metabolic stability and lipophilicity. Moreover, I wrote the manuscript.

Manuscript #4:

"Preclinical in vitro & in vivo evaluation of [^{11}C]SNAP-7941 - the first PET tracer for the melanin concentrating hormone receptor 1"

Cécile Philippe, Lukas Nics, Markus Zeilinger, Claudia Kuntner, Thomas Wanek, Severin Mairinger, Karem Shanab, Helmut Spreitzer, Helmut Viernstein, Wolfgang Wadsak, Markus Mitterhauser

Nuclear Medicine and Biology 2013, in press (doi:10.1016/j.nucmedbio.2013.05.010)

I performed every radiosynthesis and participated in the determination and data interpretation of the binding affinity, metabolic stability and lipophilicity. Further, I performed all *in vivo* metabolic stability experiments and participated in the design of the biodistribution and small-animal PET experiments. Moreover, I wrote the manuscript.

Manuscript #5:

"Comparative in vitro autoradiographic investigation of melanin concentrating hormone receptor 1 ligands in the central nervous system"

Cécile Philippe, Daniela Haeusler, Florian Fuchshuber, Helmut Spreitzer, Helmut Viernstein, Wolfgang Wadsak, Markus Mitterhauser

European Journal of Pharmacology, submitted 8th May 2013

I participated in the design of the study, the autoradiographic experiments and the data interpretation, as well as in the writing of the manuscript.

Mag. Cécile Philippe Vienna, July 2013

2.2. Manuscript #1

Radiosynthesis of [^{11}C]SNAP-7941 – the first PET-tracer for the melanin concentrating hormone receptor 1 (MCHR1)

Applied Radiation and Isotopes 2012; 70:2287-2294

Cécile Philippe[a,b], Eva Schirmer[c], Markus Mitterhauser[a,b,d], Karem Shanab[c], Rupert Lanzenberger[e], Georgios Karanikas[a], Helmut Spreitzer[c], Helmut Viernstein[b], Wolfgang Wadsak[a,f]

[a]Radiochemistry and Biomarker Development Unit, Department of Nuclear Medicine, Medical University of Vienna, A-1090 Vienna, Austria

[b]Department of Pharmaceutical Technology and Biopharmaceutics, University of Vienna, Austria

[c]Department of Drug and Natural Product Synthesis, University of Vienna, Austria

[d]Hospital Pharmacy of the General Hospital of Vienna, Austria

[e]Department of Psychiatry and Psychotherapy, Medical University of Vienna, 1090 Vienna, Austria

[f]Department of Inorganic Chemistry, University of Vienna, Austria

Abstract

The melanin concentrating hormone (MCH) system is a new target to treat human disorders. Our aim was the preparation of the first PET-tracer for the MCHR1. [^{11}C]SNAP-7941 is a carbon-11 labelled analogue of the published MCHR1 antagonist SNAP-7941. The optimum reaction conditions were: 2 min reaction time, ≤ 25°C reaction temperature, 2 mg/mL precursor (SNAP-acid) in acetonitrile, using [^{11}C]CH_3OTf as methylation agent. [^{11}C]SNAP-7941 was prepared in a reliable and feasible manner with high radiochemical yields (2.9 ± 1.6 GBq; 11.5 ± 6.4% EOB, n=15).

Keywords: MCHR1, SNAP-7941, Carbon-11, Radioligand, PET

1. Introduction

Melanin concentrating hormone (MCH) is a cyclic polypeptide, which was first isolated from the pituitary gland of the salmon as a hormone responsible for skin pigmentation (Kawauchi et al., 1983). In mammals, MCH is predominantly expressed in the lateral hypothalamus and zona incerta (Bittencourt et al., 1992; Casatti et al. 2002), but is also found in peripheral organs and tissues, such as the pancreas (Tadayyon et al., 2000), colonic epithelial cells (Kokkotou et al., 2008) or adipocytes (Bradley et al., 2000, 2002). It plays a key role in energy homeostasis, e.g. the control of food intake, body weight and metabolism (Ito et al., 2003; Marsh et al., 2002). Furthermore, it is involved in diabetes, gut inflammation and adiposity (Bradley et al., 2000, 2002; Kokkotou et al., 2008; Tadayyon et al., 2000). The biological function of MCH is mediated by two G-protein coupled receptors, MCH receptor 1 and 2 (MCHR1 (Chambers et al. 1999; Lembo et al.; 1999; Saito et al., 1999; Shimomura et al., 1999) and MCHR2 (An et al., 2001; Hill et al., 2001; Sailer et al. 2001; Wang et al., 2001)). The widespread distribution of MCH and its receptors and the involvement in a variety of pathologies makes the MCH system interesting as a new target to treat human disorders. Several MCHR1 antagonists were presented in the last decade; some of them have entered clinical trials for the treatment of obesity (Luthin, 2007), some are in discussion of becoming anti-diabetic drugs (Gattrell et al., 2012). However, to enable confidence in preclinical to clinical translation of central MCHR1 pharmacology, a suitable Positron Emission Tomography (PET) tracer needs to be developed. Borowsky et al. (2002) presented the evaluation of a very potent MCHR1 antagonist, SNAP-7941 ((+)-methyl (4S)-3-{[(3-{4-[3-(acetylamino)phenyl]-1-piperidinyl}propyl)amino]carbonyl}-4-(3,4-difluorophenyl)-6-(methoxymethyl)-2-oxo-1,2,3,4-tetrahydro-5-pyrimidinecarboxylate hydrochloride, **1**) as shown in Fig. 1. It is described to reduce food consumption and to decrease body weight in rats. The excellent binding affinity (K_d = 0.18 nM) for the MCHR1 was one of the main reasons to choose this compound as target for radioactive labelling.

Hence, our aims were

1. the preparation and characterization of a suitable labelling precursor (**4**, Fig. 1);

2. the establishment of a radiosynthetic procedure for the preparation of the carbon-11 labelled analogue, [^{11}C]SNAP-7941 (**2**, Fig. 1) and its optimization;
3. up-scaling and set-up of a fully automated preparation of [^{11}C]SNAP-7941, including purification and formulation;
4. set-up of a suitable quality control.

2. Experimental

2.1. Materials

All chemicals and solvents were obtained from commercial sources with analytical grade and used without further purification. Thin layer chromatography (TLC) was performed using TLC aluminium plates from Merck (silica gel 60 F_{254}, no. 1.05554, 0.2 mm × 20 cm × 20 cm; reversed phase (RP)-18 F_{254s}, no. 1.05559, 0.2 mm × 20 cm × 20 cm). Preparative TLC was performed using plates from the same company (silica gel 60 F_{254}, no. 1.05717, 2 mm × 20 cm × 20 cm; RP-18 F_{254s}, no. 1.05434, 0.2 mm × 20 cm × 20 cm). For column chromatography, silica gel 60 (70-230 mesh ASTM, no. 1.07734) or LiChroprep RP-18 silica gel (40-63 µm, 1.13900) from Merck was used. All chemicals and solvents for the synthesis of the precursor and reference compound were purchased from Sigma-Aldrich, Acros or VWR. Iodine (sublimated grade for analysis; ACS, Pharm.Eur.) was purchased from Merck (Darmstadt, Germany; product number: 1.04761.0100). Silver triflate impregnated carbon was prepared by dissolving 1 g of silver trifluoromethanesulfonate (Sigma Aldrich, Vienna, Austria) in 20 mL acetonitrile (for DNA synthesis, ≤10ppm H_2O, Merck, Darmstadt, Germany). To this solution 3 g of Graphpac™-GC (80/100 mesh, Alltech, Deerfield, Illinois, USA) were added and the suspension was stirred in the dark for about 30 min. The solvent was removed under reduced pressure and the obtained powder was further dried in the dark for 2 hours (rotary evaporator). Acetonitrile, ammonium acetate and ethanol (absolute) were purchased from Merck (Darmstadt, Germany). Tetrabutylammonium hydroxide 30-hydrate (≥98.0%) (TBAH), acetic acid, acetone, 2-butanone and methanol were obtained from Sigma Aldrich (Vienna, Austria). Dimethylformamide (DMF) was obtained from Fluka (Buchs, Switzerland). 0.9% saline solution was purchased from B. Braun

(Melsungen, Germany). 3% saline solution was obtained from a local pharmacy (Landesapotheke Salzburg, Austria). 125 mM phosphate buffer was prepared by dissolving 0.224 g sodium dihydrogenphosphate-monohydrate and 1.935 g disodiumhydrogenphosphate-dihydrate (both from Merck, Darmstadt, Germany) in 100 mL sterile water. Sterile water was purchased from Meditrade Medicare Medizinprodukte (Kufstein, Austria). Solid phase extraction (SPE) cartridges (SepPak® C18-plus) were purchased from Waters (Waters® Associates Milford, MA, USA). Semi-preparative high-performance liquid chromatography (HPLC) column (Chromolith® SemiPrep RP-18e; 100-10mm, precolumn: Chromolith® Guard Cartridge RP-18e; 5-4.6 mm) and analytical HPLC column (Chromolith® Performance RP-18e; 100-4.6 mm) were purchased from Merck (Darmstadt, Germany). Gas chromatography (GC) capillary column (forte GC Capillary Column ID-BP20; 12 m × 0.22 mm × 0.25 μm) was purchased from SGE Analytical Sciences Pty Ltd (Victoria, Australia).

2.2. Instrumentation

^{1}H- and ^{13}C-nuclear magnetic resonance (NMR) spectra were recorded on a Bruker Avance DPX-200 spectrometer at 27°C (200.13 MHz for ^{1}H, 50.32 MHz for ^{13}C), a Varian UnityPlus 300 spectrometer at 28°C (299.95 MHz for ^{1}H, 75.43 MHz for ^{13}C) or a Bruker Avance 500 spectrometer at 20°C (500.13 MHz for ^{1}H, 125.77 MHz for ^{13}C, 470.59 MHz for ^{19}F). Infrared spectroscopy (IR) spectra were recorded on a Perkin Elmer FT-IR spectrophotometer (Spectrum 1000). Mass spectra were obtained on a SHIMADZU GC/MS-Q95050A GC-17A instrument. High resolution mass spectra were recorded on a Finnigan MAT 8230 (EI 70 eV) or a Finnigan MAT 900 S (ESI, 4 kV, 3 μA, ACN/MeOH). Elemental analyses were performed at the Microanalytical Laboratory of the University of Vienna. $[^{11}C]CO_2$ was produced at a GE PET trace cyclotron (General Electric Medical System, Uppsala, Sweden) via the $^{14}N(p,\alpha)^{11}C$ nuclear reaction by irradiation of a gas target (Aluminium) filled with N_2 (+1% O_2) (Air Liquide, Vienna, Austria). Typical beam currents were 48-50 μA and the irradiation was stopped as soon as the desired activity level was reached (approx. 50-65 GBq $[^{11}C]CO_2$, calculated by cyclotron operating software; corresponding to 30-40 min irradiation time). Generally, 7-12 GBq $[^{11}C]CH_3$ and 7-14 GBq $[^{11}C]CH_3OTf$, respectively, were obtained. The production of $[^{11}C]CH_4$,

[^{11}C]CH_3I, [^{11}C]CH_3OTf and [^{11}C]SNAP-7941 including semi-preparative HPLC were performed on a TRACERlab™ FX C Pro synthesis module (GE Healthcare, Uppsala, Sweden). Analytical HPLC was performed using a Merck-Hitachi LaChrom system consisting of a L-7100 pump, a Merck-Hitachi LaChrom L7400 UV-detector (operated at 254nm) and a lead shielded NaI-radiodetector (Raytest Isotopenmessgeräte GmbH, Straubenhardt, Germany). Gas chromatography was performed using a 430-GC system (Burker Daltonik GmbH, Bremen, Germany). The osmolality was measured using a Wescor osmometer Vapro® 5600 (Sanova Medical Systems, Vienna, Austria) and pH was measured using a WTW inoLab 740 pH meter (WTW, Weilheim, Germany).

2.3. Organic Chemistry

2.3.1. Precursor (SNAP-acid)

A reaction scheme is presented in Scheme 1. 6.40 g (29.60 mmol) of 5-(methoxyacetyl)-2,2-dimethyl-1,3-dioxane-4,6-dione (**5**; prepared in one step by condensation reaction of 2,2-dimethyl-1,3-dioxane-4,6-dione and methoxyacetyl chloride) and allyl alcohol (5.13 g, 88.33 mmol) were heated in toluene (90-100 mL) for 24 h at 80°C. After distillation, the crude product was purified using column chromatography yielding 3.81 g (74.8 %) prop-2-en-1-yl 4-methoxy-3-oxobutanoate (**6**) as yellowish oil. To a mixture of 3.70 g (21.50 mmol) of **6**, 3,4-difluorobenzaldehyde (3.15 g, 22.17 mmol), and urea (1.94 g, 32.30 mmol) in THF (18.4 ml) were added Cu_2O (310 mg, 2.17 mmol) and acetic acid (130 µl) at room temperature, followed by dropwise addition of boron trifluoride diethyletherate (3.4 mL, 3.89 g, 24.43 mmol). The slurry was refluxed for 8 h, cooled, poured on a mixture of ice (30 g) and $NaHCO_3$ (6 g) and filtered through Celite. After extraction with CH_2Cl_2 the solvent was evaporated and the purification of the residue was performed using column chromatography yielding 6.65 g (91.5%) prop-2-en-1-yl 4-(3,4-difluorophenyl)-6-(methoxymethyl)-2-oxo-1,2,3,4-tetrahydropyrimidine-5-carboxylate (**7**) as yellowish oil. To pyrimidinone **7** (6.54 g, 19.33 mmol) and 4-nitrophenyl chloroformate (13.65 g, 67.72 mmol) in THF (242.0 mL) was slowly added LiHMDS (9.05 g, 54.06 mmol, 1 M in THF) at -78°C. After 10 min the reaction was quenched with H_2O (6.1 mL) and warmed to 0°C. K_2CO_3 (10.68 g,

77.27 mmol) and 3-aminopropylbromide hydrobromide (12.69 g, 57.96 mmol) were added and stirred overnight at room temperature. After washing with a solution of $NaHCO_3$, extraction with Et_2O, and subsequent column chromatography, prop-2-en-1-yl 3-[(3-bromopropyl)carbamoyl]-4-(3,4-difluorophenyl)-6-(methoxymethyl)-2-oxo-1,2,3,4-tetrahydropyrimidine-5-carboxylate (**8**) was obtained in good yield (8.50 g, 87.7%). 4.60 g (21.07 mmol) of N-[3-(piperidin-4-yl)phenyl]acetamide (**9**; prepared according to Schönberger (2006) in a 5-step-synthesis staring from N-Boc-piperidinone) were solved in acetonitrile and after addition of **8** (6.90 g, 13.74 mmol) and K_2CO_3 (21.08 g, 152.52 mmol) stirred under argon atmosphere for 37 h at 35°C. After filtration and evaporation *in vacuo* of the solvent, the residue was washed twice with a solution of $NaHCO_3$, extracted with ethyl acetate purified *via* column chromatography to obtain allyl-SNAP **3** (allyl-3-(3-(4-(3-acetamindoophenyl)piperidin-1-yl)propylcarbamoyl)-4-(3,4-difluorphenyl)-6-(methoxymethyl)-2-oxo-1,2,3,4-tetrahydropyrimidine-5-carboxylic ester)(3.70 g, 42.1%) as a pale yellow solid. After dissolving **3** (2.44 g, 3.81 mmol) in THF, $(PPh_3)_4Pd$ (530 mg, 0.46 mmol) and morpholine (3.98 g, 44.38 mmol) were added under argon atmosphere. After 17 h THF was evaporated and the residue was purified using column chromatography. 660 mg of SNAP-acid **4** (3-(3-(4-(3-acetamidophenyl)piperidin-1-yl)propylcarbamoyl)-4-(3,4-difluorophenyl)-6-(methoxymethyl)-2-oxo-1,2,3,4-tetrahydropyrimidine-5-carboxylic acid) (28.9 %) were obtained after purification as an amorphic pale yellow solid.

All intermediates and products were analyzed spectroscopically *via* NMR, MS, and HRMS. For NMR analysis, the solvent signal was used as an internal standard which was related to TMS with δ = 7.26 ppm (^1H in $CDCl_3$) and δ = 77.0 ppm (^{13}C in $CDCl_3$), respectively.

6: **^{1}H-NMR** (200 MHz, $CDCl_3$): δ (ppm) 3.39 (s, 3H, OC<u>H</u>$_3$), 3.51 (s, 2H, 2-C<u>H</u>$_2$), 4.05 (s, 2H, 4-OC<u>H</u>$_2$), 4.61 (d, *J* = 5.7 Hz, 2H, Allyl-OC<u>H</u>$_2$), 5.20-5.35 (m, 2H, Allyl-C<u>H</u>$_2$), 5.79-5.98 (m, 1H, Allyl-C<u>H</u>) **^{13}C-NMR** (50 MHz, $CDCl_3$): δ (ppm) 45.6 (2-<u>C</u>H$_2$), 59.3 (O<u>C</u>H$_3$), 65.9 (Allyl-O<u>C</u>H$_2$), 77.3 (4-O<u>C</u>H$_2$), 118.7 (Allyl-<u>C</u>H$_2$), 131.4 (Allyl-<u>C</u>H), 166.6 (1-<u>C</u>OO), 201.4 (3-<u>C</u>O) **MS**: m/z (%) 173 (1), 172 (1), 115 (47), 84 (6), 69 (14), 55 (11), 45 (100), 43 (8), 42 (7), 41 (24) **HRMS**: m/z calculated for $C_8H_{12}O_4$: 172.0736. Found: 172.0735.

7: **^{1}H-NMR** (500 MHz, $CDCl_3$): δ (ppm) 3.44 (s, 3H, 7-OC$\underline{H}_3$), 4.48-4.56 (m, 2H, Allyl-OC$\underline{H}_2$), 4.64 (d, 2H, J = 16.5 Hz, 6-OC$\underline{H}_2$), 5.17 (m, 2H, Allyl-C$\underline{H}_2$), 5.34 (d, 2H, J = 3.0 Hz, 3-C$\underline{H}$), 5.79 (m, 1H, Allyl-C$\underline{H}$), 6.77 (s, 1H, 2a-N$\underline{H}$), 7.02 (m, 1H, 15-C$\underline{H}$), 7.06 (m, 1H, 14-C$\underline{H}$), 7.11 (m, 1H, 11-C$\underline{H}$), 7.66 (s, 1H, 1-N$\underline{H}$) **^{13}C-NMR** (126 MHz, $CDCl_3$): δ (ppm) 54.5 (53-$\underline{C}$H), 59.1 (7-O$\underline{C}H_3$), 68.5 (6-O$\underline{C}H_2$), 98.2 (4-C), 115.7 (d, J = 17.6 Hz, 11-$\underline{C}$H), 117.4 (d, J = 17.4 Hz, 14-$\underline{C}$H), 118.4 (Allyl-$\underline{C}H_2$), 122.5 (15-$\underline{C}$H), 131.8 (Allyl-$\underline{C}$H), 140.4 (t, J = 4.1 Hz, 10-C), 147.8 (5-C), 149.9 (12-$\underline{C}$F), 150.3 (13-$\underline{C}$F), 152.2 (2-$\underline{C}$O), 164.3 (8-$\underline{C}$OO) **^{19}F-NMR** (471 MHz, $CDCl_3$): δ (ppm) -136.7 (m, 12-C$\underline{F}$), -138.5 (m, 13-C$\underline{F}$) **MS**: m/z (%) 338 (11), 297 (47), 265 (53), 261 (34), 253 (32), 225 (100), 194 (28), 184 (51), 169 (35), 167 (33), 151 (32), 140 (27), 45 (33), 41 (98) **HRMS**: m/z calculated for $C_{16}H_{16}F_2N_2O_4$: 339.1156. Found: 339.1150.

8: **^{1}H-NMR** (200 MHz, $CDCl_3$): δ (ppm) 1.20-1.30 (m, 2H, 20-C$\underline{H}_2$Br), 2.02-2.15 (m, 2H, 19-C$\underline{H}_2$), 3.38 (t, J = 6.4 Hz, 2H, 18-C$\underline{H}_2$), 3.46 (s, 3H, 7-OC$\underline{H}_3$), 4.59-4.62 (m, 2H, Allyl-OC$\underline{H}_2$), 4.67 (s, 2H, 6-C$\underline{H}_2$), 5.17-5.26 (m, 2H, Allyl-C$\underline{H}_2$), 5.74-5.94 (m, 1H, Allyl-C$\underline{H}$), 6.66 (s, 1H, 3-C$\underline{H}$), 7.02-7.21 (m, 3H, 11-C$\underline{H}$, 14-C$\underline{H}$, 15-C$\underline{H}$), 7.88 (s, 1H, 1-N$\underline{H}$), 9.08 (t, 1H, J = 5.6 Hz, 17-N$\underline{H}$) **^{13}C-NMR** (50 MHz, $CDCl_3$): δ (ppm) 30.2 (20-$\underline{C}H_2$), 31.9 (19-$\underline{C}H_2$), 39.3 (18-$\underline{C}H_2$), 53.4 (3-$\underline{C}$H), 59.1 (7-$\underline{C}H_3$), 65.6 (Allyl-O$\underline{C}H_2$), 68.0 (6-$\underline{C}H_2$), 101.4 (4-C), 115.9/116.2 (11-$\underline{C}$H), 117.3/117.6 (14-$\underline{C}$H), 118.8 (Allyl-$\underline{C}H_2$), 122.8/122.88/122.93/123.0 (15-$\underline{C}$H), 131.3 (Allyl-$\underline{C}$H), 141.0 (10-C), 146.3 (5-C), 152.4 (2-$\underline{C}$O), 153.8 (16-$\underline{C}$O), 163.8 (8-$\underline{C}$OO) **MS**: m/z (%) 502 (1), 463 (12), 420 (5), 337 (23), 279 (13), 261 (14), 168 (22), 142 (16), 56 (15), 45 (15), 43 (15), 41 (100) **HRMS**: m/z calculated for $C_{20}H_{22}F_2N_3O_5BrNa$ $[M + Na]^+$: 524.0609. Found: 524.0611.

3: **^{1}H-NMR** (500 MHz, $CDCl_3$): δ (ppm) 1.73-1.83 (m, 4H, 22,22´-($\underline{C}H_2$)$_2$), 1.74 (m, 2H, 19-C$\underline{H}_2$), 1.99 und 2.99 (m, 4H, 21,21´-($\underline{C}H_2$)$_2$), 2.16 (s, 3H, 32-C$\underline{H}_3$), 2.40 (t, 2H, J = 7.0 Hz, 20-C$\underline{H}_2$), 2.44 (m, 1H, 23-C$\underline{H}$), 3.32 und 3.40 (m, 2H, 18-C$\underline{H}_2$), 3.43 (s, 3H, 7-C$\underline{H}_3$), 4.54-4.64 (m, 2H, Allyl-C$\underline{H}_2$), 4.67 (s, 2H, 6-C$\underline{H}_2$), 5.20-5.21 (m, 2H, Allyl-C$\underline{H}_2$), 5.85 (m, 1H, Allyl-C$\underline{H}$), 6.69 (s, 1H, 3-C$\underline{H}$), 6.95 (d, 1H, J = 7.6 Hz, 29-C$\underline{H}$), 7.05 (m, 1H, 14-C$\underline{H}$), 7.10 (m, 1H, 15-C$\underline{H}$), 7.19 (m, 1H, 11-C$\underline{H}$), 7.20 (m, 1H, 28-C$\underline{H}$), 7.28 (d, 1H, J = 8.0 Hz, 27-C$\underline{H}$), 7.47 (s, 1H, 25-C$\underline{H}$), 7.58 (s, 1H, 30-N$\underline{H}$), 8.00 (s, 1H, 1-N$\underline{H}$), 8.99 (t, 1H, J = 5.4 Hz, 17-N$\underline{H}$) **^{13}C-NMR** (126 MHz, $CDCl_3$): δ (ppm) 24.5 (32-$\underline{C}H_3$), 26.4 (19-$\underline{C}H_2$), 33.0 (22,22´-($\underline{C}H_2$)$_2$), 39.7 (18-$\underline{C}H_2$), 42.7 (23-$\underline{C}$H), 53.0 (3-$\underline{C}$H), 54.33, 54.37 (21,21´-($\underline{C}H_2$)$_2$), 56.7 (20-$\underline{C}H_2$), 59.0 (7-$\underline{C}H_3$), 65.2 (Allyl-$\underline{C}H_2$), 68.0 (6-$\underline{C}H_2$),

101.6 (4-C), 116.2 (11-CH), 117.2 (14-CH), 117.5 (27-CH), 118.3 (25-CH), 118.6 (Allyl-CH_2), 122.8 (29-CH), 123.1 (15-CH), 128.8 (28-CH), 131.6 (Allyl-CH), 137.7 (10-C), 138.0 (26-C), 146.5 (5-C), 147.4 (24-C), 149.9 (12- oder 13-CF), 150.1 (12- oder 13-CF), 152.2 (2-CO), 153.1 (16-CO), 163.8 (8-COO), 168.5 (31-CON) **^{19}F-NMR** (471 MHz, $CDCl_3$): δ (ppm) -136.9 (m, 12- oder 13-CF), -138.5 (m, 12- oder 13-CF) **MS**: m/z (%) 641 (7), 640 (19), 628 (8), 346 (2), 345 (13), 324 (3), 303 (19), 302 (100) **HRMS**: m/z calculated $C_{33}H_{40}F_2N_5O_6$ $[M + H]^+$: 640.2947. Found: 640.2956. **IR**: (v) (cm^{-1}) 3311, 3147, 3087, 2937, 2809, 2771, 1718, 1674, 1647, 1610, 1593, 1541, 1517, 1490, 1468, 1437, 1393, 1371, 1306, 1280, 1211, 1115, 1077, 766

4: **^{1}H-NMR** (200 MHz, d_6-DMSO): δ (ppm) 1.52-1.66 (m, 6H, 19-CH_2, 22,22´-$(CH_2)_2$), 1.89-2.01 (m, 5H, 21,21´-CH_2, 32-CH_3), 2.36 (m, 3H, 20-CH_2, 23-CH), 2.98-2.99 (m, 2H, 21,21´-CH_2), 3.22 (m, 5H, 7-OCH_3, 18-CH_2), 4.59 (dd, 2H, J = 12.7 Hz, J = 84.0 Hz, 6-CH_2), 6.61 (s, 1H, 3-CH), 6.87 (d, 1H, J = 6.4 Hz, 29-CH), 7.03-7.48 (m, 7H, 11-CH, 14-CH, 15-CH, 25-CH, 27-CH, 28-CH, 30-NH), 7.77-7.83 (m, 1H, 1-NH), 8.96 (m, 1H, 17-NH), 9.89 (s, 1H, 8-COOH) **^{13}C-NMR** (50 MHz, d_6-DMSO): δ (ppm) 24.0 (32-CH_3), 25.8 (19-CH_2), 32.4 (22,22´-$(CH_2)_2$), 38.9 (18-CH_2), 41.7 (23-CH), 52.5 (3-CH), 53.5 (21,21´-$(CH_2)_2$), 55.6 (20-CH_2), 57.7 (7-OCH_3), 66.3 (6-OCH_2), 115.0/115.3 (11-CH), 116.9/117.2 (14-CH), 117.4 (27-CH), 117.7 (25-CH), 121.5 (29-CH), 122.6/122.8/122.8 (15-CH), 128.6 (28-CH), 139.1 (10-C), 139.4 (26-C), 146.1 (5-C), 146.6 (24-C), 152.9 (2-CO), 153.2 (16-CO), 168.1 (31-CON), 168.2 (8-COOH) **MS**: m/z (%) 601 (4), 600 (15), 579 (7), 345 (11), 324 (8), 303 (18), 302 (100), 301 (26), 279 (5) **HRMS**: m/z calculated for: $C_{30}H_{34}F_2N_5O_6$ $[M - H]^-$: 598.2477. Found: 598.2462 **IR**: (v) (cm^{-1}) 3416, 3256, 2961, 2925, 2853, 1711, 1685, 1651, 1610, 1556, 1514, 1489, 1424, 1375, 1261, 1223, 1096, 1021, 874, 799, 703

2.3.2. Reference standard (rac-SNAP-7941)

Reference standard rac-SNAP-7941 (**1**, Fig. 1) was obtained according to Schönberger (2006). Preparation of all intermediates took place in analogy to the route described in 2.3. and is shown in Scheme 1. Purification was performed using column chromatography. 4.51 g (77 %) rac-SNAP-7941 were obtained after purification as a yellow oil. NMR analysis (^{1}H and ^{13}C) of the final compound was in full accordance with the literature (Schönberger, 2006).

2.4. Radiochemistry

2.4.1. Synthesis of [^{11}C]SNAP-7941

A reaction scheme is presented in Scheme 2. Using the TRACERlab™ FX C Pro synthesis module, [^{11}C]CH_3I and [^{11}C]CH_3OTf, respectively, were bubbled through a solution of SNAP-acid (0.01-4mg/mL, 0.02-6.67 mmol) in 500 µL solvent containing TBAH (1 equiv). Different solvents (DMF (only for reactions with [^{11}C]CH_3I), acetone, 2-butanone and acetonitrile (≤10ppm H_2O; only for reactions with [^{11}C]CH_3OTf) and different reaction temperatures (DMF: 100-140°C; acetone: 50°C; 2-butanone: 20-75°C and acetonitrile: 0-75°C) were tested. After 1-10 min reaction time, the reaction mixture was quenched with water and the radiochemical yield was determined using analytical radio-HPLC (mobile phase: (water/acetic acid 97.5/2.5 v/v; 2.5 g/L ammonium acetate; pH 3.5)/acetonitrile 70/30 v/v; flow: 1 mL/min). Chromatograms were registered using an UV-detector (254 nm) and a NaI radioactivity detector in series.

2.4.2. Purification of [^{11}C]SNAP-7941

The crude reaction mixture was injected into the build-in HPLC system (mobile phase: (water/acetic acid 97.5/2.5 v/v; 2.5 g/L ammonium acetate; pH 3.5)/acetonitrile 75/25 v/v; flow: 8 mL/min, after 6.5 min: 10 mL/min). Chromatograms were registered using an UV-detector (254 nm) and a NaI radioactivity detector in series. The retention times were 2.8-3.6 min (k'= 1.8-2.6) for SNAP-acid and 8.1-9.7 min (k'=7.1-8.7) for [^{11}C]SNAP-7941. The [^{11}C]SNAP-7941 fraction was cut and diluted with 100 mL water. The resulting solution was then pushed through a C18 SPE cartridge. After washing with 10 mL water the purified product was completely eluted with 1.5 mL of ethanol and 5 mL 0.9% saline solution. Formulation was done with a further 9 mL of physiological saline (0.9%), 1 mL of saline solution (3%) and 1 mL of phosphate buffer (125 nM). Hence, the final total volume was 17.5 mL.

2.4.3. Quality control of [^{11}C]SNAP-7941

Chemical and radiochemical impurities were detected using analytical radio-HPLC (for conditions see Radiosynthesis section). Retention times were 3.1-4.1 min (k'=0.6-1.1) for SNAP-acid and 5.3-7.9 min (k'=1.7-3.0) for [^{11}C]SNAP-7941. The

chemical identity of [^{11}C]SNAP-7941 was determined by co-injection of the unlabeled reference compound, SNAP-7941. Residual solvents were analyzed by GC. Osmolality and pH were checked with dedicated equipment.

3. Results and discussion

3.1. Organic synthesis

A synthetic route to the precursor compound SNAP-acid (**4**) (660 mg, 28.9%) could be established via deallylation of allyl-SNAP (**3**). The use of other protecting groups (i.e. t-butyl, trimethylsilyl and p-methoxybenzyl) could not provide the desired precursor. The reference standard rac-SNAP-7941 (**1**) could be synthesized in good yields (4.51 g, 77%) and purity for the evaluation of the radiosynthesis.

3.2. Radiochemistry

The first preparation of [^{11}C]SNAP-7941 followed by a fully-automated synthesis and purification was successful. Using [^{11}C]CH_3I as methylation agent, the radiochemical incorporation yield of [^{11}C]SNAP-7941 was below 4% in all tested conditions (reaction solvent, reaction temperature, reaction time, precursor concentration). Using [^{11}C]CH_3OTf as methylation agent, the radiochemical incorporation yield was still unsatisfactory low in acetone (< 2.5%). Reasonable yields could be achieved using 2-butanone (up to 45%) or acetonitrile (up to 50%) as reaction solvent. Acetonitrile evinced as the most suitable solvent regarding yield and avoidance of separation problems in preparative HPLC.

The evaluation of the precursor concentration, reaction temperature and reaction time using [^{11}C]CH_3OTf as methylation agent in acetonitrile is shown in Fig. 2. Highest radiochemical incorporation yields could be obtained using 4 mg/mL (49.0 ± 2.0%) and 2 mg/mL (48.7 ± 0.5%), respectively. No significant difference in the radiochemical incorporation yield was found between these two precursor concentrations. Significantly ($P < 0.01$) lower yields were obtained with ≤ 1 mg/mL of precursor. The radiochemical incorporation yields ($n \geq 2$) of [^{11}C]SNAP-7941 (75°C, 5 min) ranged from 8.8 ± 6.4% using 0.05 mg/mL of precursor up to 49.0 ±

2.0% using 4 mg/mL of precursor. No radiochemical conversion was observed using precursor concentrations < 0.05 mg/mL (Fig. 2a).

A clear inverse trend was found between temperatures versus radiochemical incorporation yields. At 1 mg/mL precursor for 5 min the radiochemical incorporation decreases with higher temperature: 45.7 ± 0.3% at 0°C, 41.4 ± 0.6% at 25°C, 36.2 ± 0.6% at 50°C and 35.3 ± 0.6% at 75°C (Fig. 2b). This trend was not due to the production of more side-products at higher temperatures, but due to the better conversion of [^{11}C]CH_3OTf at lower temperatures.

Regarding the reaction time (1 mg/mL precursor, 75°C), the maximum radiochemical incorporation yield (41.1 ± 1.0%) was achieved after 2 min (Fig. 2c). Although the maximum yield was achieved after 2 min reaction time, there was no significant difference within the tested conditions (1-10 min). Hence, the optimum reaction conditions were determined to be 2 min reaction time at ≤ 25°C reaction temperature using 2 mg/mL precursor in 500 µL acetonitrile (Table 1).

Purification using semi-preparative HPLC was straight forward using a monolithic reversed-phase column at moderate flow rates (8-10 mL/min). Sample chromatograms are shown in Fig. 3. Subsequent SPE purification resulted in a recovery of > 95% of [^{11}C]SNAP-7941. Until now, 15 complete high-scale radiosyntheses were performed (2 mg/mL precursor, 25°C, 2 min). 2.9 ± 1.6 GBq of formulated [^{11}C]SNAP-7941 (17.5 ± 3.6%, based on [^{11}C]CH_3OTf; 11.5 ± 6.4% EOB) were produced within < 40 min.

Full quality control was completed within 9 min. Radiochemical purity always exceeded 99% as determined by radio-HPLC. No residual precursor mass was detected but 9.6 ± 6.4 µg of ^{12}C-SNAP-7941 were found in the final product solution. Specific activity was determined via HPLC and found to be 28.9 ± 9.4 GBq/µmol at the end of synthesis (EOS). Sample chromatograms are shown in Fig. 4. Residual solvent analysis revealed <5 ppm acetonitrile and no other impurities except ethanol (8.5%). Osmolality was 291 ± 14 mosmol/kg and pH was 7.5 ± 0.2.

Achieved yields are sufficient to allow for preclinical and potentially clinical investigations. Due to general problems with the production of [^{11}C]CO_2 during the time frame of the presented study, specific activity was relatively low (28.9 ± 9.4 GBq/µmol). Higher specific activities of [^{11}C]SNAP-7941 are expected for future syntheses. Thus, the presented work is the basis for future applications that will

further elucidate the role of MCHR1 in obesity, diabetes and several other pathologies.

4. Conclusion

[^{11}C]SNAP-7941, the first PET-tracer for the MCHR1, was prepared in a reliable and feasible manner, starting from a suitable labelling precursor (SNAP-acid). The optimized reaction conditions evinced sufficient overall yields for subsequent preclinical and clinical investigations.

Acknowledgment

This research was part of an ongoing study, funded by the Austrian Science Fund (FWF P20977-B09; P.I.: M. Mitterhauser).

References

An, S., Cutler, G., Zhao, J.J., Huang, S.G., Tian, H., Li, W., Liang, L., Rich, M., Bakleh, A., Du, J., Chen, J.L., Dai, K., 2001. Identification and characterization of a melanin-concentrating hormone receptor. Proc. Natl. Acad. Sci. USA 98, 7576-7581.

Bittencourt, J.C., Presse, F., Arias, C., Peto, C., Vaughan, J., Nahon, J.L., Vale, W., Sawchenko, P.E., 1992. The melanin-concentrating hormone system of the rat brain: An immuno- and hybridization histochemical characterization. J. Comp. Neurol. 319, 218-245.

Borowsky, B., Durkin, M.M., Ogozalek, K., Marzabadi, M.R., DeLeon, J., Lagu, B., Heurich, R., Lichtblau, H., Shaposhnik, Z., Daniewska, I., Blackburn, T.P., Branchek, T.A., Gerald, C., Vaysse, P.J., Forray, C., 2002. Antidepressant, anxiolytic and anorectic effects of a melanin-concentrating hormone-1 receptor antagonist. Nat. Med. 8, 825-830.

Bradley, R.L., Kokkotou, E.G., Maratos-Flier, E., Cheatham, B., 2000. Melanin-concentrating hormone regulates leptin synthesis and secretion in rat adipocytes. Diabetes 49, 1073-1077.

Bradley, R.L., Mansfield, J.P., Maratos-Flier, E., Cheatham, B., 2002. Melanin-concentrating hormone activates signaling pathways in 3T3-L1 adipocytes. *Am. J.* Physiol. Endocrinol. Metab. 283, E584-E592.

Casatti, C.A., Elias, C.F., Sita, L.V., Frigo, L., Furlani, V.C.G., Bauer, J.A., Bittencourt, J.C., 2002. Distribution of melanin-concentrating hormone neurons projecting to the medial mammillary nucleus. Neuroscience 115, 899-915.

Chambers, J., Ames, R.S., Bergsma, D., Muir, A., Fitzgerald, L.R., Hervieu, G., Dytko, G.M., Foley, J.J., Martin, J., Liu, W.S., Park, J., Ellis, C., Ganguly, S., Konchar, S., Cluderay, J., Leslie, R., Wilson, S., Sarau, H.M., 1999. Melanin-concentrating hormone is the cognate ligand for the orphan G-protein-coupled receptor SLC-1. Nature 400, 261-265.

Gattrell, W.T., Sambrook Smith C.P., Smith, A.J., 2012. An example of designed multiple ligands spanning protein classes: Dual MCH-1R antagonists/DPPIV inhibitors. Bioorg. Med. Chem. Lett. 22, 2464-2469.

Hill, J., Duckworth, M., Murdock, P., Rennie, G., Sabido-David, C., Ames, R. S., Szekeres, P., Wilson, S., Bergsma, D.J., Gloger, I.S., Levy, D.S., Chamber; J.K., Muir, A.I., 2001. Molecular cloning and functional characterization of MCH2, a novel human MCH receptor. J. Biol. Chem. 276, 20125-20129.

Ito, M., Gomori, A., Ishihara, A., Oda, Z., Mashiko, S., Matsushita, H., Yumoto, M., Ito, M., Sano, H., Tokita, S., Moriya, M., Iwaasa, H., Kanatani, A., 2003. Characterization of MCH-mediated obesity in mice. Am. J. Physiol. Endocrinol. Metab., 284, E940-E945.

Kawauchi, H., Kawazoe, I., Tsubokawa, M., Kishida, M., Baker, B. I., 1983. Charakterization of the melanin-concentrating hormone in chum salmon pituitaries. Nature 305, 321-323.

Kokkotou, E., Moss, A.C., Torres, D., Karagiannides, I., Cheifetz, A., Liu, S., O'Brian, M., Maratos-Flier, E., Pothoulakis, C., 2008. Melanin-concentrating hormone as a mediator of intestinal inflammation. Proc. Natl. Acad. Sci. USA 105, 10613-10618.

Lembo, P.M.C., Grazzini, E., Cao, J., Hubatsch, D.A., Pelletier, M., Hoffert, C., St-Onge, S., Pou, C., Labreque, J., Groblewski, T., O'Donnell, D., Payza, K., Ahmad, S., Walker, P., 1999. The receptor for the orexigenic peptide melanin-concentrating hormone is a G-protein-coupled receptor. Nat. Cell. Biol. 1, 267-271.

Luthin, D.R., 2007. Anti-obesity effects of small molecule melanin-concentrating hormone receptor1 (MCHR1) antagonists. Life Sciences 81, 423-440.

Marsh, D.J., Weingarth, D.T., Novi, D.E., Chen, H.Y., Turmbauer, M.E., Chen, A.S., Guan, X.M., Jiang, M.M., Feng, Y., Camacho, R.E., Shen, Z., Frazier, E.G., Yu, H., Metzger, J.M., Kuca, S.J., Shearman, L.P., Gopal-Truter, S., MacNeil, D.J., Strack, A.M., MacIntyre, D.E., Van der Ploeg, L.H.T., Qian, S., 2002. Melanin-concentrating hormone 1 receptor-deficient mice are lean, hyperactive, and hyperphagic and have altered metabolism. Proc. Natl. Acad. Sci. USA 99, 3240-3245.

Sailer, A.W., Sano, H., Zeng, Z., McDonald, T.P., Pan, J., Pong, S.S., Feighner, S.D., Tan, C.P., Fukami, T., Iwaasa, H., Hreniuk, D.L., Morin, N.R., Sadowski, S.J., Ito, M., Ito, M., Bansal, A., Ky, B., Figueroa, D.J., Jiang, Q., Austin, C.P., MacNeil, D.J., Ishihara, A., Ihara, M., Kanatani, A., Van der Ploeg, L.H.T., Howard A.D., Liu, Q., 2001. Identification and characterization of a second melanin-concentrating hormone receptor, MCH-2R. Proc. Natl. Acad. Sci. USA 98, 7564-7569.

Saito, Y., Nothacker, H.P., Wang, Z., Lin, S.H., Leslie, F., Civelli, O., 1999. Molecular characterization of the melanin-concentrating-hormone receptor. Nature 400, 265-269.

Schönberger, J., 2006. Studie zur Entwicklung neuer Leitstrukturen für die medikamentöse Adipositastherapie. Dissertation, Techn. Univ. Darmstadt.

Shimomura, Y., Mori, M., Sugo, T., Ishibashi, Y., Abe, M., Kurokawa, T., Onda, H., Nishimura, O., Sumino, Y., Fujino, M., 1999. Isolation and identification of melanin-concentrating hormone as the endogenous ligand of the SLC-1 receptor. Biochem. Biophys. Res. Commun. 261, 622-626.

Tadayyon, M., Welters, H.J., Haynes, A.C., Cluderay, J.E., Hervieu, G., 2002. Expression of melanin-concentrating hormone in insulin-producing cells: MCH stimulates insulin release in RINm5F and CRI-G1 cell-lines. Biochem. Biophys. Res. Commun. 275, 709-712.

Wang, S., Behan, J., O'Neill, K., Weig, B., Fried, S., Laz, T., Bayne, M., Gustafson, E., Hawes, B.E., 2001. Identification and pharmacological characterization of a novel human melanin-concentrating hormone receptor, MCH-R2. J. Biol. Chem. 276, 34664-34670.

Captions

Fig. 1. SNAP-7941 derivatives **1-4** (**1**: SNAP-7941; **2**: [^{11}C]SNAP-7941; **3**: Allyl-SNAP; **4**: SNAP-acid)

Fig. 2. The dependence of the radiochemical incorporation yield of [^{11}C]SNAP-7941 ($n \geq 2$) on (a) amount of precursor (75°C, 5 min), (b) reaction temperature (1 mg/mL, 5min) (c) and reaction time (1 mg/mL, 75°C). If not visible, error bars are within the margin of the symbols.

Fig. 3. Semi-preparative HPLC chromatogram of the reaction solution of [^{11}C]SNAP-7941.

Fig. 4. Typical chromatogram of purified and formulated [^{11}C]SNAP-7941 using analytical HPLC.

Scheme 1. Reaction scheme for the preparation of the precursor SNAP-acid (**4**) and the reference standard rac-SNAP-7941 (**1**).

Scheme 2. Reaction scheme of the radiosynthesis of [^{11}C]SNAP-7941 (**2**).

Table 1. Optimum reaction conditions and outcome for large scale preparation of [^{11}C]SNAP-7941 (n=15).

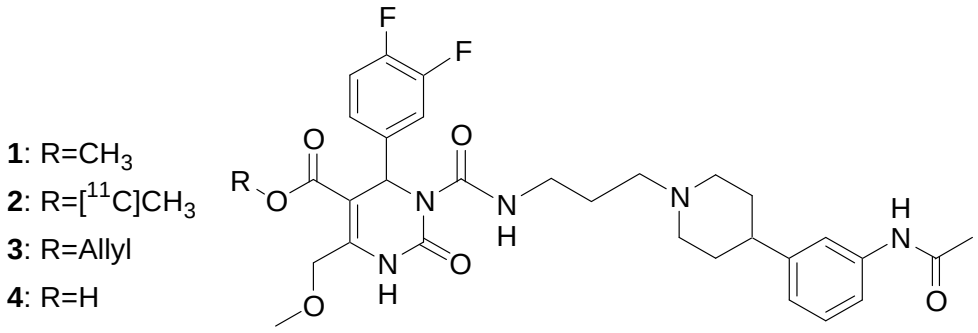

Fig. 1. SNAP-7941 derivatives **1**-**4** (**1**: SNAP-7941; **2**: [^{11}C]SNAP-7941; **3**: Allyl-SNAP; **4**: SNAP-acid)

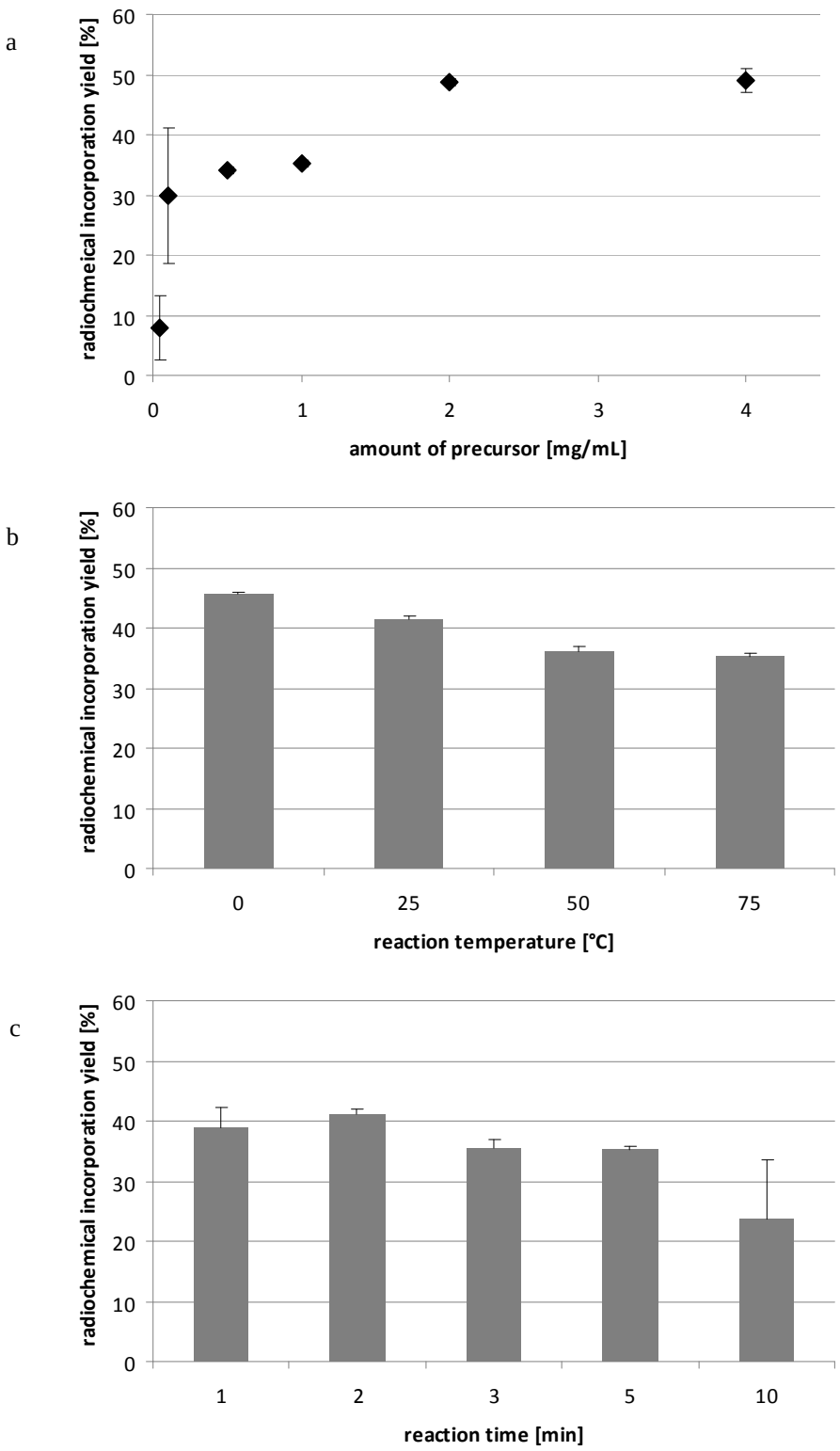

Fig. 2. The dependence of the radiochemical incorporation yield of [^{11}C]SNAP-7941 ($n \geq 2$) on (a) amount of precursor (75°C, 5 min), (b) reaction temperature (1 mg/mL, 5min) (c) and reaction time (1 mg/mL, 75°C). If not visible, error bars are within the margin of the symbols.

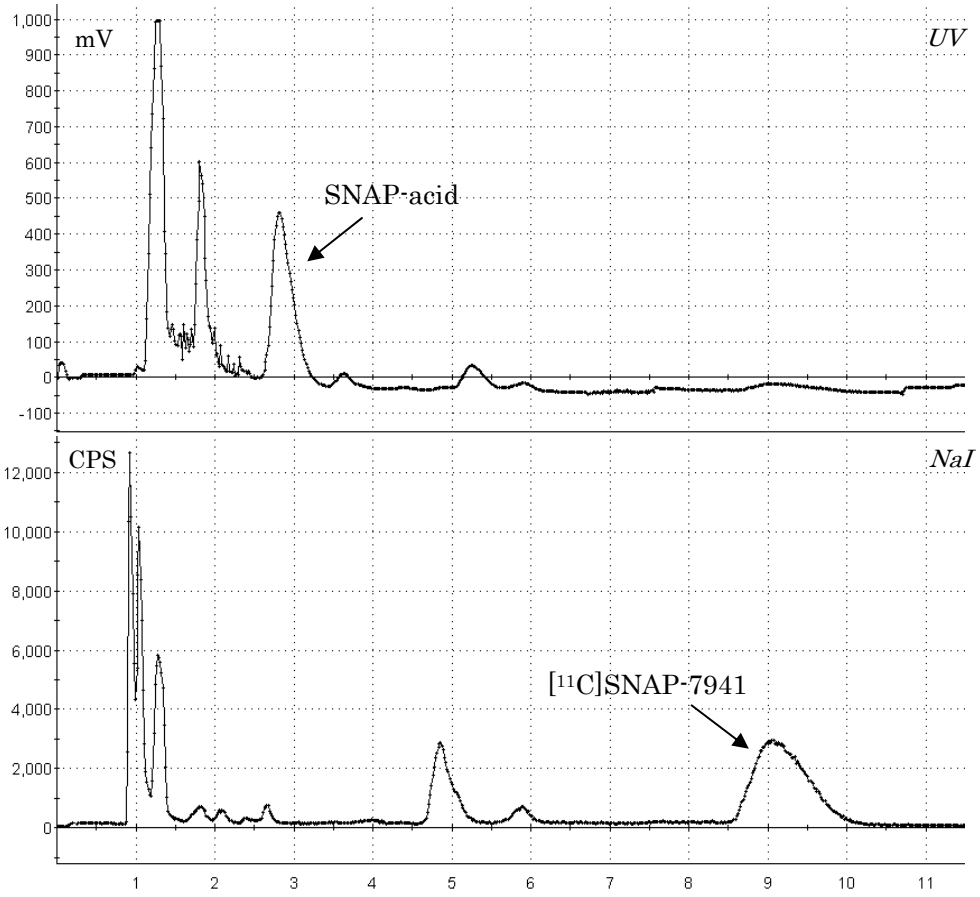

Fig. 3. Semi-preparative HPLC chromatogram of the reaction solution of [^{11}C]SNAP-7941.

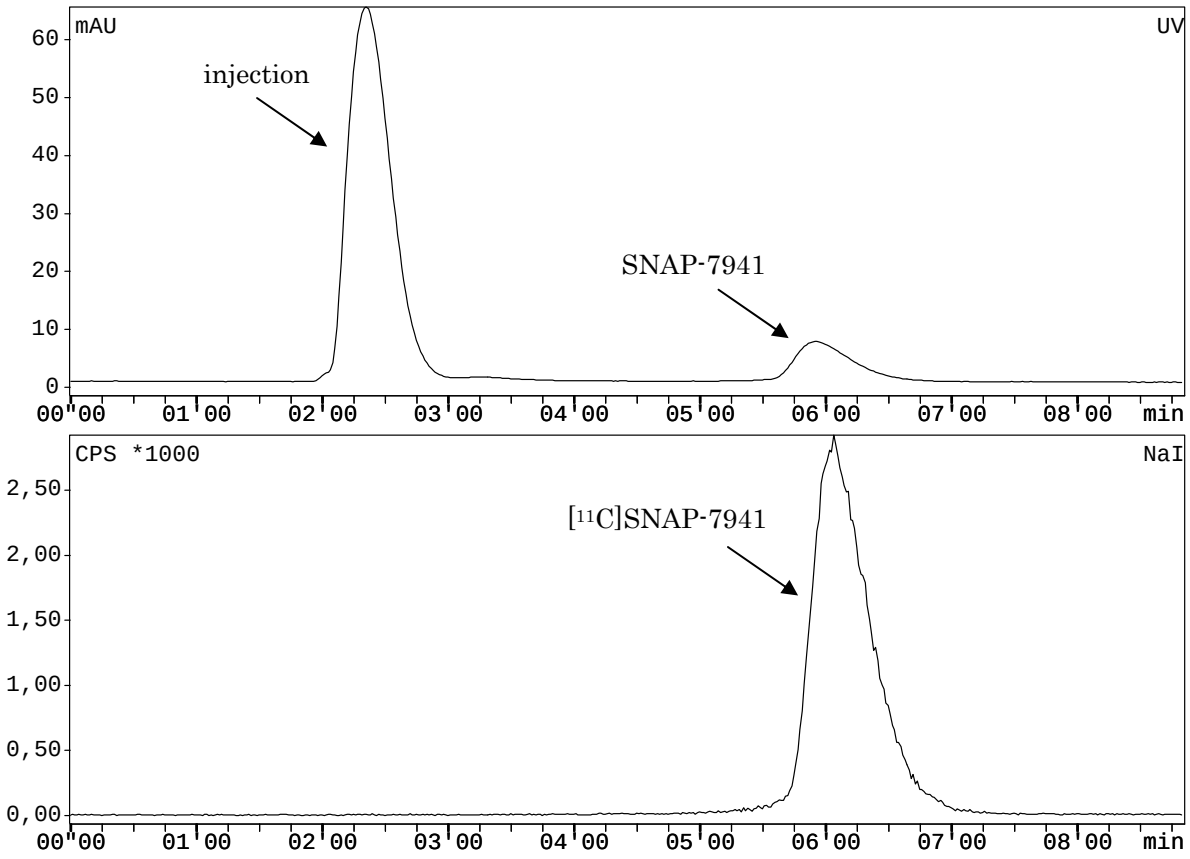

Fig. 4. Typical chromatogram of purified and formulated [^{11}C]SNAP-7941 using analytical HPLC.

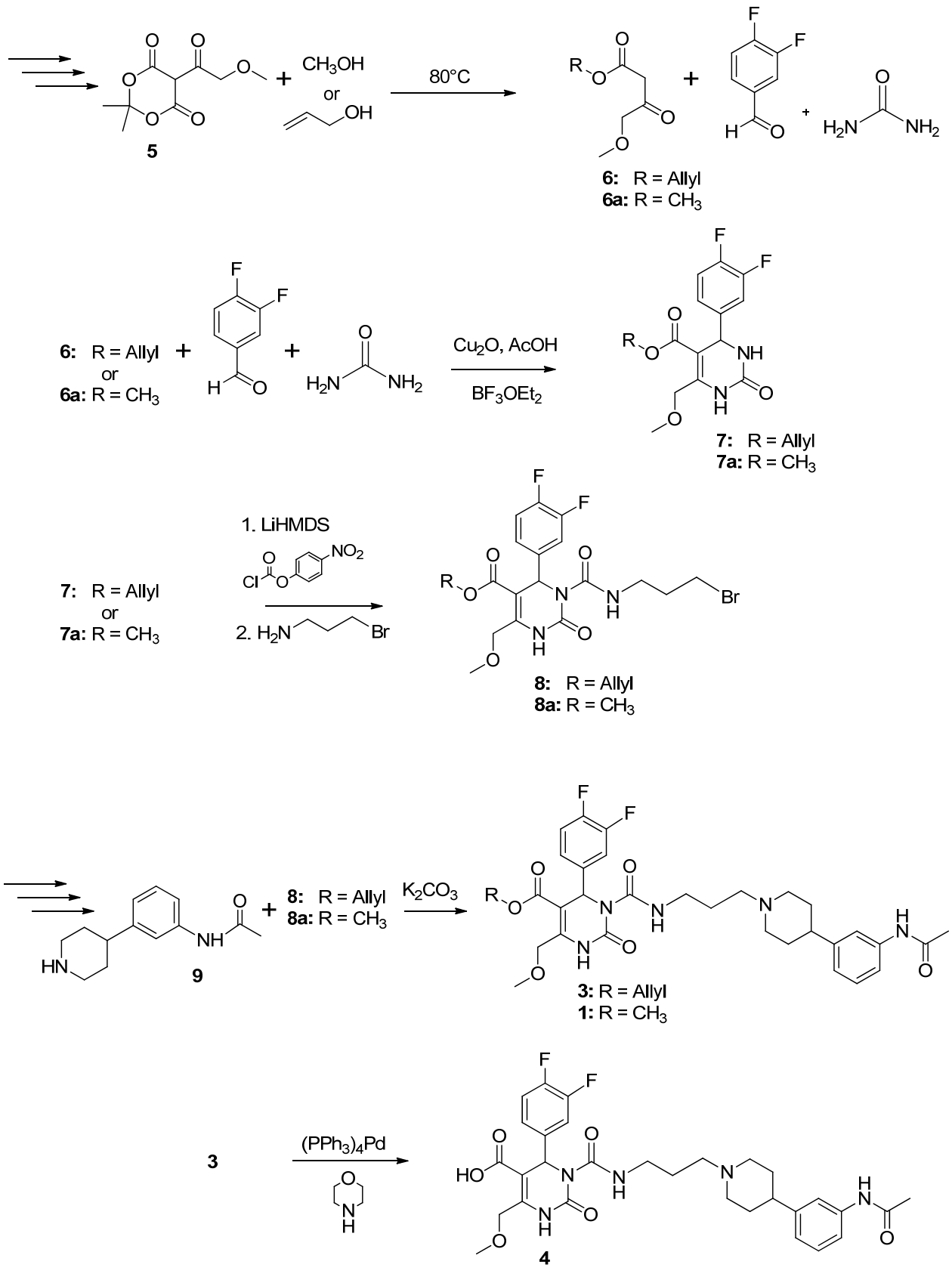

Scheme 1. Reaction scheme for the preparation of the precursor SNAP-acid (**4**) and the reference standard rac-SNAP-7941 (**1**).

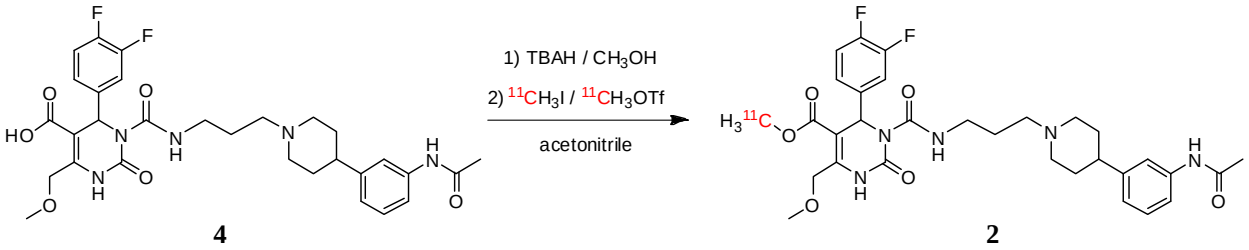

4 **2**

Scheme 2. Reaction scheme of the radiosynthesis of [^{11}C]SNAP-7941 (**2**).

Reaction temperature (°C)	≤ 25
Reaction time (min)	2
Amount of precursor (mg/mL)	2
Yield (GBq)[a]	2.9 ± 1.6
Yield (%)[b]	17.5 ± 3.6
Specific activity (GBq/µmoL)[a]	28.9 ± 9.4
Radiochemical purity (%)	> 99

[a] at end of synthesis (EOS).
[b] based on [^{11}C]CH_3OTf, corrected for decay.

Table 1. Optimum reaction conditions and outcome for large scale preparation of [^{11}C]SNAP-7941 (n=15).

2.3. Manuscript #2

[^{18}F]FE@SNAP - a new PET tracer for the melanin concentrating hormone receptor 1 (MCHR1): microfluidic and vessel-based approaches

Bioorganic & Medicinal Chemistry 2012; 20:5936-5940

Cécile Philippe[a,b,#], Johanna Ungersboeck[a,c,#], Eva Schirmer[d], Milica Zdravkovic[b], Lukas Nics[a,e], Markus Zeilinger[a], Karem Shanab[d], Rupert Lanzenberger[f], Georgios Karanikas[a], Helmut Spreitzer[d], Helmut Viernstein[b], Markus Mitterhauser[a,b,g], Wolfgang Wadsak[a,c]

[a]Radiochemistry and Biomarker Development Unit, Department of Nuclear Medicine, Medical University of Vienna, 1090 Vienna, Austria

[b]Department of Pharmaceutical Technology and Biopharmaceutics, University of Vienna, 1090 Vienna, Austria

[c]Department of Inorganic Chemistry, University of Vienna, 1090 Vienna, Austria

[d]Department of Drug and Natural Product Synthesis, University of Vienna, 1090 Vienna, Austria

[e]Department of Nutritional Sciences, University of Vienna, 1090 Vienna, Austria

[f]Department of Psychiatry and Psychotherapy, Medical University of Vienna, 1090 Vienna, Austria

[g]Hospital Pharmacy of the General Hospital of Vienna, 1090 Vienna, Austria

[#] These authors contributed equally to this manuscript.

Abstract

Changes in the expression of the melanin concentrating hormone receptor 1 (MCHR1) are involved in a variety of pathologies, especially obesity and anxiety disorders. To monitor these pathologies in-vivo positron emission tomography (PET) is a suitable method. After the successful radiosynthesis of [^{11}C]SNAP-7941 – the first PET-Tracer for the MCHR1, we aimed to synthesize its [^{18}F]fluoroethylated analogue: [^{18}F]FE@SNAP. Therefore, microfluidic and vessel-based approaches were tested. [^{18}F]fluoroethylation was conducted via various [^{18}F]fluoroalkylated synthons and direct [^{18}F]fluorination. Only the direct [^{18}F]fluorination of a tosylated

precursor using a flow-through microreactor was successful, affording [^{18}F]FE@SNAP in 44.3 ± 2.6%.

Keywords: MCHR1; Fluorine-18; PET; Microfluidic; SNAP-7941; Radioligand

1. Introduction

Melanin concentrating hormone (MCH) is a cyclic neuropeptide originally isolated from the salmon pituitary gland as a hormone responsible for skin pigmentation in teleost fish.[1] In mammals, MCH is predominantly expressed in the lateral hypothalamus and zona incerta,[2,3] but is also found in peripheral organs and tissues, such as the pancreas,[4] colonic epithelial cells[5] or adipocytes.[6,7] It plays a key role in energy homeostasis, e.g. the control of food intake, body weight and metabolism.[8,9] Furthermore, it is involved in anxiety,[10-14] diabetes,[4] gut inflammation[5] and adiposity.[6,7] The biological function of MCH is mediated by two G-protein coupled receptors, MCH receptor 1 and 2 (MCHR1[15-18] and MCHR2[19-22]). The widespread distribution of MCH and its receptors and the involvement in a variety of pathologies makes the MCH system interesting as a target to treat human disorders.

Several MCHR1 antagonists were presented in the last decade; some of them have entered clinical trials for the treatment of obesity,[23] some are in discussion of becoming anti-diabetic drugs.[24] However, to enable confidence in preclinical to clinical translation of central MCHR1 pharmacology, a suitable positron emission tomography (PET) tracer needs to be developed. Borowsky et al.[25] presented the evaluation of the very potent MCHR1 antagonist SNAP-7941 ((+)-methyl (4S)-3-{[(3-{4-[3-(acetylamino)phenyl]-1-piperidinyl}propyl)amino]carbonyl}-4-(3,4-difluorophenyl)-6-(methoxymethyl)-2-oxo-1,2,3,4-tetrahydro-5-pyrimidinecarboxylate hydrochloride, **1,** Fig. 1) (K_d = 0.18 nM, evaluated on Cos-7 cells expressing the human MCHR1 (hMCHR1)).[25] We previously reported the successful radiosynthesis of its radiolabelled analogue, [^{11}C]SNAP-7941 – the first PET tracer for the MCHR1.[26] Due to the practical advantages of the longer-lived radioisotope ^{18}F ($t_{1/2}$=110 min) instead of ^{11}C ($t_{1/2}$=20 min) and the comparable

stability of methyl- and fluoroethylesters,[27] we aimed to synthesize a [18F]fluoroethylated analogue: [18F]FE@SNAP (**2**, Fig. 1). We performed preliminary stability tests by incubation in human plasma at 37°C which showed almost no degradation (<5%) within 120 minutes; and incubation with carboxyl esterase in a standard assay revealed only 20% cleavage within 6 hours. Additionally, in preliminary binding experiments on CHO-hMCHR1 cell membranes, FE@SNAP evinced similar binding affinity as the parent compound SNAP-7941 (K_d = 0.18 nM). In general, 18F-fluoroalkyl radiolabels can be introduced using either a direct [18F]fluorination of a suitable precursor-compound (already containing a leaving group at the alkyl side chain) or via two step labelling reaction using an 18F-fluoroalkylating synthon. Even for flow-through microreactor procedures both synthesis strategies have already been reported for various radiotracer syntheses: For example, direct radio-fluorinations were presented for 2-[18F]FDG,[28-31] [18F]fallypride,[32] [18F]annexin,[29,31] and N-[18F]fluoroacetyl-N-(2,5-dimethoxybenzyl)-2-phenoxyaniline;[33] furthermore, the [18F]fluoroethylation of carboxylic acids,[34] [18F]fluoroalkylation of diverse [18F]fluorocholine derivatives using either [18F]fluoroethyl tosylate or [18F]fluoropropyl tosylate[35,36] and the syntheses of [18F]fluoroarenes from diaryliodonium salts[37] have been presented.

The aim of this work was the preparation of [18F]FE@SNAP in sufficient amounts for future pre-clinical applications. For this purpose, vessel-based as well as microfluidic approaches were conducted, starting from two different precursors: SNAP-acid (**3**, Fig. 1) (for the two step [18F]fluoroalkylation) and Tos@SNAP (**4**, Fig. 1) (for direct radiolabelling).

2. Results and discussion

2.1. General

TLC Rf-values were 0.00-0.02 for [18F]fluoride and 0.63-0.69 for [18F]FE@SNAP. A typical radio-TLC sample chromatogram is presented in Figure 2. HPLC retention times were 2.3-2.6 min (k'=0.5-0.7) for Tos@SNAP and 5.1-5.9 min (k'=2.4-2.9) for [18F]FE@SNAP. All values were verified by inactive reference substances. The TLC R_f-values of the two additional, unknown radio-labelled side products were 0.76-

0.82 and 0.87-0.93, respectively; HPLC retention times were 3.6-4.3 min (k'=1.4-1.7) and 6.9-7.7 min (k'=3.6-4.1).

2.2. Vessel-based preparation

The production of all [^{18}F]fluoroalkylation agents ([^{18}F]BFE, [^{18}F]FEtTos, [^{18}F]FEtTf) was successful: 2.9 ± 0.9 GBq [^{18}F]BFE (23.1 ± 10.4% EOB), 0.3 ± 0.1 GBq [^{18}F]FEtTos (24.0 ± 0.7% EOB) and 0.3 ± 0.2 GBq [^{18}F]FEtTf (19.2 ± 9.6% EOB) were achieved. However, the [^{18}F]fluoroethylation of SNAP-acid via these synthons did not succeed. No radiochemical incorporation was observed regardless of the conditions applied (reaction temperature, reaction time, solvent, synthon). Furthermore, the direct fluorination of Tos@SNAP in the conventional approach was not successful, either. Again, no radiochemical incorporation was observed.

2.3. Microfluidic preparation

Radiolabelling of the [^{18}F]fluoroalkylation agent [^{18}F]FEtTos was in accordance to the literature.[35,36] However, the second step - the [^{18}F]fluoroethylation of SNAP-acid - was not successful using this approach.

The direct [^{18}F]fluorination via the microfluidic system finally resulted in the production of [^{18}F]FE@SNAP. The RCIY was increasing with higher reaction temperatures and increasing amounts of precursor. Highest RCIYs were obtained at 170°C using 4 mg/mL of precursor in the reaction mixture (43.8 ± 2.2%). Further raise of precursor amount did not improve synthetic outcome (Fig. 3). Reasonable radiolabelling yields and no formation of any side products could be observed at 100°C. At 140°C radiochemical incorporation was increased but two unknown radiolabelled side products were formed additionally. When increasing the reaction temperature up to 170°C side product formation was even more pronounced. At the same time degradation of precursor with increasing temperature could be observed in the UV channel of the HPLC chromatogram. This degradation also increased with slow flow rates. Therefore, the dependency upon the flow rate was determined both at 140°C and 170°C (7.5 mg/mL Tos@SNAP, Fig. 4). At 170°C the RCIY increased with increasing flow rates. The inverse trend was observed at 140°C. RCIYs decreased with increasing flow rates. However, best RCIYs were observed

using fast flow rates up to 150 µL/min at 170°C. In this set-up the residence time within the heated microreactor (15.6 µL) was only 6.24 seconds. This time was sufficient to radiolabel the tosylated precursor and short enough to avoid extensive precursor degradation. RCIY of [^{18}F]FE@SNAP was increased from 25.1 ± 1.8% (20 µL/min) to 44.3 ± 2.6% (150 µL/min) applying 7.5 mg/mL precursor at 170°C.

Due to previous findings,[38] the reaction volume was examined as additional parameter. No "bolus volume effect" could be observed for this set-up. For reactions using 3 mg/mL Tos@SNAP at 170°C and a flow rate of 150 µL/min, RCIY was similar for small-scale reactions (20µL) and for enlarged reaction boluses (300µL): 30.5 ± 8.9%.

All these results led to the optimum reaction conditions for the radiochemical preparation of [^{18}F]FE@SNAP summarized in Table 1.

3. Conclusion

[^{18}F]FE@SNAP could not be synthesized in any vessel-based approach neither using direct radio-fluorination of the tosylated precursor nor through the coupling of a [^{18}F]fluoroalkylation agent to SNAP-acid. Once again, flow-through microreactor technology was demonstrated to be a valuable addition in the portfolio of radiolabelling techniques for the preparation of new PET tracers. Solely, a microfluidic procedure enabled the radiosynthesis of [^{18}F]FE@SNAP. Further experiments comprising an up-scaling, purification and formulation of [^{18}F]FE@SNAP will enable its use in preclinical investigations.

4. Experimental section

4.1. General

Chemicals and solvents were purchased from Merck (Darmstadt, Germany) and Sigma-Aldrich (Vienna, Austria). All reagents were at least of analytical grade and used without purification. [^{18}F]fluoride was produced via the ^{18}O(p,n)^{18}F reaction in a GE PETtrace cyclotron (16.5-MeV protons; GE Medical Systems, Uppsala,

Sweden). $H_2{}^{18}O$ (HYOX18; > 98%) was purchased from Rotem Europe (Leipzig, Germany). Anion-exchange cartridges (PS-HCO_3) for [^{18}F]fluoride trapping were obtained from Macherey-Nagel (Dueren, Germany). 2-bromoethyl triflate[39] (BETfO) and ethylene glycol bis triflate[40] were synthesized in cooperation with the Department of Drug and Natural Product Synthesis of the University of Vienna (Austria). Alumina cartridges (Sep-Pak® Light Alum N) were purchased from Waters (Waters® Associates Milford, MA, USA). For conventional small-scale preparations, the reactions were carried out in Wheaton 1.0 mL v-vials (clear glass) assembled with TFE/silicone septa. Microfluidic reactions were carried out within an Advion NanoTek® unit (Ithaca, NY, USA) comprising a concentrator unit (CE) and a liquid flow reaction unit (LF) with dedicated control software (Advion, version 1.4). The set-up is illustrated in Figure 5. Microreactors were made of fused silica tubing (inner diameter 0.1 µm; length 2.0 m), wound-up and held in a brass ring filled with a thermoresistant polymer to hold the tubing in its place. Drying and collecting v-vials (3.0 and 5.0 mL, clear glass) were obtained from Alltech (Deerfield, IL, USA). Radiochemical incorporation yields (RCIYs) were determined by analysing the reaction mixtures by radio-analytical thin-layer chromatography (radio-TLC) and analytical high performance liquid chromatography (HPLC). Radio-TLC was performed using silica gel 60 RP-18 $F_{254}S$ plates from Merck (Darmstadt, Germany) (mobile phase: acetonitrile/water 95/5 v/v). Analyses of radio-TLC plates were done using a Canberra-Packard Instant Imager (Perkin Elmer, Watford, UK). Analytical HPLC was performed using an Agilent system (Boeblingen, Germany) consisting of an autosampler 1100, a quaternary pump 1200 (flow: 1 mL/min), a diode array detector 1200 (operated at 255nm) and a lead-shielded NaI-radiodedector (Raytest Isotopenmessgeräte GmbH, Straubenhardt, Germany). HPLC column (Chromolith® Performance RP-18e; 100-4.6 mm) was purchased from Merck (Darmstadt, Germany). HPLC mobile phase consisted of (water/acetic acid 97.5/2.5 v/v; 2.5 g/L ammonium acetate; pH 3.5)/acetonitrile 70/30 v/v.

4.2. Preparation of precursor compounds and reference standard

Syntheses of precursor compounds (SNAP-acid[26] and Tos@SNAP[41,42]) and reference standard (FE@SNAP[43]) were performed in cooperation with the Department of

Drug and Natural Product Synthesis of the University of Vienna (Austria). ^{1}H- and ^{13}C-NMR data and spectra as well as ^{19}F-NMR, MS, HRMS and IR data, are available as supplementary data.

4.3. Azeotropic drying

Azeotropic drying of cyclotron produced [^{18}F]fluoride was always performed within the concentrator unit of the Advion NanoTek® synthesizer using a programmed procedure, in order to avoid differences between manual and automatic azeotropic drying. N.C.A [^{18}F]fluoride (1.5-31.7 GBq) was trapped on to an anion exchange cartridge (PS-HCO3) and released with a solution containing Kryptofix 2.2.2 (4,7,13,16,21,24-hexaoxa-1,10-diaza-bi-cyclo[8.8.8]hexacosane; 10 mg, 26.6 µmol) and potassium carbonate (2.25 mg, 16.6 µmol) in acetontrile/water (70/30 v/v; V=0.5 mL). Iterative azeotropic drying was performed at 110°C by addition of 3 times 300 µL of dry acetonitrile.

4.4. Vessel-based preparation

4.4.1. Fluoroethylation via 1-bromo-2 [^{18}F]fluoroethane ([^{18}F]BFE)

[^{18}F]BFE was produced according to Zuhayra et al.[44] Briefly, to the dried [^{18}F]fluoride-aminopolyether a mixture of 30 µL BETfO and 500 µL 1,2-dichlorobenzene (o-DCB) was added. After heating at 100°C for 10 min, [^{18}F]BFE was distilled at 130°C under helium flow into the respective solvent (DMF, DMSO and 2-butanone). The precursor SNAP-acid (4 mg/mL) was activated by adding an equimolar amount of tetrabutylammonium hydroxide (TBAH) and dissolved in the respective solvent. The [^{18}F]BFE solution was added to the precursor solution (1:1) and the reaction mixture was heated at 75-140°C for 10-20 min.

4.4.2. Fluoroethylation via [^{18}F]fluoroethyl tosylate ([^{18}F]FEtTos)

Ethylene glycol di-p-tosylate (9.25 mg/mL in acetonitrile) was added to the dried [^{18}F]fluoride-aminopolyether and heated at 85°C for 15 min. The resulted [^{18}F]FEtTos was added to SNAP-acid (activated with TBAH, 4 mg/mL in acetonitrile) (1:1) and the reaction mixture was heated at 75°C for 10-30 min.

4.4.3. Fluoroethylation via [^{18}F]fluoroethyl triflate ([^{18}F]FEtTf)

[^{18}F]FEtTf was produced according to Kiesewetter et al.[40] Briefly, a solution of ethylene glycol bis triflate (1.0 mg in 100 µL acetonitrile) was added to the dried [^{18}F]fluoride-aminopolyether. After heating at 125°C for 1 min, the solution was cooled in an ice bath and triflic anhydride (5 µL) was added. The solution was loaded onto an alumina cartridge and [^{18}F]FEtTf was eluted with acetonitrile (500 µL). The solution of [^{18}F]FEtTf was added to SNAP-acid (activated with TBAH, 4 mg/mL in acetonitrile) (1:1) and heated at 75°C for 10-30 min.

4.4.4. Direct [^{18}F]fluorination

The tosylated precursor Tos@SNAP (2 mg/mL) was dissolved in acetonitrile and added to the dried [^{18}F]fluoride-aminopolyether. The reaction mixture was heated at 75°C for 10-90 min.

4.5. Microfluidic preparation

4.5.1. Fluoroethylation via [^{18}F]fluoroethyl tosylate ([^{18}F]FEtTos)

Reaction educts were dissolved in acetonitrile and drawn into the respective loops (loop 1: ethylene glycol di-p-tosylate (10 mg/mL); loop 2: SNAP-acid (activated with TBAH, 20 mg/mL); loop 3: dried [^{18}F]fluoride-aminopolyether in 500 µL acetonitrile). Before starting the experiments, transfer-lines were filled with the solutions from the storage loops and the reactors were finally swept with the reaction solvent via pump 3 (Fig. 2). The synthesis was carried out within the Advion NanoTek® using the "discovery mode" for two step reactions. The conversion to [^{18}F]FEtTos (first reaction) was performed by pushing the previously filled solutions simultaneously from loop 1 and 3 through the first temperature controlled (180°C) flow-through microreactor (flow rate: 30-50 µL/min). In a second phase the [^{18}F]FEtTos-mixture was swept out of the reactor through the storage line towards the other reactor. The second reaction starts when the [^{18}F]FEtTos-mixture and the precursor solution (loop 2) are pushed through the second microreactor (100-180°C) with defined velocity (20-150 µL/min) followed by a final sweeping where the reaction mixture is finally flushed out of the system into a collecting vial filled with 200 µL of solvent. Total reaction bolus volumes between 28 µL and 90 µL (7+7+14 and 15+15+60 µL) were tested.

4.5.2. Direct [^{18}F]fluorination

Dried [^{18}F]fluoride-aminopolyether dissolved in 500 µL acetonitrile and Tos@SNAP (3-10 mg/mL in acetonitrile) precursor solution were drawn and stored in the respective loops of pumps 1 and 3 of the LF unit. Before starting the experiments, transfer lines 1 and 3 were filled with the solutions from the storage loops and the reactor was swept with the reaction solvent via pump 3. Optimal reaction conditions were determined using the pre-installed "discovery" mode for one step reactions: small volumes (5-200 µL) of the previously filled solutions were simultaneously pushed through the temperature-controlled reactor (100°C-200°C) with defined overall flow rates (60-150 µL/min). Subsequently, the crude product solution was swept out of the micro reactor with a defined volume of 200 µL of acetonitrile into collection vials.

4.6. Statistical analyses

Quantitative data (both in text and figures) are expressed as arithmetic mean ± standard deviation. If not stated otherwise all experiments were performed in triplicates.

Acknowledgement

This research was part of an ongoing study, funded by the Austrian Science Fund (FWF P20977-B09; P.I.: M. Mitterhauser).

References

1. Kawauchi, H.; Kawazoe, I.; Tsubokawa, M.; Kishida, M.; Baker, B. I. *Nature* **1983**, *305*, 321.

2. Bittencourt, J. C.; Presse, F.; Arias, C.; Peto, C.; Vaughan, J.; Nahon, J. L.; Vale, W.; Sawchenko, P. E. *J. Comp. Neurol.* **1992**, *319*, 218.

3. Casatti, C. A.; Elias, C. F.; Sita, L. V.; Frigo, L.; Furlani, V. C. G.; Bauer, J. A.; Bittencourt, J. C. *Neuroscience* **2002**, *115*, 899.

4. Tadayyon, M.; Welters, H. J.; Haynes, A. C.; Cluderay, J. E.; Hervieu, G. *Biochem. Biophys. Res. Commun.* **2000**, *275*, 709.

5. Kokkotou, E.; Moss, A. C.; Torres, D.; Karagiannides, I.; Cheifetz, A.; Liu, S.; O'Brian, M.; Maratos-Flier, E.; Pothoulakis, C. *Proc. Natl. Acad. Sci. USA* **2008**, *105*, 10613.

6. Bradley, R. L.; Kokkotou, E. G.; Maratos-Flier, E.; Cheatham, B. *Diabetes* **2000**, *49*, 1073.

7. Bradley, R. L.; Mansfield, J. P.; Maratos-Flier, E.; Cheatham, B. *Am. J. Physiol. Endocrinol. Metab.* **2002**, *283*, E584.

8. Marsh, D. J.; Weingarth, D. T.; Novi, D. E.; Chen, H. Y.; Turmbauer, M. E.; Chen, A. S.; Guan, X. M.; Jiang, M. M.; Feng, Y.; Camacho, R. E.; Shen, Z.; Frazier, E. G.; Yu, H.; Metzger, J. M.; Kuca, S. J.; Shearman, L. P.; Gopal-Truter, S.; MacNeil, D. J.; Strack, A. M.; MacIntyre, D. E.; Van der Ploeg, L. H. T.; Qian, S. *Proc. Natl. Acad. Sci. USA* **2002**, *99*, 3240.

9. Ito, M.; Gomori, A.; Ishihara, A.; Oda, Z.; Mashiko, S.; Matsushita, H.; Yumoto, M.; Ito, M.; Sano, H.; Tokita, S.; Moriya, M.; Iwaasa, H.; Kanatani, A. *Am. J. Physiol. Endocrinol. Metab.* **2003**, *284*, E940.

10. Monzón, M. E.; De Barioglio, S. R. *Physiol. Behav.* **1999**, *67*, 813.

11. Kela, J.; Salmi, P.; Rimondini-Giorgini, R.; Heilig, M.; Wahlestedt, C. *Regulatory Peptides* **2003**, *114*, 109.

12. Smith, D. G.; Davis, R. J.; Rorick-Kehn, L.; Morin, M.; Witkin, J. M., McKenzie, D. L.; Nomikos, G. G; Gehlert, D. R. *Neuropsychopharmacology* **2006**, *31*, 1135.

13. Roy, M.; David, N. K.; Danao, J. V.; Baribault, H.; Tian, H.; Giorgetti, M. *Neuropsychopharmacology* **2006**, *31*, 112.

14. Roy, M.; David, N.; Cueva, M.; Giorgetti, M. *Biol. Psychiatry* **2007**, *61*, 174.

15. Saito, Y.; Nothacker, H. P.; Wang, Z.; Lin, S. H.; Leslie, F.; Civelli, O. *Nature* **1999**, *400*, 265.

16. Shimomura, Y.; Mori, M.; Sugo, T.; Ishibashi, Y.; Abe, M.; Kurokawa, T.; Onda, H.; Nishimura, O.; Sumino, Y.; Fujino, M. *Biochem. Biophys. Res. Commun.* **1999**, *261*, 622.

17. Chambers, J.; Ames, R. S.; Bergsma, D.; Muir, A.; Fitzgerald, L. R.; Hervieu, G.; Dytko, G. M.; Foley, J. J.; Martin, J.; Liu, W. S.; Park, J.; Ellis, C.; Ganguly, S.; Konchar, S.; Cluderay, J.; Leslie, R.; Wilson, S.; Sarau, H. M. *Nature* **1999**, *400*, 261.

18. Lembo, P. M. C.; Grazzini, E.; Cao, J.; Hubatsch, D. A.; Pelletier, M.; Hoffert, C.; St-Onge, S.; Pou, C.; Labreque, J.; Groblewski, T.; O'Donnell, D.; Payza, K.; Ahmad, S.; Walker, P. *Nat. Cell. Biol.* **1999**, *1*, 267.

19. Sailer, A. W.; Sano, H.; Zeng, Z.; McDonald, T. P.; Pan, J.; Pong, S. S.; Feighner, S. D.; Tan, C. P.; Fukami, T.; Iwaasa, H.; Hreniuk, D. L.; Morin, N. R.; Sadowski, S. J.; Ito, M.; Ito, M.; Bansal, A.; Ky, B.; Figueroa, D. J.; Jiang, Q.; Austin, C. P.; MacNeil, D. J.; Ishihara, A.; Ihara, M.; Kanatani, A.; Van der Ploeg, L. H. T.; Howard A. D.; Liu, Q. *Proc. Natl. Acad. Sci. USA* **2001**, *98*, 7564.

20. Hill, J.; Duckworth, M.; Murdock, P.; Rennie, G.; Sabido-David, C.; Ames, R. S.; Szekeres, P.; Wilson, S.; Bergsma, D. J.; Gloger, I. S.; Levy, D. S.; Chambers; J. K.; Muir, A. I. *J. Biol. Chem.* **2001**, *276*, 20125.

21. Wang, S.; Behan, J.; O'Neill, K.; Weig, B.; Fried, S.; Laz, T.; Bayne, M.; Gustafson, E.; Hawes, B. E. *J. Biol. Chem.* **2001**, *276*, 34664.

22. An, S.; Cutler, G.; Zhao, J. J.; Huang, S. G.; Tian, H.; Li, W.; Liang, L.; Rich, M.; Bakleh, A.; Du, J.; Chen, J. L.; Dai, K. *Proc. Natl. Acad. Sci. USA* **2001**, *98*, 7576.

23. Luthin, D. R. *Life Sciences* **2007**, *81*, 423.

24. Gattrell, W. T.; Sambrook Smith C. P.; Smith, A. J. *Bioorg. Med. Chem. Lett.* **2012**, *22*, 2464.

25. Borowsky, B.; Durkin, M. M.; Ogozalek, K.; Marzabadi, M. R.; DeLeon, J.; Lagu, B.; Heurich, R.; Lichtblau, H.; Shaposhnik, Z.; Daniewska, I.; Blackburn, T. P.; Branchek, T. A.; Gerald, C.; Vaysse, P. J.; Forray, C. *Nat. Med.* **2002**, *8*, 825.

26. Philippe, C.; Schirmer, E.; Mitterhauser, M.; Shanab, K.; Lanzenberger, R.; Karanikas, G.; Spreitzer, H.; Viernstein, H.; Wadsak, W. *Appl. Radiat. Isot.* **2012**; accepted.

27. Nics, L.; Haeusler, D.; Wadsak, W.; Wagner, K. H.; Dudczak, R.; Kletter, K.; Mitterhauser, M. *Nucl. Med. Biol.* **2011**, *38*, 13.

28. Lee, C. C.; Sui, G.; Elizarov, A.; Shu, C. J.; Shin, Y. S.; Dooley, A. N.; Huang, J.; Daridon, A.; Wyatt, P.; Stout, D.; Kolb, H. C.; Witte, O. N.; Satyamurthy, N.; Heath, J. R.; Phelps, M. E.; Quake, S. R.; Tseng, H. R. *Science* **2005**, *310*, 1793.

29. Gillies, J. M.; Prenant, C.; Chimon, G. N.; Smethurst, G. J.; Dekker, B.A.; Zweit, J. *Appl. Radiat. Isot.* **2006**, *64*, 333.

30. Steel, C.J.; O'Brien, A. T.; Luthra, S. K.; Brady, F. *J. Labelled. Compd. Radiopharm.* **2007**, *50*, 308.

31. Gillies, J. M.; Prenant, C.; Chimon, G. N.; Smethurst, G. J.; Perrie, W.; Hamblett, I.; Dekker, B.A.; Zweit, J. *Appl. Radiat. Isot.* **2006**, *64*, 325.

32. Lu, S.; Giamis, A. M.; Pike, V. W. *Curr. Radiopharm.* **2009**, *2*, 49.

33. Briard, E.; Zoghbi, S. S.; Simeon, F. G; Imaizumi, M.; Gourley, J. P.; Shetty, H. U.; Lu, S.; Fujita, M.; Innis, R. B.; Pike, V. W. *J. Med. Chem.* **2009**, *52*, 688.

34. Lu, S. Y.; Watts, P.; Chin, F. T.; Hong, J.; Musachio, J. L.; Briard, E.; Pike, V. W. *Lab on a chip* **2004**, *4*, 523.

35. Pascali, G.; Mazzone, G.; Saccomanni, G.; Manera, C.; Salvadori, P. A. *Nucl. Med. Biol.* **2010**, *37*, 547.

36. Pascali, G.; Nannavecchia, G.; Pitzianti, S.; Salvadori; P. A. *Nucl. Med. Biol.* **2011**, *38*, 637.

37. Chun, J. H.; Lu, S.; Lee, Y. S.; Pike, V. W. *J. Org. Chem.* **2010***, 75*, 3332.

38. Ungersboeck, J.; Richter, S.; Collier, L.; Mitterhauser, M.; Karanikas, G.; Lanzenberger, R.; Dudczak, R.; Wadsak, W. *Nucl. Med. Biol.* **2012**, in press (doi:10.1016/j.nucmedbio.2012.04.004).

39. Chi, D. Y.; Kilbourn, M. R.; Katzenellenbogen, J. A; Welch, M. J. J. Org. Chem. 1987, *52*, 658.

40. Kiesewetter, D. O.; Brücke, T.; Finn, R. D. *Appl. Radiat. Isot.* **1989**, *40*, 455.

41. Schirmer, E. EHEC 2010 - XXIVth European Colloquium on Heterocyclic Chemistry, August 23-27 **2010**, Vienna, Austria, book of abstracts, publ.: book-of-abstracts.com, H. Krebs, Gumpoldskirchen, Austria. ISBN: 978-3-9502992-0-5, PO-57.

42. Schirmer, E. PACCON 2010 - Pure and Applied Chemistry International Conference, January 21-23 **2010**, Ubon Ratchathani, Thailand, book of abstracts, ISBN: 978-974-523-221-1, ORC-PO-47.

43. Schirmer, E. JMMC 2011 - VII Joint Meeting on Medicinal Chemistry, Catania, Italy, June 30th-July 2nd **2011**, book of abstracts, 127, www.jmmc2011.it

44. Zuhayra, M.; Alfteimi, A.; Papp, L.; Lützen, U.; Lützen, A.; Von Forstner, C.; Meller, B.; Henze, E. *Bioorg. Med. Chem.* **2008**, *16*, 9121.

Captions

Figure 1. SNAP-7941 derivatives **1-4** (**1**: SNAP-7941; **2**: [^{18}F]FE@SNAP; **3**: SNAP-acid; **4**: Tos@SNAP).

Figure 2. Typical radio-TCL chromatogram of the crude reaction mixture (7.5 mg/mL, 170°C, 150 µL/min) with results after integration.

Figure 3. Dependency of the RCIY upon precursor concentration. Reactions were performed with a flow rate of 60 µL/min at 100°C, 140°C and 170°C. Values are decay-corrected and given as arithmetic means ± SD (n≥3). Error bars are depicted unidirectional for better visualization but represent deviations in both directions.

Figure 4. Influence of the overall flow rate on the RCIY. Reactions were conducted using 7.5 mg/mL Tos@SNAP in reaction mixture. Values are decay-corrected and given as arithmetic means ± SD (n≥3).

Figure 5. Schematic illustration of the set-up of the Advion NanoTek® system for two-step reactions.

Table 1. Optimum reaction conditions and outcome for the preparation of [^{18}F]FE@SNAP.

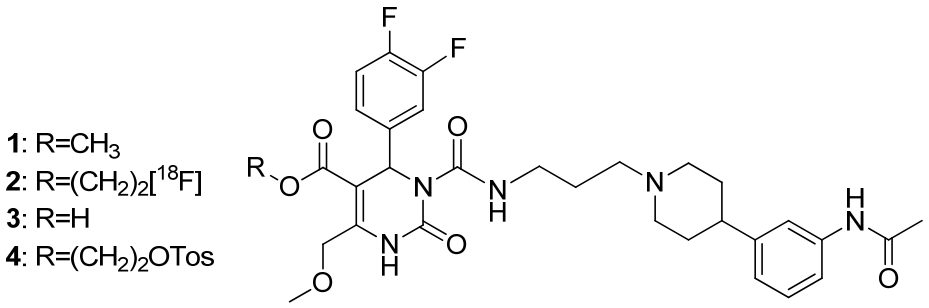

Figure 1. SNAP-7941 derivatives **1-4** (**1**: SNAP-7941; **2**: [^{18}F]FE@SNAP; **3**: SNAP-acid; **4**: Tos@SNAP).

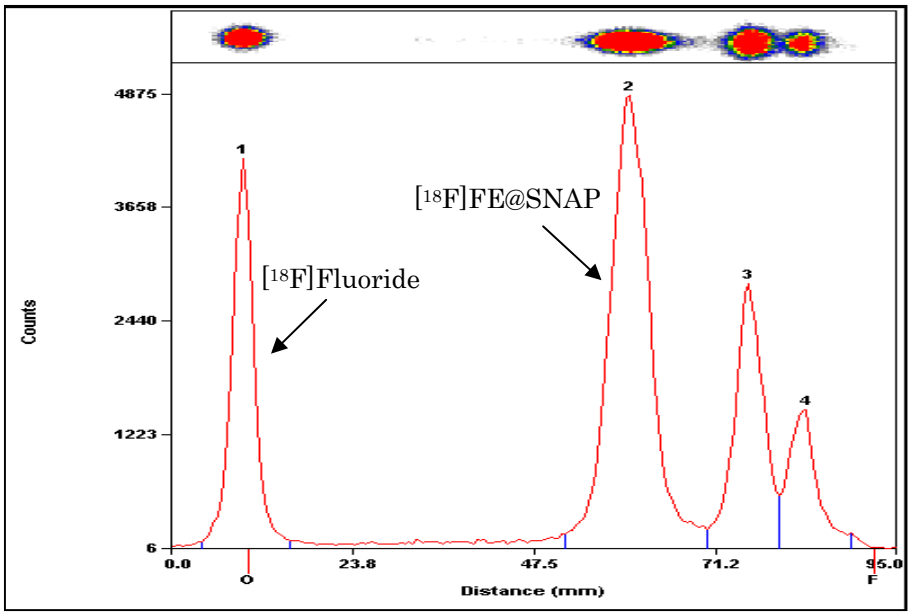

Figure 2. Typical radio-TCL chromatogram of the crude reaction mixture (7.5 mg/mL, 170°C, 150 µL/min) with results after integration.

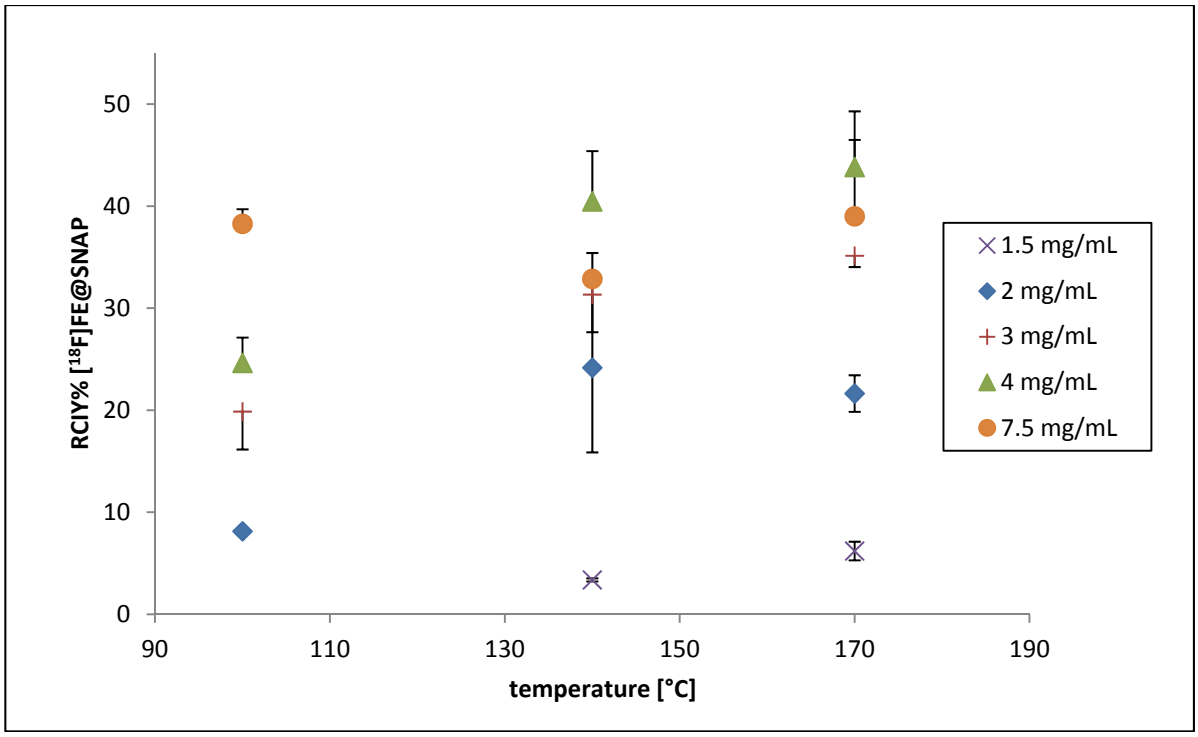

Figure 3. Dependency of the RCIY upon precursor concentration. Reactions were performed with a flow rate of 60 µL/min at 100°C, 140°C and 170°C. Values are decay-corrected and given as arithmetic means ± SD (n≥3). Error bars are depicted unidirectional for better visualization but represent deviations in both directions.

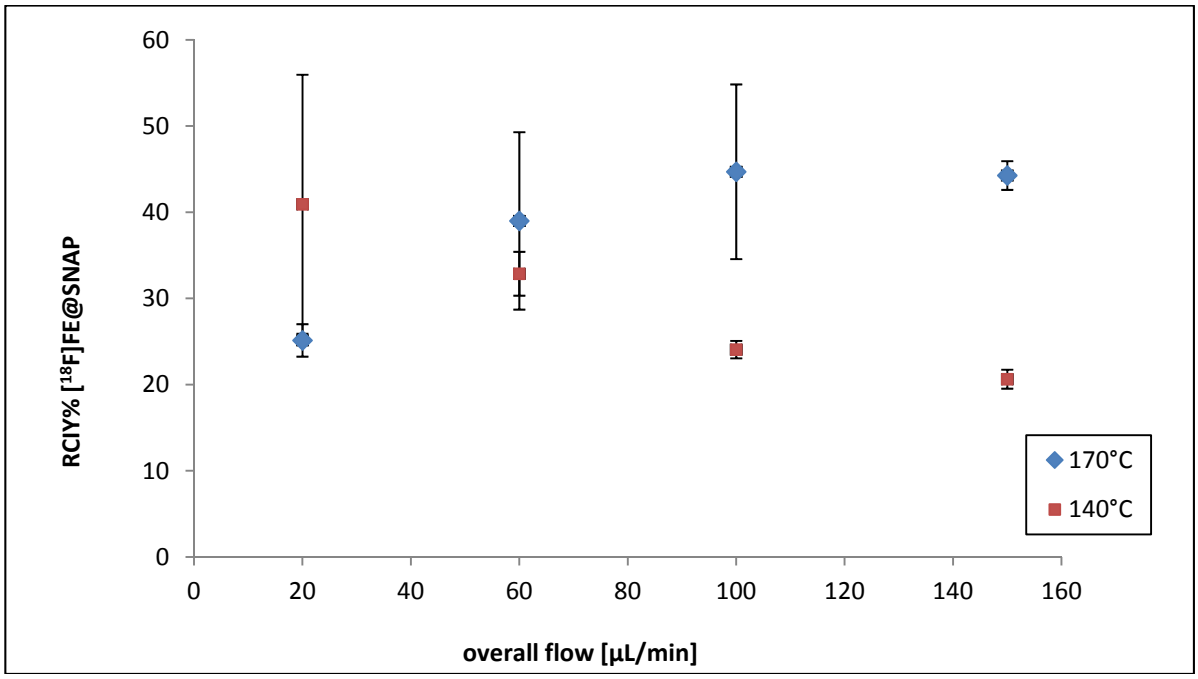

Figure 4. Influence of the overall flow rate on the RCIY. Reactions were conducted using 7.5 mg/mL Tos@SNAP in reaction mixture. Values are decay-corrected and given as arithmetic means ± SD (n≥3).

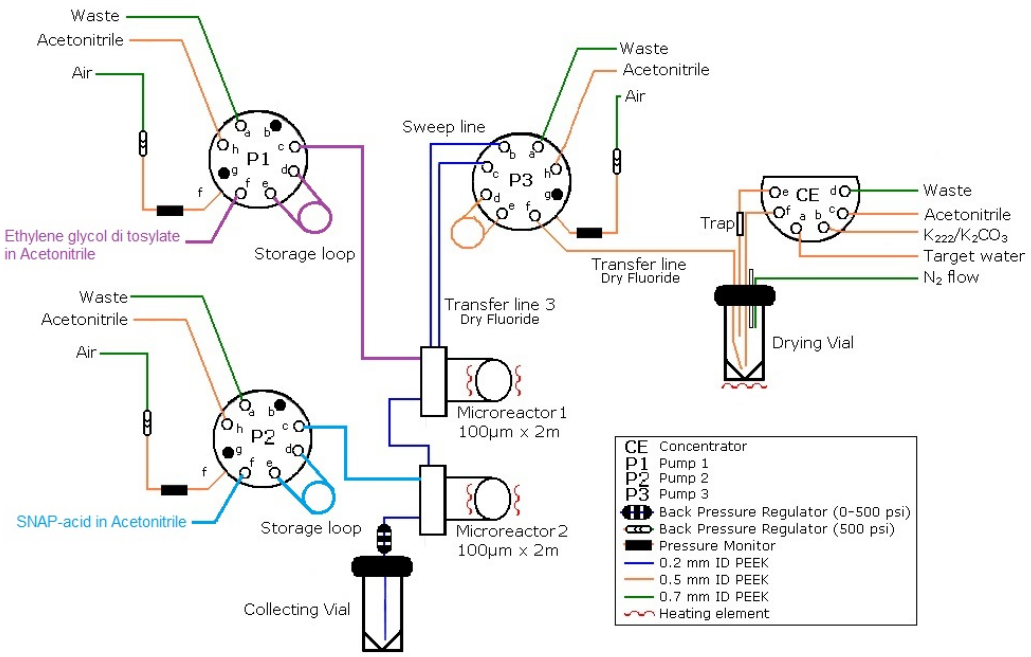

Figure 5. Schematic illustration of the set-up of the Advion NanoTek® system for two-step reactions.

Amount of precursor (mg/mL)	4
Reaction temperature (°C)	170
Flow rate (µL/min)	150
RCIY (%)	43.8 ± 2.2

Table 1. Optimum reaction conditions and outcome for the preparation of [^{18}F]FE@SNAP.

2.4. Manuscript #3

Preparation and first preclinical evaluation of [^{18}F]FE@SNAP: a potential PET tracer for the melanin concentrating hormone receptor 1 (MCHR1)

Scientia Pharmaceutica 2013, in press (doi:10.3797/scipharm.1306-02)

Cécile Philippe[1,2], Lukas Nics[1,3], Markus Zeilinger[1], Eva Schirmer[4], Helmut Spreitzer[4], Georgios Karanikas[1], Rupert Lanzenberger[5], Helmut Viernstein[2], Wolfgang Wadsak[1,6], Markus Mitterhauser[1,2,]

[1]Radiochemistry and Biomarker Development Unit, Department of Nuclear Medicine, Medical University of Vienna, 1090 Vienna, Austria

[2]Department of Pharmaceutical Technology and Biopharmaceutics, University of Vienna, 1090 Vienna, Austria

[3]Department of Nutritional Sciences, University of Vienna, 1090 Vienna, Austria

[4]Department of Drug and Natural Product Synthesis, University of Vienna, 1090 Vienna, Austria

[5]Department of Psychiatry and Psychotherapy, Medical University of Vienna, 1090 Vienna, Austria

[6]Department of Inorganic Chemistry, University of Vienna, 1090 Vienna, Austria

Abstract

The melanin concentrating hormone (MCH) system is a new target for the treatment of human disorders. Since the knowledge about the involvement of the MCH system in a variety of pathologies (obesity, diabetes, deregulation of metabolic feedback mechanism) bases on *in vitro* or preclinical studies, a suitable positron emission tomography (PET) tracer needs to be developed. We herein present the preparation and first preclinical evaluation of [^{18}F]FE@SNAP – a new PET tracer for the MCH receptor 1 (MCHR1).

The synthesis was performed using a microfluidic device. Preclinical evaluation included binding affinity, plasma stability, plasma free fraction, stability against the Cytochrom P-450 (CYP450) system using liver microsomes, stability against

carboxylesterase and methods to assess the penetration of the blood brain barrier (BBB) such as logD analysis and immobilized artificial membrane (IAM) chromatography.
374 ± 202 MBq [^{18}F]FE@SNAP were obtained after purification. The obtained K_d value of [^{18}F]FE@SNAP was 2.9 nM. [^{18}F]FE@SNAP evinced high stability against carboxylesterase, CYP450 enzymes and in human plasma. LogD (3.83) and IAM chromatography results (P_m=0.51) were in the same range as for known BBB penetrating compounds.
The synthesis of [^{18}F]FE@SNAP was reliable and successful. Due to high binding affinity and stability, [^{18}F]FE@SNAP is a promising tracer for the MCHR1.

Keywords: MCHR1; Fluorine-18; PET; SNAP-7941; Radioligand

Introduction

Melanin concentrating hormone (MCH) is a cyclic nonadeca-peptide, predominantly expressed in the lateral hypothalamus and zona incerta [1,2]. Beside, it is also found in peripheral organs and tissues, such as the pancreas [3], colonic epithelial cells [4] or adipocytes [5,6]. The biological function of MCH is mediated by two G-protein coupled receptors, MCH receptor 1 and 2 (MCHR1 [7-10] and MCHR2 [11-14]). MCH plays a key role in energy homeostasis, e.g. the control of food intake and body weight [15, 16]. Furthermore, it is involved in diabetes, gut inflammation and adiposity [3-6]. The widespread distribution of MCH and its receptors and the involvement in a variety of pathologies makes the MCH system an interesting new target for the treatment of human disorders. Several MCHR1 antagonists were presented in the last decade; some of them have been entered in clinical trials for the treatment of obesity [17] and some are in discussion of becoming anti-diabetic drugs [18]. However, to enable confidence in preclinical to clinical translation of MCHR1 pharmacology and for further studies on the involvement and distribution of the MCHR1 in energy homeostasis, a suitable positron emission tomography (PET) tracer needs to be developed. PET is a non-invasive technique to visualize molecular effects directly *in vivo*. Borowsky et al. [19] presented the evaluation of the very potent MCHR1 antagonist SNAP-7941 ((+)-methyl (4S)-3-{[(3-{4-[3-

(acetylamino)phenyl]-1-piperidinyl}propyl)amino]carbonyl}-4-(3,4-difluorophenyl)-6-(methoxymethyl)-2-oxo-1,2,3,4-tetrahydro-5-pyrimidinecarboxylate hydrochloride, **1**, Fig. 1) (K_d=0.18 nM, evaluated on Cos-7 cells expressing the human MCHR1 (hMCHR1) [19]). We previously reported the successful radiosyntheses of its radiolabelled analogues, [^{11}C]SNAP-7941 [20] (**2**, Fig. 1) and [^{18}F]FE@SNAP [21] (**3**, Fig. 1). The present work focuses on:

1. the up-scaling, purification and formulation of [^{18}F]FE@SNAP, and
2. on the *in vitro* assessment of its potential as a PET tracer through preclinical evaluation of its main biological and physicochemical properties.

Results

Radiochemistry

From a single synthesis in the microfluidic system 374 ± 202 MBq (range: 98-662 MBq) [^{18}F]FE@SNAP were obtained after purification (n=6). Radiochemical purity always exceeded 98%. 3.1 ± 0.5 µg FE@SNAP were detected in the final product solution. Precursor mass was below the limit of detection (< 0.5 µg/mL). Specific radioactivity was 24.8 ± 12 GBq/µmol at the end of synthesis (EOS). Residual solvent analysis revealed < 10 ppm acetonitrile and no other impurities. Osmolality was 222 ± 4 mosmol/kg and pH was 7.4 ± 0.2.

Biological evaluation

The binding experiments on the hMCHR1 revealed a K_d of 2.9 nM (n=2) for [^{18}F]FE@SNAP (Fig. 2). Preliminary competition binding experiments against [^{125}I]MCH on the hMCHR2 showed poor binding of FE@SNAP (K_i > 1000 nM).

The degradation of [^{18}F]FE@SNAP in human plasma (n=6) was 0.48 ± 0.5% after 0 min and 3.87 ± 3.9% after 120 min. In rat plasma (n=11) the degradation was 32.44 ± 33.5% initially and, after 120 min, [^{18}F]FE@SNAP was completely metabolized. The formation of a radioactive hydrophilic metabolite could be observed.

The plasma free fraction (f_1) of [^{18}F]FE@SNAP was 12.6 ± 0.2% in human plasma (n=3). Due to the fast metabolism of [^{18}F]FE@SNAP in rat plasma, it was not possible to determine f_1 in that medium.

The enzymatic degradation of [^{18}F]FE@SNAP by CYP450 after 60 min was 5.39 ± 1.6% using human liver microsomes (n=4) and 2.59 ± 1.8% using rat liver microsomes (n=4) (Fig. 3).
The Michaelis-Menten constant (K_m) of FE@SNAP was 347.3 µM and the limiting velocity (V_{max}) was 0.874 µM/min (Fig. 4).

Physicochemical parameters

The logD value of FE@SNAP was 3.83 ± 0.1 (n=3) and the value of the permeability through the membrane (P_m) was 0.51 ± 0.1(n=3). Preliminary experiments on the hMCHR2 showed poor binding of FE@SNAP (K_i > 1000 nM).

Discussion

Due to the low density of the MCH receptors in the human brain (B_{max}=5.8 ± 0.3 fmol/mg, [22]), a high binding affinity in a low nanomolar range of [^{18}F]FE@SNAP is mandatory. [^{18}F]FE@SNAP evinced a high affinity in saturation binding assays (K_d=2.9 nM). Moreover, FE@SNAP revealed high selectivity to the hMCHR1 (K_i on hMCHR2 > 1000 nM) in competition binding assays.
Starting from 29 ± 4 GBq [^{18}F]fluoride, 374 ± 202 MBq (2.6 ± 1.5% at the end of bombardment (EOB)) [^{18}F]FE@SNAP were obtained. 3 different circumstances led to this unexpected low radiochemical yield:
1. Due to incomplete priming of the solution into the loop to guarantee bubble-free filling (which is a systematic problem in the used microfluidic system), 16.1 ± 0.3% of activity remained in the concentrator vial of the microfluidic system after aceotropic drying and were not assessable for the synthesis [23].
2. Further 8.0 ± 3.5% remained in the lines and thereby were not accessible for the reaction [23].
3. The syntheses were performed in the discovery mode of the microfluidic system. There, approximately only half the amount of activity from the loop was used for the synthesis. The residual activity was kept as reserve in the loop to have the option for a second consecutive synthesis.

However, 374 ± 202 MBq [^{18}F]FE@SNAP were sufficient for any subsequent preclinical evaluation studies. Higher radiochemical yields will be achieved using the sequence mode of the microfluidic system.

The tested quality control parameters of the physiologically formulated [^{18}F]FE@SNAP solution were in accordance with the standards for human application. Specific activity was relatively low (24.8 ± 12 GBq/µmol). Higher specific activities are expected for future syntheses with higher yields. We note that no conversion of [^{18}F]FE@SNAP could be achieved using conventional synthesizing modules [21].

We evaluated the stability of [^{18}F]FE@SNAP not only in human but also in rat tissues (plasma, liver microsomes) to be prepared for species differences in future small animal PET experiments. [^{18}F]FE@SNAP was highly stable against human and rat liver microsomes (consisting of the multi enzyme complex Cytochrom P-450: 5.39 ± 1.6% (human) and 2.59 ± 1.8% (rat) decomposition after 60 min) and in human plasma (only 3.87 ± 3.9% metabolism after 120 min). In contrast, [^{18}F]FE@SNAP was completely metabolized in rat plasma within 120 min.

The amount of unbound (free) [^{18}F]FE@SNAP (f_1=12.6 ± 0.2%) in the human plasma should be sufficient for potential future clinical PET-studies targeting the brain. For comparison: the $5HT_{1A}$ ligand [carbonyl-^{11}C]WAY-100635 has a plasma free fraction of 5.8 ± 0.2% [24].

Porcine carboxylesterase was used to assess MMK, due to its wide use as biochemical model for in vitro studies [25]. With a K_m of 347.3 µM, FE@SNAP showed again very high stability.

For prediction of blood brain barrier (BBB) penetration the lipohilicity expressed as logD was measured in a first step. Since logP/logD values were shown to be poor predictors for BBB penetration [26], immobilized artificial membrane (IAM) chromatography was additionally performed. Under the modified conditions from Tavares et al. [27] FE@SNAP (P_m=0.51) is situated well in between of ß-CIT (P_m=0.31) and DASB (P_m=1.23) – two known BBB penetrating compounds. Therefore, considering only the passive diffusion, a penetration through the BBB seems possible.

Compared to [^{11}C]SNAP-7941, which we evaluated previously [34], [^{18}F]FE@SNAP was only accessible via microfluidic chemistry. Both tracers evinced a high binding affinity and selectivity to the hMCHR1 and a high metabolic stability in human plasma and against liver microsomes and carboxylesterase. The rapid enzymatic degradation in rat plasma was also observed with [^{11}C]SNAP-7941. These similarities confirm the analogy of methyl- and fluoroethylesters described by Nics et al. [32]. The logD and P_m values of both tracers were similar too. Summing up, [^{18}F]FE@SNAP is comparable to [^{11}C]SNAP-7941 in its biological behaviour with the advantage of the longer-lived radioisotope ^{18}F ($t_{1/2}$=110 min) instead of ^{11}C ($t_{1/2}$=20 min).

Conclusion

The synthesis of [^{18}F]FE@SNAP yielded sufficient amounts (374 ± 202 MBq) for subsequent preclinical evaluations. Our main criteria to pursuit the evaluation of [^{18}F]FE@SNAP as a PET tracer for the MCHR1 were:

- a high binding affinity to the MCHR1 in a low nanomolar range,
- high metabolic stability to assure enough intact tracer for visualization of MCHR1 specific tissues and
- reasonable lipophilicity to expect BBB penetration.

FE@SNAP binds to hMCHR1 in a nanomolar range (K_d=2.9 nM) and is highly selective to this receptor subtype. It showed very high stability against porcine carboxylesterase, the Cytochrom P-450 fraction of human and rat liver microsomes and in human plasma. Furthermore, the human plasma free fraction (f_1=12.6 ± 0.2%) is high enough for potential brain imaging. The fact, that decomposition in rat plasma is complete within 120 min, has to be considered for further preclinical studies in rats. As IAM chromatography experiments showed comparable behavior to known BBB penetrating compounds, passive BBB penetration is possible. Collectively, [^{18}F]FE@SNAP is a promising tracer for the MCHR1 and further preclinical evaluation steps (e.g. autoradiography and small-animal PET) will elucidate its potential.

Methods

General

Materials

[^{18}F]fluoride was produced via the $^{18}O(p,n)^{18}F$ reaction in a GE PETtrace cyclotron (16.5-MeV protons; GE Medical Systems, Uppsala, Sweden). $H_2{}^{18}O$ (HYOX18; > 98%) was purchased from Rotem Europe (Leipzig, Germany). Typical beam currents were 48-52 μA and the irradiation was stopped as soon as the desired activity level was reached (approx. 25-30 GBq). Anion-exchange cartridges (PS-HCO_3) for [^{18}F]fluoride trapping were obtained from Macherey-Nagel (Dueren, Germany). The precursor compound (Tos@SNAP; **4**, Fig. 1)) and the reference standard (FE@SNAP) were synthesized in cooperation with the Department of Drug and Natural Product Synthesis of the University of Vienna (Austria) [28, 29]. Solid phase extraction (SPE) cartridges SepPak® C18-plus and Oasis HLB 6cc Vac (200 mg) were purchased from Waters (Waters® Associates, Milford, MA, USA). Sterile water Ecotainer® and 0.9% saline solution were purchased from B. Braun (Melsungen, Germany). 3% saline solution was obtained from a local pharmacy (Landesapotheke Salzburg, Austria). 125 mM phosphate buffer was prepared by dissolving 0.224g sodium dihydrogenphosphate-monohydrate and 1.935g disodiumhydrogenphosphate-dihydrate (both from Merck, Darmstadt, Germany) in 100 mL sterile water. Phosphate buffered saline (PBS) concentrate (10:1) was obtained from Morphisto (Frankfurt, Germany). NADPH regenerating system solution-A and solution-B were obtained from BD Biosciences (Bedford, MA, USA). Acetonitrile, acetic acid, tetrahydrofuran (THF) anhydrous, methanol, ethylendiaminetetraacetic acid (EDTA), bacitracin, bovine serum albumin and porcine liver carboxylesterase (EC 3.1.1.1) were purchased from Sigma Aldrich (Vienna, Austria). Ammonium acetate, acetonitrile (for DNA synthesis, ≤ 10 ppm H_2O), Krypotofix 2.2.2, K_2CO_3, $MgCl_2$, Tris(hydroxymethyl)-aminomethane (Tris), triphenylene, toluol and ethanol were purchased from Merck (Darmstadt, Germany). Pooled human liver microsomes (Lot No. 34689), pooled male rat liver mircosomes (Lot No. 85157) and pooled female rat liver microsomes (Lot No. 59232) (both from Sprague Dawley rats) were purchased from BD Biosciences (Woburn, MA, USA). The male and female rat liver microsomes were homogenized. Pooled

lithium-heparinised human plasma (No. IPLA-N) and pooled lithium-heparinised rat plasma (No. IRT-N) were purchased from Innovative Research (Novi, MI, USA). Centrifugal Filter Units (Centrifree®-30K) were purchased from Merck Millipore (Tullagreen, Ireland). [^{125}I]MCH and CHO-K1 cell membranes expressing the hMCHR1/hMCHR2 were purchased from PerkinElmer (Waltham, MA, USA). The vials for the binding affinity assay were purchased from Beckman Coulter Inc. (Brea, CA, USA; Bio-Vial™, 4 mL, 14 × 55 mm) and from Seton Scientific (Petaluma, CA, USA; Open-Top Centrifuge Tubes Polyclear, 13 × 64 mm). Semi-preparative high-performance liquid chromatography (HPLC) column (Chromolith® SemiPrep RP-18e; 100-4.6 mm), analytical HPLC column (LiChroCART® 250-4 mm) and the column for metabolic stability testing (Chromolith® Performance RP-18e; 100-4.6 mm precolumn: Chromolith® Guard Cartridge RP-18e; 5-4.6 mm) were purchased from Merck (Darmstadt, Germany). Gas chromatography capillary column (forte GC Capillary Column ID-BP20; 12 m × 0.22 mm × 0.25 µm) was purchased from SGE Analytical Science Pty. Ltd. (Victoria, Autralia). IAM (immobilized artificial membrane) chromatography was performed using a IAM.PC.DD2 column (15 cm × 4.6 mm) (Regis Technologies Inc., Morton Grove, IL, USA). The ODP-50 column for logD measurement was purchased from Shodex™ (Showa Denko Europe GmbH, Munich, Germany).

Instrumentation

The radiosynthesis of [^{18}F]FE@SNAP was carried out within an Advion NanoTek® unit (Ithaca, NY, USA) comprising a concentrator unit (CE) and a liquid flow reaction unit (LF) with dedicated control software (Advion, version 1.4). Microreactors were made of fused silica tubing (ID, 0.1 µm; length 2.0 m), wound-up and held in a brass ring filled with a thermoresistant polymer to hold the tubing in its place. The purification of the resulting crude product solution and the final formulation of [^{18}F]FE@SNAP was carried out within an Nuclear Interface® PET synthesizer (GE Medical Systems, Uppsala, Sweden) remotely controlled via GINAstar software (Raytest Isotopenmessgeräte GmbH, Straubenhardt, Germany) installed on a standard PC. Analytical HPLC was performed using an Agilent system (Boeblingen, Germany) consisting of an autosampler 1100, a quartenary pump 1200, a diode array detector 1200 (operated at 254 nm) and a lead-shielded

BGO-radiodetector. The osmolality was measured using a Wescor osmometer Vapro® 5600 (Sanova Medical Systems, Vienna, Austria), pH was measured using a WTW inoLab 740 pH meter (WTW, Weilheim, Germany). Gas chromatography was performed using a 430-GC system (Burker Daltonik GmbH, Bremen, Germany). For binding experiments a Sorvall Ultracentrifuge Combi OTD (Thermo Fisher Scientific Inc, Waltham, MA, USA) and a 2480 WIZARD^2 Automatic Gamma Counter (PerkinElmer, Waltham, MA, USA) were used. For stability experiments sample incubation was conducted within a Thermomixer compact from Eppendorf® (Vienna, Austria) and sample centrifugation with a Universal 30 RF centrifuge (Hettich, Tuttlingen, Germany). The same centrifuge was used for determination of the plasma free fraction.

Radiochemistry

Radiosynthesis

The azeotropic drying of cyclotron produced [^{18}F]fluoride and the radiosynthesis of [^{18}F]FE@SNAP were carried out within a microfluidic system (Advion NanoTek®) as described in detail elsewhere [21]. Briefly, n.c.a [^{18}F]fluoride (25-30 GBq) was trapped on an anion exchange cartridge (PS-HCO3) and released with a solution containing Kryptofix 2.2.2 (4,7,13,16,21,24-hexaoxa-1,10-diaza-bi-cyclo[8.8.8]hexacosane; 10 mg, 26.6 µmol) and potassium carbonate (2.25 mg, 16.6 µmol) in acetontrile/water (70/30 v/v; V=0.5 mL). Iterative azeotropic drying was performed at 110°C by addition of 3 times 300 µL of dry acetonitrile. Subsequently, the dried [^{18}F]fluoride-aminopolyether was dissolved in 500 µL acetonitrile. 150 – 200 µL of Tos@SNAP (6 mg/mL in acetonitrile (for DNA synthesis)) and the same volume of the [^{18}F]fluoride-aminopolyether in acetonitrile (final precursor concentration: 3mg/mL) were simultaneously pushed through the microreactor at 170°C with a total flow rate of 170 µL/min. Subsequently, the crude product solution was swept out of the microreactor with a defined volume of 200 µL acetonitrile. The crude product solution was transferred into the Nuclear Interface® synthesizer unit, quenched with 1 mL water and subsequently injected onto the semi-preparative HPLC column (mobile phase: (water/acetic acid 97.5/2.5 v/v; 2.5 g/L ammonium acetate; pH 3.5)/acetonitrile 75/25 v/v; flow: 8 mL/min, after 9 min: 10 mL/min). Chromatograms were registered using an UV-detector (245 nm) and a

NaI radioactivity detector in series. The retention times were 2'20-3'10 (k'=0'16-0'63) for Tos@SNAP and 14'05-16'35 min (k'=5'11-6'11) for [^{18}F]FE@SNAP (Fig. 5). The [^{18}F]FE@SNAP fraction was cut and diluted with 100 mL water. This aqueous product solution was then pushed through a C18 SPE cartridge. After washing with 10 mL water, the pure product was eluted with 1.5 mL ethanol and 5 mL 0.9% saline solution. Formulation was done with an additional 9 mL physiological saline (0.9%), 1 mL of saline solution (3%) and 1 mL phosphate buffer (125 nM). Hence, the final total volume was 17.5 mL. For stability and binding affinity experiments, [^{18}F]FE@SNAP was eluted from the SPE cartridge with only 1 mL ethanol and 0.5 mL water in order to enhance the activity concentration in the product solution.

Quality control

Chemical and radiochemical impurities were detected using analytical HPLC (mobile phase: 0.1 M ammonium acetate/acetonitrile 60/40 v/v; flow: 1 mL/min). The retention time of [^{18}F]FE@SNAP was 11.8-12.5 min (k'=4.9-5.3). The chemical identity of [^{18}F]FE@SNAP was determined by co-injection of the unlabeled reference compound, FE@SNAP. The physiological formulated product solutions were further checked on residual solvents (analyzed by GC), osmolality and pH (checked with dedicated equipment).

Biological evaluation

Binding affinity

The method used was conducted according to Mashiko et al. [30] with minor modifications. CHO-K1 cell membranes expressing the hMCHR1 (10 μg/mL) were dissolved in 500 μL 50 mM Tris buffer (pH 7.4) (containing 10 mM $MgCl_2$, 2 mM EDTA, 0.1% bacitracin and 0.2% BSA). For the evaluation of the equilibrium dissociation constant (K_d) of [^{18}F]FE@SNAP, several concentrations (0-500 nM) of [^{18}F]FE@SNAP were added. The membranes were incubated in vials at room temperature for 120 min. Bound and free fractions of radioligand were separated by centrifugation at 40.000 × g for 20 min. The supernatants were removed into new vials. The pellets were washed with 800 μL ice cold Tris buffer, which was added to the supernatant and the pellets were dissolved in 1300 μL Tris buffer. The

radioactivity in the vials was measured in a Gamma Counter. The K_d values were calculated by using GraphPad Prism software Version 5.0 (La Jolla, CA, USA).

Plasma stability

Stability of [^{18}F]FE@SNAP in human and rat plasma was determined according to Nics et al. [31]. 1800 µL lithium-heparinized plasma (rat and human, respectively) were pre-incubated under physiological conditions (PBS, pH 7.4, 37°C) in a shaking incubator for 5 minutes. 36 µL [^{18}F]FE@SNAP (corresponding to 2% ethanol v/v in the total volume) were added and the plasma vial was vortexed for at least 10 seconds. After defined time points (0 and 120 min) 500 µL of the incubation-mixture were added to a preconditioned (with 5 mL methanol followed by 5 mL water) SPE-cartridge (Oasis). The cartridge was then eluted into a collection tube, washed with 5 mL of 5% methanol in water (v/v) into a second tube and eluted with 3 mL of THF into a third tube. 20 µL of the eluate-solution of tube two and three were injected into analytical HPLC (mobile phase: (water/ acetic acid 97.5/2.5 v/v; 2.5 g/L ammonium acetate; pH 3.5)/acetonitrile 70/30 v/v; flow: 2mL/min).

Plasma free fraction

The method used was modified from Parsey et al. [24]. 1 mL heparinized plasma (rat and human, respectively) were mixed with 10-50 µL [^{18}F]FE@SNAP. 200 µL aliquots were pipetted into centrifugal filter units and the total radioactivity was measured in a Gamma Counter. After the centrifugation step (2.000 × *g*, 50 min) 50 µL of the obtained filtrate was back-measured for radioactivity. For determination of the plasma free fraction (f_1), the ratio of filtrate to total activity concentration was calculated.

Stability against liver microsomes (CYP450)

The method used was described by Nics et al. [31]. Briefly, liver microsomes (pooled from human or rat origin) were pre-incubated under physiological conditions (PBS, pH 7.4, 37°C) with a NADPH-generating system (solution-A: NADP+, Glucose-6-phosphate and magnesium-chloride in H_2O and solution-B: Glucose-6-phosphate dehydrogenase in sodium citrate) for 5 min. 6 µL of [^{18}F]FE@SNAP, which correspond to 2% ethanol (v/v) in the total volume, were added. Enzymatic reactions were stopped after defined time points (0, 2, 5, 10, 20, 40 and 60 min) by adding the

same amount of ice-cold acetonitrile/methanol (10:1). The mixtures were vortexed, followed by a centrifugation step (23.000 × *g*, 5 min). Aliquots of the obtained supernatant were analyzed by analytical HPLC (for conditions see Plasma stability).

Stability against carboxylesterase

The method used was slightly modified from Nics et al. [32]. Incubations of different amounts (10, 30, 50, 70, 100, 200 µg/ml) of FE@SNAP were accomplished with constant quantity of 80 International Units (I.U.) of porcine carboxylesterase under physiological conditions (PBS, pH 7.4, 37°C). The use of selected concentrations of FE@SNAP was based on an optimal choice to create Michaelis-Menten kinetics (MMK). 35 µl of the incubation-mixture were stopped after defined time points (0, 60, 120, 180 and 240 min) by adding the same amount of ice-cold acetonitrile/methanol (10:1) and vortexed. After centrifugation of the reaction mixtures (23.000 × *g*, 5 min), 20 µL of the obtained supernatant were analyzed by analytical HPLC (for conditions see Plasma stability). The MMK of FE@SNAP was calculated by using GraphPad Prism software Version 5.0 (La Jolla, CA, USA).

Physicochemical parameters

logD analysis

LogD values were determined using an HPLC based assay according to Donovan and Pescatore [33]. A cocktail of two internal standards (toluene and triphenylene) with known logD and *k'* values and FE@SNAP in methanol was injected onto a short polymeric ODP-50 column. A linear gradient from 10% methanol/90% phosphate buffer (pH 7.4) to 100% methanol within 9.4 min at a flow rate of 1.5 mL/min was applied. Detection was performed at 260 nm and 285 nm.

IAM chromatography

IAM chromatography was modified from Tavares et al. [29]. 0.01 M phosphate buffer (pH 7.0) and acetonitrile (ranging from 50% to 35%, v/v) were used as mobile phase at a flow rate of 1 mL/min. FE@SNAP was injected onto the IAM column. As result the permeability through the membrane (P_m) was calculated and compared

with the P_m of known BBB penetrating compounds (DASB, ß-CIT) as external standards.

Acknowledgments

This research was part of an ongoing study, funded by the Austrian Science Fund (FWF P20977-B09; P.I.: M. Mitterhauser). The authors thank Matthias Hendl for his support in the IAM chromatography experiments.

References

[1] Bittencourt JC, Presse F, Arias C, Peto C, Vaughan J, Nahon JL, Vale W, Sawchenko PE.
The melanin-concentrating hormone system of the rat brain: An immuno- and hybridization histochemical characterization.
J Comp Neurol. 1992; 319: 218-245.
http://dx.doi.org/10.1002/cne.903190204

[2] Casatti CA, Elias CF, Sita LV, Frigo L, Furlani VCG, Bauer JA, Bittencourt JC.
Distribution of melanin-concentrating hormone neurons projecting to the medial mammillary nucleus.
Neuroscience. 2002; 115: 899-915.
http://dx.doi.org/10.1016/S0306-4522(02)00508-0

[3] Tadayyon M, Welters HJ, Haynes AC, Cluderay JE, Hervieu G.
Expression of melanin-concentrating hormone in insulin-producing cells: MCH stimulates insulin release in RINm5F and CRI-G1 cell-lines.
Biochem Biophys Res Commun. 2000; 275: 709-712.
http://dx.doi.org/10.1006/bbrc.2000.3357

[4] Kokkotou E, Moss AC, Torres D, Karagiannides I, Cheifetz A, Liu S, O'Brian M, Maratos-Flier E, Pothoulakis C.
Melanin-concentrating hormone as a mediator of intestinal inflammation.
Proc Natl Acad Sci USA. 2008; 105: 10613-10618.
http://dx.doi.org/10.1073/pnas.0804536105

[5] Bradley RL, Kokkotou EG, Maratos-Flier E, Cheatham B.
Melanin-concentrating hormone regulates leptin synthesis and secretion in rat adipocytes. Diabetes. 2000; 49: 1073-1077.
http://dx.doi.org/10.2337/diabetes.49.7.1073

[6] Bradley RL, Mansfield JP, Maratos-Flier E, Cheatham B.
Melanin-concentrating hormone activates signaling pathways in 3T3-L1 adipocytes.
Am J Physiol Endocrinol Metab. 2002; 283: E584-E592.
http://dx.doi.org/10.1152/ajpendo.00161.2002

[7] Saito Y, Nothacker HP, Wang Z, Lin SH, Leslie F, Civelli O.
Molecular characterization of the melanin-concentrating-hormone receptor.
Nature. 1999; 400: 265-269.
http://dx.doi.org/10.1038/22321

[8] Shimomura Y, Mori M, Sugo T, Ishibashi Y, Abe M, Kurokawa T, Onda H, Nishimura O, Sumino Y, Fujino M.
Isolation and identification of melanin-concentrating hormone as the endogenous ligand of the SLC-1 receptor.
Biochem Biophys Res Commun. 1999; 261: 622-626.
http://dx.doi.org/10.1006/bbrc.1999.1104

[9] Chambers J, Ames RS, Bergsma D, Muir A, Fitzgerald LR, Hervieu G, Dytko GM, Foley JJ, Martin J, Liu WS, Park J, Ellis C, Ganguly S, Konchar S, Cluderay J, Leslie R, Wilson S, Sarau HM.

Melanin-concentrating hormone is the cognate ligand for the orphan G-protein-coupled receptor SLC-1.
Nature. 1999; 400: 261-265.
http://dx.doi.org/10.1038/22313

[10] Lembo PM, Grazzini E, Cao J, Hubatsch DA, Pelletier M, Hoffert C, St-Onge S, Pou C, Labreque J, Groblewski T, O'Donnell D, Payza K, Ahmad S, Walker P.
The receptor for the orexigenic peptide melanin-concentrating hormone is a G-protein-coupled receptor.
Nat Cell Biol. 1999; 1: 267-271.
http://dx.doi.org/10.1038/12978

[11] Sailer AW, Sano H, Zeng Z, McDonald TP, Pan J, Pong SS, Feighner SD, Tan CP, Fukami T, Iwaasa H, Hreniuk DL, Morin NR, Sadowski SJ, Ito M, Ito M, Bansal A, Ky B, Figueroa DJ, Jiang Q, Austin CP, MacNeil DJ, Ishihara A, Ihara M, Kanatani A, Van der Ploeg LHT, Howard AD, Liu Q.
Identification and characterization of a second melanin-concentrating hormone receptor, MCH-2R.
Proc Natl Acad Sci USA. 2001; 98: 7564-7569.
http://dx.doi.org/10.1073/pnas.121170598

[12] Hill J, Duckworth M, Murdock P, Rennie G, Sabido-David C, Ames RS, Szekeres P, Wilson S, Bergsma DJ, Gloger IS, Levy DS, Chambers JK, Muir AI.
Molecular cloning and functional characterization of MCH2, a novel human MCH receptor.
J Biol Chem. 2001; 276: 20125-20129.
http://dx.doi.org/10.1074/jbc.M102068200

[13] Wang S, Behan J, O'Neill K, Weig B, Fried S, Laz T, Bayne M, Gustafson E, Hawes B.
Identification and pharmacological characterization of a novel human melanin-concentrating hormone receptor, MCH-R2.
J Biol Chem. 2001; 276: 34664-34670.
http://dx.doi.org/10.1074/jbc.M102601200

[14] An S, Cutler G, Zhao JJ, Huang S-G, Tian H, Li W, Liang L, Rich M, Bakleh A, Du J, Chen JL, Dai K.
Identification and characterization of a melanin-concentrating hormone receptor.
Proc Natl Acad Sci USA. 2001; 98: 7576-7581.
http://dx.doi.org/10.1073/pnas.131200698

[15] Marsh DJ, Weingarth DT, Novi DE, Chen HY, Turmbauer ME, Chen AS, Guan XM, Jiang MM, Feng Y, Camacho RE, Shen Z, Frazier EG, Yu H, Metzger JM, Kuca S J, Shearman LP, Gopal-Truter S, MacNeil DJ, Strack AM, MacIntyre DE, Van der Ploeg LHT, Qian S.
Melanin-concentrating hormone 1 receptor-deficient mice are lean, hyperactive, and hyperphagic and have altered metabolism.
Proc Natl Acad Sci USA. 2002; 99: 3240-3245.
http://dx.doi.org/10.1073/pnas.052706899

[16] Ito M, Gomori A, Ishihara A, Oda Z, Mashiko S, Matsushita H, Yumoto M, Ito M, Sano H, Tokita S, Moriya M, Iwaasa H, Kanatani A.
Characterization of MCH-mediated obesity in mice.
Am J Physiol Endocrinol Metab. 2003; 284: E940-E945.

http://dx.doi.org/10.1152/ajpendo.00529.2002

[17] Luthin DR.
Anti-obesity effects of small molecule melanin-concentrating hormone receptor1 (MCHR1) antagonists.
Life Sciences. 2007; 81: 423-440.
http://dx.doi.org/10.1016/j.lfs.2007.05.029

[18] Gattrell WT, Sambrook Smith CP, Smith AJ.
An example of designed multiple ligands spanning protein classes: Dual MCH-1R antagonists/DPPIV inhibitors.
Bioorg Med Chem Lett. 2012; 22: 2464-2469.
http://dx.doi.org/10.1016/j.bmcl.2012.02.010

[19] Borowsky B, Durkin MM, Ogozalek K, Marzabadi MR, DeLeon J, Lagu B, Heurich R, Lichtblau H, Shaposhnik Z, Daniewska I, Blackburn TP, Branchek TA, Gerald C, Vaysse PJ, Forray C.
Antidepressant, anxiolytic and anorectic effects of a melanin-concentrating hormone-1 receptor antagonist.
Nat Med. 2002; 8: 825-830.
http://dx.doi.org/10.1038/nm741

[20] Philippe C, Schirmer E, Mitterhauser M, Shanab K, Lanzenberger R, Karanikas G, Spreitzer H, Viernstein H, Wadsak W.
Radiosynthesis of [^{11}C]SNAP-7941 – the first PET-tracer for the melanin concentrating hormone receptor 1 (MCHR1).
Appl Radiat Isot. 2012; 70: 2287-2294.
http://dx.doi.org/10.1016/j.apradiso.2012.07.010

[21] Philippe C, Ungersboeck J, Schirmer E, Zdravkovic M, Nics L, Zeilinger M, Shanab K, Lanzenberger R, Karanikas G, Spreitzer H, Viernstein H, Mitterhauser M, Wadsak W.
[^{18}F]FE@SNAP – A new PET tracer for the melanin concentrating hormone receptor 1 (MCHR1): Microfluidic and vessel-based approaches.
Bioorg Med Chem. 2012; 20: 5936-5940.
http://dx.doi.org/10.1016/j.bmc.2012.07.051

[22] Sone M, Takahashi K, Murakami O, Totsune K, Arihara Z, Satoh F, Sasano H, Ito H, Mouri T.
Binding sites for the melanin-concentrating hormone in the human brain.
Peptides. 2000; 21: 245-250.
http://dx.doi.org/10.1016/S0196-9781(99)00206-5

[23] Ungersboeck J, Philippe C, Mien L-K, Haeusler D, Shanab K, Lanzenberger R, Spreitzer H, Keppler BK, Dudczak R, Kletter K, Mitterhauser M, Wadsak W.
Microfluidic preparation of [^{18}F]FE@SUPPY and [^{18}F]FE@SUPPY:2 – comparison with conventional radiosyntheses.
Nucl Med Biol. 2011; 38: 427-434.
http://dx.doi.org/10.1016/j.nucmedbio.2010.09.009

[24] Parsey RV, Slifstein M, Hwang D-R, Abi-Dragham A, Simpson N, Mawlawi O, Guo NN, Van Heertum R, Mann J, Laruelle M.

Validation and reproducibility of measurement of 5-HT IA receptor parameters with [carbonyl-^{11}C]WAY-100635 in humans: comparison of arterial and reference tissue input functions.
J Cereb Blood Flow Metab. 2000; 20: 1111-1133.
http://dx.doi.org/10.1097/00004647-200007000-00011

[25] Jones B.
Probing the specificity of synthetically useful enzymes.
Aldrichimica Acta. 1993; 26: 105-112.

[26] Naik P, Cucullo L.
In vitro blood-brain barrier models: Current and perspective technologies.
J Pharm Sci. 2012; 101: 1337-1354.
http://dx.doi.org/10.1002/jps.23022

[27] Tavares AA, Lewsey J, Dewar D, Pimlott SL.
Radiotracer properties determined by high performance liquid chromatography: a potential tool for brain radiotracer discovery.
Nucl Med Biol. 2012; 39: 127-135.
http://dx.doi.org/10.1016/j.nucmedbio.2011.06.011

[28] Schirmer E.
PACCON 2012 – Pure and Applied Chemistry International Conference, Ubon Ratchathani, Thailand. book of abstracts.
ISBN: 978-974-523-221-1, ORC-PO-47.

[29] Schirmer E.
JMMC 2011 – VII Joint Meeting on Medicinal Chemistry, Catania, Italy, book of abstracts, 127, www.jmmc2011.it

[30] Mashiko S, Ishihara A, Gomori A, Moriya R, Ito M, Iwaasa H, Matsuda M, Feng Y, Shen Z, Marsh DJ, Bednarek MA, MacNeil DJ, Kanatani A.
Antiobesity effect of a melanin-concentrating hormone 1 receptor antagonist in diet-induced obese mice.
Endocrinology. 2005; 146: 3080-3086.
http://dx.doi.org/10.1210/en.2004-1150

[31] Nics L, Vraka C, Hendl M, Haeusler D, Wagner KH, Shanab K, Dudczak R, Wadsak W, Mitterhauser M.
In-vitro stability of [^{18}F]FE@SUPPPY and [^{18}F]FE@SUPPY:2 against human liver-microsomes and human plasma.
Nuklearmedizin. 2011; 50: A176.

[32] Nics L, Haeusler D, Wadsak W, Wagner KH, Dudczak R, Kletter K, Mitterhauser M.
The stability of methyl-, ethyl- and fluoroethylesters against carboxylesterases in vitro: there is no difference.
Nucl Med Biol. 2011; 38: 13-17.
http://dx.doi.org/10.1016/j.nucmedbio.2010.07.004

[33] Donovan SF, Pescatore MC.
Method for measuring the logarithm of the octanol-water partition coefficient by using short octadecyl-poly(vinyl alcohol) high-performance liquid chromatography columns.
J Chromatogr A. 2002; 952: 47-61.

http://dx.doi.org/10.1016/S0021-9673(02)00064-X

[34] Philippe C, Nics L, Zeilinger M, Kuntner C, Wanek T, Mairinger S, Shanab K, Spreitzer H, Viernstein H, Wadsak W, Mitterhauser M.
Preclinical in vitro & in vivo evaluation of [^{11}C]SNAP-7941 – the first PET tracer for the melanin concentrating hormone receptor 1
Nuc Med Biol. 2013; in press.
http://dx.doi.org/10.1016/j.nucmedbio.2013.05.010

Captions

Fig. 1. SNAP-7941 derivatives **1-4** (**1**: SNAP-7941; **2**: [^{11}C]SNAP-7941; **3**: [^{18}F]FE@SNAP ; **4**: Tos@SNAP)

Fig. 2. Specific binding of [^{18}F]FE@SNAP on the hMCHR1. If not visible, error bars are within the margin of the symbols.

Fig. 3. Degradation of [^{18}F]FE@SNAP by rat and human liver microsomes.

Fig. 4. Michaelis-Menten saturation curve of FE@SNAP against carboxylesterase. If not visible, error bars are within the margin of the symbols.

Fig. 5. Representative semi-preparative HPLC chromatogram of the reaction solution of [^{18}F]FE@SNAP. Top chromatogram: UV channel (mAu, milli Absorbance Unit). Bottom chromatogram: radioactivity channel (NaI); (CPS, counts per second).

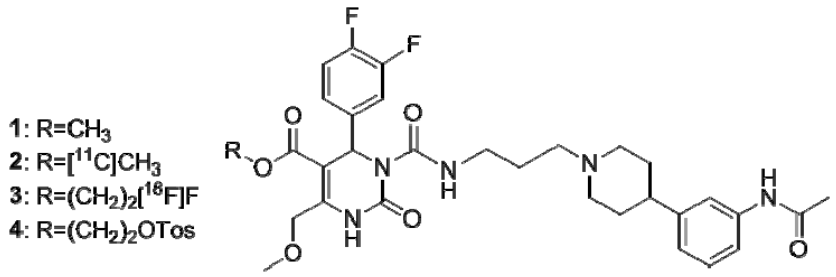

Fig. 1. SNAP-7941 derivatives **1-4** (**1**: SNAP-7941; **2**: [^{11}C]SNAP-7941; **3**: [^{18}F]FE@SNAP ; **4**: Tos@SNAP)

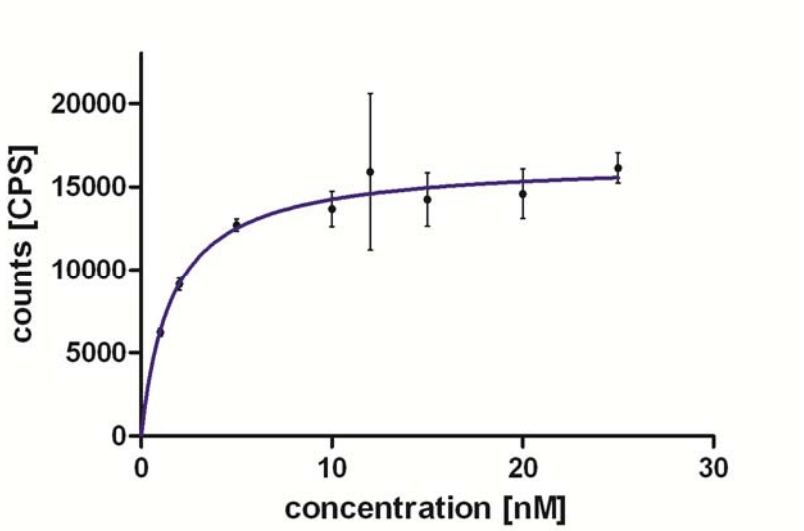

Fig. 2. Specific binding of [^{18}F]FE@SNAP on the hMCHR1. If not visible, error bars are within the margin of the symbols.

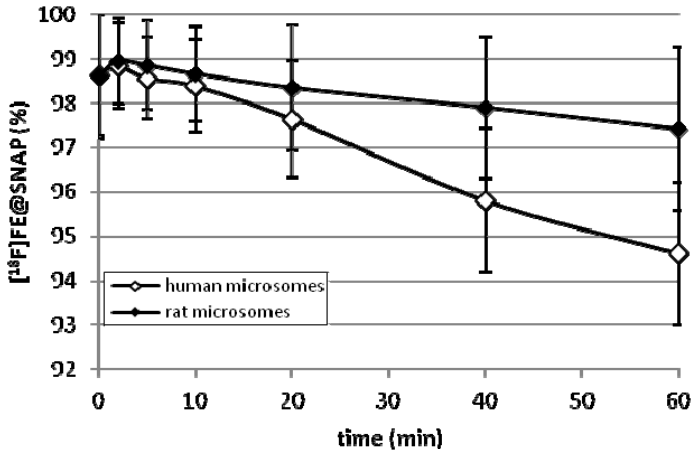

Fig. 3. Degradation of [^{18}F]FE@SNAP by rat and human liver microsomes.

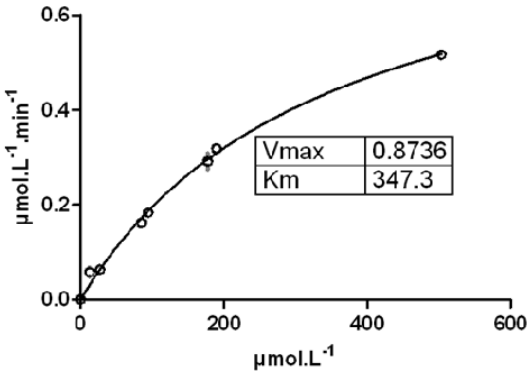

Figure 4 Michaelis-Menten saturation curve of FE@SNAP against carboxylesterase. If not visible, error bars are within the margin of the symbols.

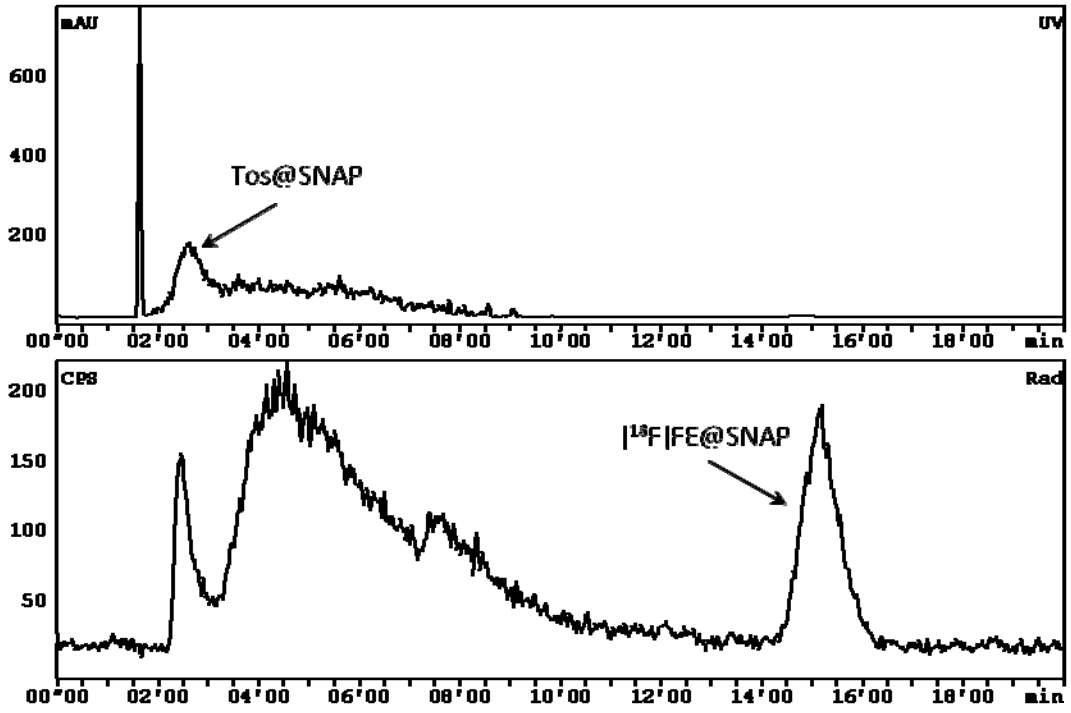

Figure 5 Representative semi-preparative HPLC chromatogram of the reaction solution of [^{18}F]FE@SNAP. Top chromatogram: UV channel (mAu, milli Absorbance Unit). Bottom chromatogram: radioactivity channel (NaI); (CPS, counts per second).

2.5. Manuscript #4

Preclinical *in vitro* & *in vivo* evaluation of [^{11}C]SNAP-7941 - the first PET tracer for the melanin concentrating hormone receptor

Nuclear Medicine and Biology 2013, in press (doi:10.1016/j.nucmedbio.2013.05.010)

Cécile Philippe[1,2], Lukas Nics[1,3], Markus Zeilinger[1], Claudia Kuntner[4], Thomas Wanek[4], Severin Mairinger[4], Karem Shanab[5], Helmut Spreitzer[5], Helmut Viernstein[2], Wolfgang Wadsak[1,6], Markus Mitterhauser[1,2]

[1]Radiochemistry and Biomarker Development Unit, Department of Nuclear Medicine, Medical University of Vienna, 1090 Vienna, Austria

[2]Department of Pharmaceutical Technology and Biopharmaceutics, University of Vienna, 1090 Vienna, Austria

[3]Department of Nutritional Sciences, University of Vienna, 1090 Vienna, Austria

[4]Biomedical Systems, Health & Environment Department, AIT Austrian Institute of Technology GmbH, 2444 Seibersdorf, Austria

[5]Department of Drug and Natural Product Synthesis, University of Vienna, 1090 Vienna, Austria

[6]Department of Inorganic Chemistry, University of Vienna, 1090 Vienna, Austria

Abstract

Introduction: Due to its involvement in a variety of pathologies (obesity, diabetes, gut inflammation and depression), the melanin concentrating hormone receptor 1 (MCHR1) is a new target for the treatment of these lifestyle diseases. We previously presented the radiosynthesis of [^{11}C]SNAP-7941, the first potential PET tracer for the MCHR1.

Methods: We herein present its *in vitro* and *in vivo* evaluation, including binding affinity, plasma stability, stability against liver mircrosomes and carboxylesterase, lipohilicity, biodistribution, *in vivo* metabolism and small-animal PET.

Results: [^{11}C]SNAP-7941 evinced high stability against liver microsomes, carboxylesterase and in human plasma. The first small-animal PET experiments revealed a 5 fold increased brain uptake after Pgp/BCRP inhibition. Therefore, it can be assumed that [^{11}C]SNAP-7941 is a Pgp/BCRP substrate. No metabolites were found in brain.

Conclusion: On the basis of these experiments with healthy rats, the suitability of [^{11}C]SNAP-7941 for the visualisation of central and peripheral MCHR1 remains speculative.

Keywords: SNAP-7941; MCHR1; PET; metabolites

1. Introduction

The melanin concentrating hormone receptor 1 (MCHR1) is a G protein-coupled receptor, predominantly expressed in the central nervous system [1, 2]. Besides, it is also found in peripheral tissues, such as the ß-cells of the pancreas [3], colonic epithelial cells [4] or adipocytes [5, 6]. Changes in its expression, both, up and down regulation, are discussed to be involved in a variety of pathologies, such as obesity [7, 8], diabetes [3], gut inflammation [4] and depression [9]. Due to its involvement in these lifestyle diseases, MCHR1 has become a very interesting pharmacological target since its discovery in 1999 [10-13]. Several MCHR1 antagonist were presented in the last decade, some of them have entered clinical trials for the treatment of obesity [14], while some are in discussion of becoming anti-diabetic drugs [15]. However, to enable confidence in preclinical to clinical translation of MCHR1 pharmacology and for further studies on the involvement and distribution of the MCHR1 in energy homeostasis, a suitable positron emission tomography (PET) tracer needs to be developed. PET is a non-invasive technique to visualize molecular effects directly *in vivo*. On the basis of the highly potent MCHR1 antagonist SNAP-7941 ((+)-methyl (4S)-3-{[(3-{4-[3-(acetylamino)phenyl]-1-piperidinyl}propyl)amino]carbonyl}-4-(3,4-difluorophenyl)-6-(methoxymethyl)-2-oxo-1,2,3,4-tetrahydro-5-pyrimidinecarboxylate hydrochloride, 1, Fig.1) (K_d = 0.18 nM,

evaluated on Cos-7 cells expressing the human MCHR1 (hMCHR1)) [16], we developed two potential PET tracers: [^{11}C]SNAP-7941 [17] and the fluoroethylated analogue [^{18}F]FE@SNAP [18]. Both were synthesized in a reliable and feasible manner and first preclinical studies were conducted. The present work focuses on the detailed preclinical *in vitro* and *in vivo* evaluation of [^{11}C]SNAP-7941 (Fig. 1), including binding affinity, plasma stability, stability against liver microsomes and carboxylesterase, lipohilicity, biodistribution, *in vivo* metabolism and small-animal PET.

2. Materials and methods

2.1 General

2.1.1. Materials

Unless otherwise stated, all chemicals were of analytical grade and purchased from Sigma Aldrich (Vienna, Austria) or Merck (Darmstadt, Germany). For the radiosynthesis, acetonitrile for DNA synthesis (≤ 10 ppm H_2O) from Merck was used. Isoflurane was obtained from Baxter Vertriebs GmbH (Vienna, Austria). [^{11}C]CH_4 was produced via the ^{14}N(p,α)^{11}C nuclear reaction by irradiating nitrogen gas containing 10% hydrogen using a PETtrace cyclotron equipped with a CH_4 target system (GE Healthcare, Uppsala, Sweden). Typical beam current was 25 μA and the irradiation was stopped as soon as the desired activity level was reached (approx. 40 GBq [^{11}C]CH_4, calculated by cyclotron operating software; corresponding to 20-25 min irradiation time). [^{11}C]CH_3I was prepared in a TRACERlab™ FX C Pro synthesis module (GE Healthcare) and converted into [^{11}C]CH_3OTf by passage through a column containing silver-triflate impregnated graphitized carbon. Syntheses of the precursor compound (SNAP-acid) and the reference standard (SNAP-7941) were performed in cooperation with the Department of Drug and Natural Product Synthesis of the University of Vienna (Austria) [17]. Tariquidar dimesylate (TQD) was kindly provided by Dr. Erker (Department of Medicinal Chemistry, University of Vienna, Austria). Solid phase extraction (SPE) cartridges SepPak® C18-plus and Oasis® HLB 6cc Vac (200 mg) were purchased from Waters (Waters® Associates, Milford, MA, USA). Phosphate buffered saline (PBS)

concentrate (10:1) was obtained from Morphisto (Frankfurt, Germany). NADPH regenerating system solution-A and solution-B were obtained from BD Biosciences (Bedford, MA, USA). Pooled human liver microsomes (Lot No. 34689), pooled male rat liver microsomes (Lot No. 85157) and pooled female rat liver microsomes (Lot No. 59232) (both from Sprague Dawley rats) were purchased from BD Biosciences (Woburn, MA, USA). The male and female rat liver microsomes were homogenized. The fresh frozen plasma (pooled lithium-heparinised human plasma (No. IPLA-N) and pooled lithium-heparinised rat plasma (No. IRT-N)) were purchased from Innovative Research (Novi, MI, USA). The porcine liver carboxylesterase (EC 3.1.1.1) was obtained from Sigma Aldrich. Centrifugal Filter Units (Centrifree®-30K) were purchased from Merck Millipore (Tullagreen, Ireland). [^{125}I]MCH and CHO-K1 cell membranes expressing the hMCHR1/hMCHR2 were purchased from PerkinElmer (Waltham, MA, USA). The vials for the binding affinity assay were purchased from Beckman Coulter Inc. (Brea, CA, USA; Bio-Vial™, 4 mL, 14 × 55 mm). Semi-preparative high-performance liquid chromatography (HPLC) column (Chromolith® SemiPrep RP-18e; 100-10mm, precolumn: Chromolith® Guard Cartridge RP-18e; 5-4.6 mm) and analytical HPLC column (Chromolith® Performance RP-18e; 100-4.6 mm) were purchased from Merck (Darmstadt, Germany). The analytical column was used with a precolumn (Chromolith® Guard Cartridge RP-18e; 5-4.6 mm) for metabolic stability testing. For binding experiments a Sorvall Ultracentrifuge Combi OTD (Thermo Fisher Scientific Inc, Waltham, MA, USA) was used. The Gamma Counter was purchased from PerkinElmer, Waltham, MA, USA (2480 WIZARD^2 Automatic Gamma Counter). For stability experiments sample incubation was conducted within a Thermomixer compact from Eppendorf® (Vienna, Austria) and sample centrifugation with a Universal 30 RF centrifuge (Hettich, Tuttlingen, Germany). The same centrifuge was used for determination of the plasma free fraction. For in vivo metabolism assessment a Hettich Rotanta/P Typ 350 and a Thermo Heraeus Fresco 17 (Thermo Fisher Scientific, Waltham, MA, USA) centrifuge were used. IAM (immobilized artificial membrane) chromatography was performed using a IAM.PC.DD2 column (15 cm × 4.6 mm) (Regis Technologies Inc., Morton Grove, IL, USA). The ODP-50 column for logD measurement was purchased from Shodex™ (Showa Denko Europe GmbH, Munich, Germany).

2.1.2. Tracer preparation

Radiosynthesis of [^{11}C]SNAP-7941 (Fig.1) was performed in the fully automated synthesizer TRACERlab™ FX C Pro as described elsewhere [17]. Briefly, [^{11}C]CH_3OTf was bubbled through a solution of SNAP-acid (2 mg/mL, 3.34 mmol) in 500 µL acetonitrile containing TBAH (1 molar equivalent). Purification of the crude reaction mixture was done via the build-in HPLC system. The collected product was passed over a C18 SPE cartridge. After washing, the purified product was eluted with ethanol. For iv injection, the ethanol was removed by heating at 100°C under a stream of argon and the product was formulated in a mixture of 0.9% aqueous saline/polyethylene glycol 300 (92.5/7.5, v/v) at an approximate concentration of 350 MBq/mL. Radiochemical purity and specific activity of [^{11}C]SNAP-7941 were determined by analytical radio-HPLC. Subsequently, [^{11}C]SNAP-7941 was injected into the animals. Due to the short half-life of carbon-11 ($t_{1/2}$ = 20 min) a distinct radiosynthesis for each animal had to be performed.

2.1.3. Animals

Adult Sprague-Dawley rats (male and female) weighing 291 ± 41 g were kept under controlled environmental conditions (22 ± 1°C; 40-70% humidity; 12h light/dark cycle) with free access to standard laboratory animal diet and tap water. Prior to each experiment, the animals were placed into an induction box and anesthetized with 2.5% isoflurane. When unconscious, the animals were taken from the box and kept under anaesthesia with 1.5-2% isoflurane administered via a mask during the whole experiment. The study was authorized by the institutional animal care and use committees, and all study procedures were performed in accordance with the European Communities Council Directive of November 24, 1986 (86/609/ECC). Every effort was made to minimize both, the suffering and the number of animals used in this study.

2.2. In vitro evaluation

2.2.1. Binding affinity

The method used was conducted according to Mashiko et al. [19] with minor modifications. CHO-K1 cell membranes expressing the hMCHR1 (10 µg/mL) were

dissolved in 500 µL 50 mM Tris buffer (pH 7.4) (containing 10 mM $MgCl_2$, 2 mM EDTA, 0.1% bacitracin and 0.2% BSA). The equilibrium inhibition constant (K_i) was evaluated using several concentrations (0-2000 nM) of SNAP-7941 in the presence of 0.1 nM [^{125}I]MCH. The membranes were incubated in vials at room temperature for 120 min. Bound and free fractions of radioligand were separated by centrifugation at 40.000 × g for 20 min. The supernatants were removed into new vials. The pellets were washed with 800 µL ice cold Tris buffer, which was added to the supernatant and the pellets were dissolved in 1300 µL Tris buffer. The radioactivity in the vials was measured in a Gamma Counter. The K_i values were calculated by using GraphPad Prism software Version 5.0 (La Jolla, CA, USA).

2.2.2. Plasma stability

Stability of [^{11}C]SNAP-7941 in human and rat plasma was determined according to Nics et al. [20]. Briefly, 1250 µL lithium-heparinized plasma were pre-incubated under physiological conditions (PBS, pH 7.4, 37°C) in a shaking incubator for 5 minutes. 25 µL [^{11}C]SNAP-7941 (corresponding to 2% ethanol v/v in the total volume) were added and the plasma vial was vortexed for at least 10 seconds. After defined time points (0 and 60 min) 500 µL of the incubation-mixture were added to a preconditioned (with 5 mL methanol followed by 5 mL water) SPE-cartridge (Oasis). The cartridge was then eluted into a collection tube, washed with 5 mL of 5% methanol in water (v/v) into a second tube and eluted with 3 mL of THF into a third tube. 20 µL of the eluate-solution of tube two and three were injected into analytical radio-HPLC (mobile phase: (water/acetic acid 97.5/2.5 v/v; 2.5 g/L ammonium acetate; pH 3.5)/acetonitrile 70/30 v/v; flow: 2 mL/min, λ=254 nm).

2.2.3. Plasma free fraction

The method used was modified from Parsey et al. [21]. 1 mL of heparinized plasma (rat and human, respectively) was mixed with approx. 10 µL [^{11}C]SNAP-7941 (corresponding to the upper level of the linear range of the Gamma Counter). 200 µL aliquots were pipetted into centrifugal filter units and the total radioactivity was measured in a Gamma Counter. After the centrifugation step (2.000 × g, 50 min) 50 µL of the obtained filtrate was back-measured for radioactivity. For determination

of the plasma free fraction (f_1) the ratio of filtrate to total activity concentration was calculated.

2.2.4. Stability against liver microsomes (CYP450)

The method used was described by Nics et al. [20]. Briefly, liver microsomes (pooled from human or rat origin) were pre-incubated under physiological conditions (PBS, pH 7.4, 37°C) with a NADPH-generating system (solution-A: NADP+, Glucose-6-phosphate and magnesium-chloride in H_2O and solution-B: Glucose-6-phosphate dehydrogenase in sodium citrate) for 5 min. 9 µL of [^{11}C]SNAP-7941, which correspond to 2% ethanol (v/v) in the total volume, were added. Enzymatic reactions were stopped after defined time points (0, 10, 20, 40 and 60 min) by adding the same amount of ice-cold acetonitrile/methanol (10:1). The mixtures were vortexed, followed by a centrifugation step (23.000 × g, 5 min). Aliquots of the obtained supernatant were analyzed by analytical radio-HPLC (for conditions see 2.2.2. Plasma stability).

2.2.5. Stability against carboxylesterase

The method used was slightly modified from Nics et al. [22]. Incubations of different amounts (10, 70, 200 µg/mL) of SNAP-7941 were accomplished with constant quantity of 80 International Units (I.U.) of porcine carboxylesterase under physiological conditions (PBS, pH 7.4, 37°C). 35 µL of the incubation-mixture were stopped after defined time points (0, 60, 120, 180 and 240 min) by adding the same amount of ice-cold acetonitrile/methanol (10:1) and vortexed. After centrifugation of the reaction mixtures (23.000 × g, 5 min), 20 µL of the obtained supernatant were analyzed by analytical HPLC (for conditions see 2.2.2. Plasma stability).

2.2.6. logD analysis

LogD values were determined using an HPLC based assay according to Donovan and Pescatore [23]. A cocktail of two internal standards (toluene and triphenylene) with known logD and k' values and SNAP-7941 in methanol was injected onto a short polymeric ODP-50 column. A linear gradient from 10% methanol/90% phosphate buffer (pH 7.4) to 100% methanol within 9.4 min at a flow rate of 1.5 mL/min was applied. Detection was performed at 260 nm and 285 nm.

2.2.7. IAM chromatography

IAM chromatography was modified from Tavares et al. [24]. 0.01 M phosphate buffer (pH 7.0) and acetonitrile (ranging from 50% to 35%) were used as mobile phase at a flow rate of 1 mL/min. SNAP-7941 was injected onto the IAM column. The permeability through the membrane (P_m) referring to the retention time of SNAP-7941 was calculated and compared with the P_m of known BBB penetrating compounds (DASB, ß-CIT), which were used as external standards.

2.3. In vivo evaluation

2.3.1. Biodistribution

Anesthetized female rats (Him:OFA/SPF, Himberg, Austria; n=4) received 83.96 ± 49.8 MBq [^{11}C]SNAP-7941 (300µL) as an iv bolus via a lateral tail vein. 20 min after injection, the animals were sacrificed. Blood, brain, eyes, muscle, bone, fat, thyroid, heart, lungs, stomach, pancreas, liver, jejunum, ileum, large intestine (cecum, colon and rectum), spleen, kidneys, adrenals, uterus and ovary were removed; dry weighted and measured in the Gamma Counter. Radioactivity concentrations were dose and weight normalised and expressed as standardized uptake values (SUV).

2.3.2. Small-animal PET imaging and PET data analysis

Anesthetized male rats (Him:OFA/SPF, Himberg, Austria) were positioned in the imaging chamber of a microPET Focus220 scanner (Siemens, Medical Solutions, Knoxville, USA) and were warmed throughout the whole experiment at around 38°C. Three groups of rats were scanned with [^{11}C]SNAP-7941. The first group (n=6) received only the tracer [^{11}C]SNAP-7941 (baseline group); the second group (n=3) received SNAP-7941 (15 mg/kg; freshly dissolved in ethanol (5%) and 0.9% saline solution, 2 mL/kg) 30 min prior to tracer application; the third group (n=3) received the P-glycoprotein (Pgp) and breast cancer resistant protein (BCRP) inhibitor TQD (15 mg/kg; freshly dissolved in 2.5% (w/v) aqueous dextrose solution, 3 mL/kg) 60 min prior to radiotracer application. SNAP-7941, TQD and 73.17 ± 22.9 MBq [^{11}C]SNAP-7941 (250 µL) were injected as an iv bolus via a tail vein. Dynamic PET imaging was performed over 60 min for all animals. At the end of each PET scan, venous blood was withdrawn by retro-orbital puncture, animals were

sacrificed and the whole brain was removed. Blood samples and brains were counted in a Gamma Counter.

PET images were reconstructed by Fourier rebinning followed by 2-dimensional filtered back projection with a ramp filter. The standard data correction protocol (normalization, attenuation, decay correction and injection decay correction) was applied to the data. Whole brain was manually outlined on multiple planes of the PET summation images using the image analysis software PMOD 3.1 (version 3.1, Pmod Ltd, Zurich, Switzerland). Volumes of interest (VOIs) were transferred to the PET images of the individual time frames and time activity curves (TACs) were calculated. To facilitate comparison of TACs of different animals, radioactivity concentrations were expressed as SUV.

2.3.3. Metabolism

[^{11}C]SNAP-7941 metabolism was assessed in plasma and brain 20 min after tracer application. Venous blood was withdrawn by retro-orbital puncture, animals (male rats, Him:OFA/SPF, Himberg, Austria; n=3) were sacrificed and the whole brain was removed. Additionally, brains from the group pre-treated with TQD (60 min after tracer application) were analysed, too.

Blood samples (3 mL) were collected in heparin buffered tubes; 100 µL thereof were analyzed in a Gamma Counter. The blood was centrifuged (2.000 × g, 5 min) to separate cellular components. Sample clean-up was performed by vortexing plasma with the equivalent amount of acetonitrile and by subsequent ultra-centrifugation (23.000 × g, 3 min) to remove precipitated proteins. The obtained supernatant was spiked with unlabelled SNAP-7941 and analyzed by radio-HPLC (for conditions see 2.2.2. Plasma stability).

Rat brains were counted in a Gamma Counter and, afterwards, homogenized with 0.8 mL 0.9% saline solution) using an IKA T10 basic Ultra-turrax (IKA Laboratory Equipment, Staufen, Germany). Acetonitrile (1.5 mL) was added to the brain homogenate, vortexed and subsequently centrifuged (23.000 × g, 4 min) to remove precipitated proteins. The obtained supernatant was spiked with unlabelled SNAP-7941 and analyzed by radio-HPLC (for conditions see Plasma stability).

3. Results

Starting from 40.94 ± 4.1 GBq [^{11}C]CH_4, 393 ± 160 MBq of [^{11}C]SNAP-7941 were produced (3.7 ± 1.4 % EOB, n=22). Radiochemical purity always exceeded 99% and the specific activity was 108.21 ± 55.8 GBq/µmol at the end of synthesis (EOS). No residual precursor mass was detected.

In vitro evaluation

The binding experiments on the hMCHR1 revealed a K_i of 4.52 ± 0.7 nM (n=2; each in triplicate) for SNAP-7941. Preliminary experiments on the hMCHR2 showed poor binding of SNAP-7941 (K_i > 1000 nM).

Over 60 min no degradation of [^{11}C]SNAP-7941 could be observed in human plasma (n=6; triplicates). In rat plasma (n=3; triplicates), 50.40 ± 0.7% [^{11}C]SNAP-7941 were found after 60 min. The formation of a radioactive hydrophilic metabolite could be observed.

The plasma free fraction of [^{11}C]SNAP-7941 was 20.96 ± 1.0% in human plasma (n=6; triplicates) and 32.44 ± 0.8% in rat plasma (n=3; triplicates).

The enzymatic degradation of [^{11}C]SNAP-7941 by CYP450 after 60 min was 9.59 ± 0.7% using human liver microsomes (n=4; triplicates) and 1.27 ± 0.8% using rat liver microsomes (n=4; triplicates).

SNAP-7941 was significantly stable against porcine carboxylesterase (no decomposition was observed). Therefore, no Michaelis-Menten constant could be calculated.

The logD value of SNAP-7941 was 3.29 (n=3; triplicates). The P_m value was 0.79 (n=3; triplicates).

In vivo evaluation

Biodistribution experiments in healthy female rats carried out 20 minutes after intravenous injection of [^{11}C]SNAP-7941 displayed highest uptake in adrenals (4.29 ± 1.80 SUV), followed by high uptake in spleen (3.02 ± 1.39 SUV) and kidneys (2.98 ± 1.86 SUV). Other organs with pronounced uptake were lungs (2.36 ± 1.11 SUV), liver (1.96 ± 1.32 SUV), jejunum (1.48 ± 0.86 SUV), pancreas (1.41 ± 0.69 SUV), thyroid (1.38 ± 0.68 SUV) and heart (1.37 ± 0.38 SUV). Moderate uptake was found

in the ileum (0.87 ± 0.35 SUV), stomach (0.82 ± 0.44 SUV), eyes (0.66 ± 0.45 SUV), uterus/ovary (0.64 ± 0.35 SUV), bone (0.50 ± 0.25 SUV), large intestine (0.27 ± 0.10 SUV) and muscle (0.23 ± 0.09 SUV). Low uptake was found in blood (0.13 ± 0.05 SUV), brain (0.05 ± 0.03 SUV) and fat (0.05 ± 0.04 SUV). Additionally, a tissue-to-blood ratio was calculated (Fig.2).

Mean brain TACs of [^{11}C]SNAP-7941 in male rats over 60 min of the baseline group and after pre-treatment with SNAP-7941 or TQD are shown in Fig. 3. Peak brain uptake in the baseline group was 0.34 ± 0.1 SUV at 1 min after tracer injection. At 55 min after tracer injection, brain activity uptake had declined to 0.22 ± 0.0 SUV. Rats, pre-treated with SNAP-7941, evinced no significant difference ($P = 0.52$) in the brain uptake (peak brain uptake: 0.32 ± 0.0 SUV after 1 min; 0.16 ± 0.0 SUV after 55 min). Highest brain uptake was found in rats pre-treated with TQD: 1.04 ± 0.1 SUV at 55 min after tracer injection, which was 3 times higher compared to the maximum SUV of the two other groups. In the TQD pre-treatment group the brain uptake was continuously rising whereas in the two other groups the uptake remained stable after the first 5 min. Representative triplanar scans of all three groups are shown in Fig. 4.

Since the brains of all groups were counted in the Gamma Counter, too, the findings of the PET scans could be confirmed: Brains of the baseline and SNAP-7941 pre-treatment group evinced the same activities (0.07 ± 0.0 SUV) whereas the activity of the brains of the TQD pre-treated group (0.35 ± 0.0 SUV) was even 5 times higher compared to the two other groups. The brain to blood ratio was 0.37 for the baseline group, 0.24 for the SNAP-7941 pre-treatment group and 2 for the TQD pre-treatment group.

In plasma, 20.0 ± 3% (n=3) of a hydrophilic metabolite was found after 20 min. Neither in the baseline group (20 min after tracer injection) nor in the pre-treatment with TQD group (60 min after tracer injection), a brain metabolite was found.

Discussion

[^{11}C]SNAP-7941 and the reference compound SNAP-7941 are the racemate of the compound presented by Borowsky et al. [16], who used the (+)-enantiomer. This

could be the explanation for the lower binding affinity of SNAP-7941 (K_i = 4.52 ± 0.7 nM) compared to (+)-SNAP-7941 (K_d = 0.18 nM, [13]). Additionally, the well-known discrepancy between K_i and K_d values (due to the different binding properties of molecules in competition and saturation assays) could contribute to that deviation.

[^{11}C]SNAP-7941 was highly stable against porcine carboxylesterase, human and rat liver microsomes. These microsomes consist of the multi enzyme complex Cytochrom P-450 and produce 9.59 ± 0.7% (human) and 1.27 ± 0.8% (rat) decomposition after 60 min. In human plasma no decomposition at all was observed. In contrast, [^{11}C]SNAP-7941 was rapidly metabolized in rat plasma. 50.40 ± 0.7% of intact [^{11}C]SNAP-7941 were observed after 60 min. The stability against liver microsomes and in plasma is comparable with the fluoroethylated analogue [^{18}F]FE@SNAP, which was also highly stable against human and rat liver microsomes and in human plasma, but completely metabolized in rat plasma within 120 min [25]. The plasma free fraction of [^{11}C]SNAP-7941 is high enough for potential brain imaging (f_1=20.96 ± 1.0% in human plasma, f_1=32.44 ± 0.8% in rat plasma) and is even higher than that of [^{18}F]FE@SNAP (f_1=12.6 ± 0.2% in human plasma, no data in rat plasma) [25]. For better understanding of the in vivo data, which were obtained from rats, in vitro metabolism experiments were also performed with rat plasma and enzymes.

For prediction of blood-brain barrier (BBB) penetration the lipophilicity, expressed as logD, was measured in a first step. SNAP-7941 has an acceptable logD of 3.29. Since logP/logD values were shown to be poor predictors for BBB penetration [26], IAM chromatography was performed additionally. Under the modified conditions from Tavares et al. [24] SNAP-7941 (P_m=0.79) is situated well in between of ß-CIT (P_m=0.31) and DASB (P_m=1.23) – two compounds known to penetrate the BBB. Therefore, considering only the passive diffusion, a prediction of a BBB penetration seems reasonable.

The small-animal PET experiments showed low but stable uptake in the brain of the baseline and SNAP-7941 pre-treatment group and continuously rising uptake in the TQD pre-treatment group. It can be assumed, that [^{11}C]SNAP-7941 is a Pgp/BCRP substrate, since brain uptake as measured with PET of this group was 3 times higher compared to the two other groups. No metabolite was found in the

brain. The hydrophilic metabolite found in the rat plasma (in vivo) was in accordance with the fast metabolism observed in the in vitro tests in rat plasma.

The fact, that [^{11}C]SNAP-7941 could be a Pgp/BCRP substrate, was surprising, since Borowsky et al. [16] observed a significant reduction in food intake and body weight after ip application (3-30mg/kg) of (+)-SNAP-7941 and drugs have to cross the BBB for a reduction of food intake [27]. An explanation could be the lower density of MCHR1 in healthy rats, being too low for quantitative imaging.

Nevertheless, species differences in the uptake of Pgp substrates were reported for several tracers, e.g. [^{11}C]WAY-100635 or [^{18}F]altanserin. These radioligands are Pgp substrates in rodents, but serve as routine brain tracers in human applications [28, 29]. The Pgp in the BBB of rodents is discussed to be more pronounced. A recent paper [30] reported on species differences between humans and rodents and showed a 2.33-fold higher expression of Pgp at the mouse BBB.

Biodistribution experiments showed both, uptake in kidneys and intestines. At this point, a specification of the major way of excretion would be too speculative. Knowing from the small animal experiments, that [^{11}C]SNAP-7941 is a Pgp/BCRP substrate, it was not surprising that the uptake in the brain was low (0.05 ± 0.03 SUV). Highest uptake was found in adrenals, where MCHR1 expression was described by Saito et al. [31]. The uptake in the pancreas, eyes, muscle and ovary follows the described distribution [31, 32]. Low uptake in our healthy rat model was found in peripheral fat tissue. It is known that MCHR1 is expressed in fat tissue [5], but to the best of our knowledge, the extent of increase of expression in obese rats is unknown.

A series of preclinical tests have been performed, starting with the evaluation of the binding properties, as it is a prerequisite for understanding the behaviour of the drug in further experiments. Since a rapid metabolism is influencing the in vivo characteristics it is crucial to understand the enzymes involved in the cleavage and which major metabolites are formed to a significant extent. These metabolites – if occurred in the target organ – would have to be characterized regarding a potential interference on the receptors. In order to predict BBB-penetration at an early stage of the evaluations, several methods can be applied. Having done several studies with logP in recent years, we had to learn, that it is a poor predictor for BBB-penetration. The introduction of the IAM-medhod by Tavares et al [24] is a further

step for that prediction. It is well known, that rodents express Pgp to a higher extent than humans and low brain-uptake can be caused by that efflux-protein. The evaluation of the involvement of Pgp in the tracer kinetics should therefore always be considered.

Conclusion

[^{11}C]SNAP-7941 evinced high stability against liver microsomes, carboxylesterase and in human plasma. The binding affinity of the racemate is lower compared to the (+)-enantiomer, but is still in a low nanomolar range.
The first small-animal PET experiments revealed a 5 fold increased brain uptake after Pgp/BCRP inhibition. No metabolites were found in brain.
On the basis of these experiments with healthy rats, the suitability of [^{11}C]SNAP-7941 for the visualisation of central and peripheral MCHR1 remains speculative. Further experiments in obese and diabetic rats will show the applicability of the MCHR1 concept.

Acknowledgments

This research was part of an ongoing study, funded by the Austrian Science Fund (FWF P20977-B09; P.I.: M. Mitterhauser). The authors thank Johann Stanek (AIT) for his support in the radiochemistry laboratory, Michael Sauberer (AIT) for his skilful help with laboratory animal handling and Oliver Langer (AIT) for his organizing talents. Teresa Heissenberger is acknowledged for her participation in the binding experiments; Matthias Hendl is acknowledged for his support in the IAM chromatography and plasma stability experiments.

References

[1] Bittencourt JC, Presse F, Arias C, Peto C, Vaughan J, Nahon JL, et al. The melanin-concentrating hormone system of the rat brain: An immuno- and hybridization histochemical characterization. J Comp Neurol 1992;319:218-45.

[2] Casatti CA, Elias CF, Sita LV, Frigo L, Furlani VCG, Bauer JA, et al. Distribution of melanin-concentrating hormone neurons projecting to the medial mammillary nucleus. Neuroscience 2002;115:899-915.

[3] Tadayyon M, Welters HJ, Haynes AC, Cluderay JE, Hervieu G. Expression of melanin-concentrating hormone in insulin-producing cells: MCH stimulates insulin release in RINm5F and CRI-G1 cell-lines. Biochem Biophys Res Commun 2000;275:709-12.

[4] Kokkotou E, Moss AC, Torres D, Karagiannides I, Cheifetz A, Liu S, et al. Melanin-concentrating hormone as a mediator of intestinal inflammation. Proc Natl Acad Sci USA 2008;105:10613-8.

[5] Bradley RL, Kokkotou EG, Maratos-Flier E, Cheatham B. Melanin-concentrating hormone regulates leptin synthesis and secretion in rat adipocytes. Diabetes 2000;49:1073-7.

[6] Bradley RL, Mansfield JP, Maratos-Flier E, Cheatham B. Melanin-concentrating hormone activates signaling pathways in 3T3-L1 adipocytes. Am J Physiol Endocrinol Metab 2002;283:E584-92.

[7] Marsh DJ, Weingarth DT, Novi DE, Chen HY, Turmbauer ME, Chen AS, et al. Melanin-concentrating hormone 1 receptor-deficient mice are lean, hyperactive, and hyperphagic and have altered metabolism. Proc Natl Acad Sci USA 2002;99:3240-5.

[8] Ito M, Gomori A, Ishihara A, Oda Z, Mashiko S, Matsushita H, et al. Characterization of MCH-mediated obesity in mice. Am J Physiol Endocrinol Metab 2003;284:E940-5.

[9] Roy M, David N, Cueva M, Giorgetti M. A Study of the Involvement of Melanin-Concentrating Hormone Receptor 1 (MCHR1) in Murine Models of Depression. Biol Psychiatry 2007;61:174-80.

[10] Saito Y, Nothacker HP, Wang Z, Lin SH, Leslie F, Civelli O. Molecular characterization of the melanin-concentrating-hormone receptor. Nature 1999;400:265-9.

[11] Shimomura Y, Mori M, Sugo T, Ishibashi Y, Abe M, Kurokawa T, et al. Isolation and identification of melanin-concentrating hormone as the endogenous ligand of the SLC-1 receptor. Biochem Biophys Res Commun 1999;261:622-6.

[12] Chambers J, Ames RS, Bergsma D, Muir A, Fitzgerald LR, Hervieu G, et al. Melanin-concentrating hormone is the cognate ligand for the orphan G-protein-coupled receptor SLC-1. Nature 1999;400:261-5.

[13] Lembo PM, Grazzini E, Cao J, Hubatsch DA, Pelletier M, Hoffert C, et al. The receptor for the orexigenic peptide melanin-concentrating hormone is a G-protein-coupled receptor. Nat Cell Biol 1999;1:267-71.

[14] Luthin DR. Anti-obesity effects of small molecule melanin-concentrating hormone receptor1 (MCHR1) antagonists. Life Sciences 2007;81:423-40.

[15] Gattrell WT, Sambrook Smith CP, Smith AJ. An example of designed multiple ligands spanning protein classes: Dual MCH-1R antagonists/DPPIV inhibitors. Bioorg Med Chem Lett 2012;22:2464-9.

[16] Borowsky B, Durkin MM, Ogozalek K, Marzabadi MR, DeLeon J, Lagu B, et al. Antidepressant, anxiolytic and anorectic effects of a melanin-concentrating hormone-1 receptor antagonist. Nat Med 2002;8:825-30.

[17] Philippe C, Schirmer E, Mitterhauser M, Shanab K, Lanzenberger R, Karanikas G, et al. Radiosynthesis of [^{11}C]SNAP-7941 – the first PET-tracer for the melanin concentrating hormone receptor 1 (MCHR1). Appl Radiat Isot 2012;70:2287-94.

[18] Philippe C, Ungersboeck J, Schirmer E, Zdravkovic M, Nics L, Zeilinger M, et al. [^{18}F]FE@SNAP – A new PET tracer for the melanin concentrating hormone receptor 1 (MCHR1): Microfluidic and vessel-based approaches. Bioorg Med Chem 2012;20:5936-40.

[19] Mashiko S, Ishihara A, Gomori A, Moriya R, Ito M, Iwaasa H, et al. Antiobesity effect of a melanin-concentrating hormone 1 receptor antagonist in diet-induced obese mice. Endocrinology 2005;146:3080-6.

[20] Nics L, Vraka C, Hendl M, Haeusler D, Wagner KH, Shanab K, et al. In-vitro stability of [^{18}F]FE@SUPPPY and [^{18}F]FE@SUPPY:2 against human liver-microsomes and human plasma. Nuklearmedizin 2011;50:A176.

[21] Parsey RV, Slifstein M, Hwang D-R, Abi-Dargham A, Simpson N, Mawlawi O, et al. Validation and reproducibility of measurement of 5-HT IA receptor parameters with *[carbonyl-I* I C]WAY-100635 in humans: comparison of arterial and reference tissue input functions. J Cereb Blood Flow Metab 2000;20:1111-33.

[22] Nics L, Haeusler D, Wadsak W, Wagner KH, Dudczak R, Kletter K, et al. The stability of methyl-, ethyl- and fluoroethylesters against carboxylesterases in vitro: there is no difference. Nucl Med Biol 2011;38:13-7.

[23] Donovan SF and Pescatore MC. Method for measuring the logarithm of the octanol-water partition coefficient by using short octadecyl-poly(vinyl alcohol) high-performance liquid chromatography columns. J Chromatogr A 2002;952:47-61.

[24] Tavares AA, Lewsey J, Dewar D, Pimlott SL. Radiotracer properties determined by high performance liquid chromatography: a potential tool for brain radiotracer discovery. Nucl Med Biol 2012;39:127-35.

[25] Philippe C, Nics L, Zeilinger M, Schirmer E, Spreitzer H, Karanikas G, et al. Preparation and first preclinical evaluation of [^{18}F]FE@SNAP: a new PET tracer for the melanin concentrating hormone receptor 1 (MCHR1). EJNMMI Research 2013; submitted.

[26] Naik P and Cucullo L. In vitro blood-brain barrier models: Current and perspective technologies. J Pharm Sci 2012;101:1337-54.

[27] Hu XE, Wos JA, Dowty ME, Suchanek PM, Ji E, Chambers JB, et al. Small-molecule melanin-concentrating hormone-1 receptor antagonists require brain penetration for inhibition of food intake and reduction in body weight. J Pharmacol Exp Ther 2008;324:206-13.

[28] Elsinga P, Hendrikse NH, Bart J, Van Waarde A, Vaalburg W. Positron emission tomography studies on binding of central nervous system drugs and P-glycoprotein function in the rodent brain. Mol Imaging Biol 2005;7:37-40.

[29] Syvänen S, Lindhe Ö, Palner M, Kornum BR, Rahaman O, Langström B, et al. Species differences in blood-brain barrier transport of three positron emission

tomography radioligands with emphasis on P-glycoprotein transport. Drug Metab Dispos 2009;37:635-43.

[30] Uchida Y, Othsuki S, Katsukura Y, et al. Quantitative targeted absolute proteomics of human blood-brain-barrier transporters and receptors. *J Neurochem*. 2011; doi: 10.1111/j.1471-4159.2011.07208.x

[31] Saito Y, Nothacker HP, Civelli O. Melanin-concentrating hormone receptor: an orphan receptor fits the key. TEM 2000;11:299-303.

[32] Saito Y, Nothacker HP, Wang Z, Lin SH, Leslie F, Civelli O. Molecular characterization of the melanin-concentrating-hormone receptor. Nature 1999;400:265-9.

Captions

Fig 1. Chemical structure of [^{11}C]SNAP-7941.

Fig 2. Tissue-to-blood uptake ratios (mean over 4 animals) of [^{11}C]SNAP-7941. Values were calculated by division of tissue by blood for each individual subject [e.g. brain (rat 1)/blood (rat 1), etc.]. Bars represent arithmetic means ± standard deviation. If not visible, error bars are within the margin of the symbols.

Fig 3. TACs (mean SUV ± SD) of [^{11}C]SNAP-7941 in whole brain of the baseline group (filled circles, n=6), the pre-treatment with SNAP-7941 group (open circles, n=3) and the pre-treatment with TQD group (open squares, n=3). If not visible, error bars are within the margin of the symbols.

Fig 4. Exemplary coronal (left), horizontal (centre) and sagittal (right) PET summation images (0-60 min) in rats. Baseline scan (A), pre-treatment with SNAP-7941 (B) and pre-treatment with TQD (C). Anatomical structures are indicated by arrows (br, brain; sg, submandibular gland).

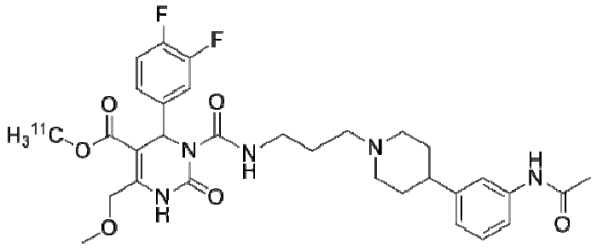

Fig 1. Chemical structure of [^{11}C]SNAP-7941.

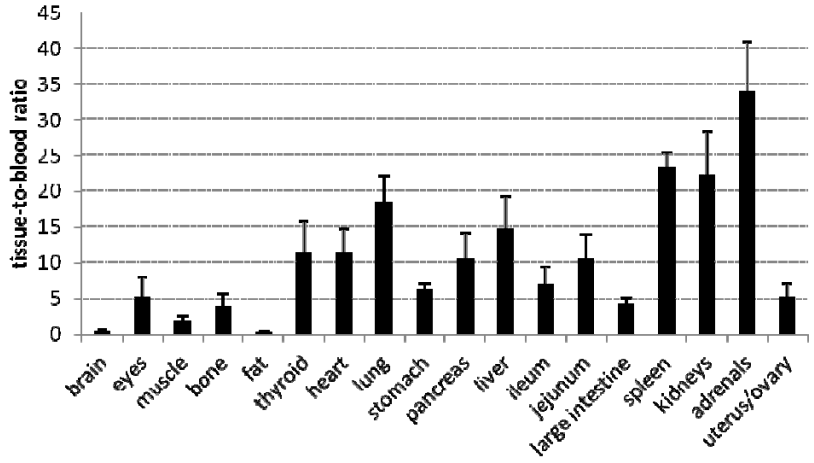

Fig 2. Tissue-to-blood uptake ratios (mean over 4 animals) of [^{11}C]SNAP-7941. Values were calculated by division of tissue by blood for each individual subject [e.g. brain (rat 1)/blood (rat 1), etc.]. Bars represent arithmetic means ± standard deviation. If not visible, error bars are within the margin of the symbols.

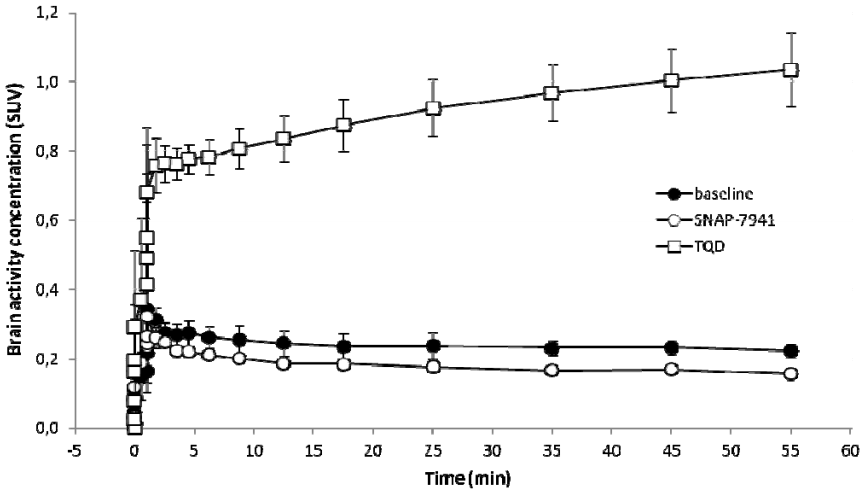

Fig 3. TACs (mean SUV ± SD) of [^{11}C]SNAP-7941 in whole brain of the baseline group (filled circles, n=6), the pre-treatment with SNAP-7941 group (open circles, n=3) and the pre-treatment with TQD group (open squares, n=3). If not visible, error bars are within the margin of the symbols.

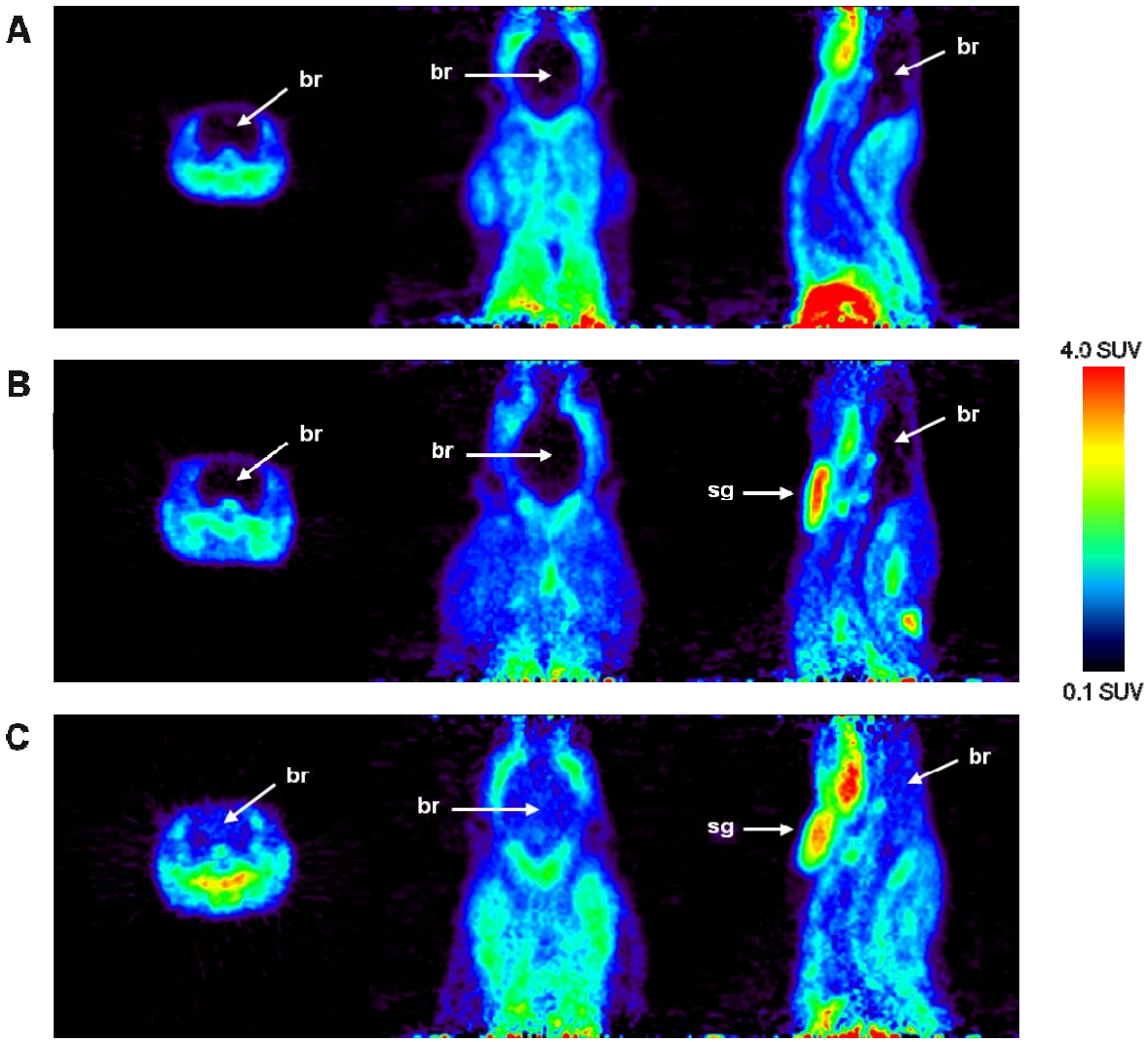

Fig 4. Exemplary coronal (left), horizontal (centre) and sagittal (right) PET summation images (0-60 min) in rats. Baseline scan (A), pre-treatment with SNAP-7941 (B) and pre-treatment with TQD (C). Anatomical structures are indicated by arrows (br, brain; sg, submandibular gland).

2.6. Manuscript #5

Comparative *in vitro* autoradiographic investigation of melanin concentrating hormone receptor 1 ligands in the central nervous system

European Journal of Pharmacology, submitted 8th May 2013

Cécile Philippe[1,2,#], Daniela Haeusler[1,#], Florian Fuchshuber[1,2], Helmut Spreitzer[3], Helmut Viernstein[2], Wolfgang Wadsak[1], Markus Mitterhauser[1,2,4]

[1]Biochemistry and Biomarker Development Unit, Department of Nuclear Medicine, Medical University of Vienna, 1090 Vienna, Austria

[2]Department of Pharmaceutical Technology and Biopharmaceutics, University of Vienna, 1090 Vienna, Austria

[3]Department of Drug and Natural Product Synthesis, University of Vienna, 1090 Vienna, Austria

[4]Hospital Pharmacy of the General Hospital of Vienna, 1090 Vienna, Austria

[#] These authors contributed equally to this manuscript.

Abstract

The MCHR1 is an interesting pharmacological and pharmaceutical target, due to its involvement in a variety of pathologies, as diabetes, gut inflammation and adiposity. Therefore, we developed two different potential PET-tracers, [^{11}C]SNAP-7941 and [^{18}F]FE@SNAP, for the *in vivo* visualization of this receptor. The potency and suitability for the MCHR1 of both molecules was evaluated in a preclinical setting. Therefore, aim of the present study was a comparative autoradiographic *in vitro* investigation in the CNS (in rat brain and 4 different human brain regions) using the two radioligands [^{125}I]-MCH and [^{125}I]-S36057. Competition was performed with specific MCHR1 ligands as PMC-3886, a commercially available MCHR1 agonist, and with SNAP-7941 and FE@SNAP, two MCHR1 antagonists. Additional immunohistochemical staining of the MCHR1 in vicinal human and rat brain tissues aimed for potential verification of the autoradiographic findings.

Specific amounts of MCHR1 competition (Δx) were found in all investigated brain tissues. Higher amounts of mean Δx of all three competitors were found in rat brain tissues (36±10%) compared to summed human brain regions (13±8%). Ranking of mean Δx in human brain tissues followed the order of hypothalamus>hippocampus>cerebellum> thalamus. MCHR1 antibody staining complemented the outcome of the autoradiographic experiments. The comparative evaluation of PMC-3886 with SNAP-7941 and FE@SNAP revealed highest competition potency for SNAP-7941, followed by FE@SNAP and PMC-3886. Thus, both novel MCHR1 antagonists qualify for further preclinical evaluation as potential MCHR1 PET-tracers.

Keywords: autoradiography, MCHR1, SNAP-7941, FE@SNAP, CNS

1. Introduction

The melanin concentrating hormone receptor 1 (MCHR1) was identified in 1999 (Chambers et al., 1999; Lembo et al., 1999; Saito et al., 1999; Shimomura et al., 1999) and is generally involved in energy homeostasis (Ito et al., 2003; Marsh et al., 2002). Changes in its expression, both, up- and down-regulation were discussed to be associated with central and peripheral pathologies such as obesity, diabetes, deregulation of metabolic feedback mechanisms and gut inflammation (Bradley et al. 2002, 2002; Kokkotou et al., 2008; Tadayyon et al., 2002). Several MCHR1 antagonists were introduced in the past decade, some of them even entered clinical trials for obesity treatment (Luthin, 2007). Furthermore, this receptor is involved in the control of sleep and in psychiatric disorders as depression and anxiety (Lagos et al., 2009; Roy et al., 2007). The MCHR1 is widespread throughout the central nervous system (CNS), especially in hypothalamic and thalamic neurons (Bittencourt et al., 1992; Casatti et al. 2002). Sone et al. (2000) found a regional distribution in humans in the following order: hypothalamus>thalamus>pons>medulla oblongata>cerebellum>cortex. In rats, the MCHR1 is present in high abundance in amygdala, hypothalamus, hippocampus, cortex, nucleus accumbens and substantia nigra (Hervieu et al., 2002; Saito et al.,

2001). Comparing human and rat MCHR1, the amino acid sequence displays high correlation of 96% (Pissios and Maratos-Flier, 2003). Due to its widespread appearance and involvement in the human organism, this receptor is a very promising and interesting pharmacological target for a variety of applications. So far, most investigations regarding the MCHR1 were conducted in-vitro and in preclinical settings. To enable translation from preclinical data to clinic, the development and evaluation of a suitable positron emission tomography (PET) tracer is mandatory. PET is a high end technique allowing non-invasive in-vivo quantification and visualization of receptors systems, enzymes and transporters. Most PET tracers for receptor systems are antagonists, to prevent potential reaction cascades of agonists. On the basis of the highly potent MCHR1 antagonist (+)-SNAP-7941 (K_d=0.18nM; Borowsky et al., 2002), we developed [^{11}C]SNAP-7941 - the first PET tracer for the MCHR1 (Philippe et al., 2012a). Additionally, we created a fluoroethylated derivative of SNAP-7941, [^{18}F]FE@SNAP, as a second potential PET-tracer for this receptor (Philippe et al., 2012b), with the advantage of the longer half-life of fluorine-18 (110min for ^{18}F vs. 20min for ^{11}C). After the successful synthesis of [^{11}C]SNAP-7941 and [^{18}F]FE@SNAP, the next consequential step in the preclinical evaluation process was an autoradiographic study on human and rat brain tissues. To prove suitability of the two newly developed PET tracers, aim of the present study was a comparative in-vitro autoradiographic investigation of the MCHR1 ligands in the CNS. In detail, we aimed at

1. the comparison of PMC-3886, a well-known and commercially available MCHR1 agonist, with the antagonists SNAP-7941 and FE@SNAP in an autoradiographic evaluation; and
2. the additional immunohistochemical staining of the MCHR1 in the dedicated brain regions.

2. Materials and Methods

2.1. Materials

Human post-mortem tissue was obtained from the neurobiobank of the Medical University of Vienna approved by the local ethics committee ("Molecular

neuropathologic investigation of neurodegenerative diseases" Nr. 396/2011) following the principles of the Helsinki declaration.

Male wild-type rats (200-300g) were deeply anesthetized by diethylether and rapidly decapitated; brains were removed and subsequently quick-frozen. Research using animal tissues was carried out under institutional approval and was in accordance with the Austrian Animal Care Law.

2.1.1. Autoradiographic experiments

Different anatomical regions (hippocampus, hypothalamus, thalamus and cerebellum) sampled from human post-mortem brains (7-9 hours post-mortem time, no history of neurological disease) were quick-frozen in isopentane (2-Methylbutane, CAS Number: 78-78-4, Sigma Aldrich, Vienna, Austria). For cutting the various tissues, a micro-cryotome (Thermo Scientific Microm HM 560, HistoCom, Wiener Neudorf, Austria) was used. Frozen samples were thaw-mounted onto superfrost slides (Thermo Scientific, Menzel-Gläser SUPERFROST® PLUS, microscope slides, Braunschweig, Germany). A barrier pen was purchased from Invitrogen (Mini PAP PEN, Zymed® Laboratories, Carlsbad, CA, USA). The radioligands [^{125}I]-MCH (Fig.1 (1a), Table 1) and [^{125}I]-S36057 (Fig.1 (1b), Table 1) were purchased from Perkin Elmer (Brunn am Gebirge, Austria). PMC-3886 (Fig.1 (2), Table 1) was purchased from Peptides International (Louisville, Kentucky, USA). Title compounds SNAP-7941 (methyl-3-{[(3-{4-[3-(acetylamino)phenyl]-1-piperidinyl}propyl)amino]carbonyl}-4-(3,4-difluorophenyl)-6-(methoxymethyl)-2-oxo-1,2,3,4-tetrahydro-5-pyrimidinecarboxylate hydrochloride) (Fig.1 (3a), Table 1) and FE@SNAP (2-fluoroethyl-3-{[(3-{4-[3-(acetylamino)phenyl]-1-piperidinyl}propyl)amino]carbonyl}-4-(3,4-difluorophenyl)-6-(methoxymethyl)-2-oxo-1,2,3,4-tetrahydro-5-pyrimidinecarboxylate hydrochloride) (Fig.1 (3b), Table 1) were synthesized at the Department of Drug and Natural Product Synthesis of the University of Vienna, Austria. Captopril was obtained from EMD Chemicals (Cat. 211875, San Diego, USA). $MgCl_2$ and $CaCl_2$ were purchased from Merck (Darmstadt, Germany). HEPES, bovine serum albumin (BSA), phenylmethanesulfonyl fluoride (PMSF), phosphoramidon and all other chemicals were purchased from Sigma Aldrich (Vienna, Austria).

The Cyclone Phosphor Imager (Cyclone Plus Storage Phosphor System) and Phosphor Imager plates (Multisensitive Phosphor Screens Long Type MS, PPN 7001724) were purchased from Perkin Elmer (Brunn am Gebirge, Austria); lead shielded cassettes (Fisher Biotech Autoradiography Cassette FBCS 1417) from Fisher Scientific (Pittsburgh, PA, USA).

2.1.2. Immunohistochemical staining

Primary antibody (MCH-1R (C-17):sc-5534) was purchased from Santa Cruz Biotechnology (Santa Cruz, CA, USA). Secondary Antibody (biotinylated anti-goat IgG), the Avidin-Biotin-Complex (Vectastain ABC Kit, PK 4001), aqueous mounting medium (VectaMount™) and AEC solution (AEC Substrate Kit for peroxidase, SK-4200) were obtained from Vector Laboratories (Burlingame, CA, USA). The reflected-light microscope (Olympus IMT-2) equipped with a camera (Olympus XC50) and imaging software were purchased from Olympus Soft Imaging Solutions GmbH (Münster, Germany). Phosphate buffered saline (PBS) was purchased from Morphisto® Evolutionsforschung und Anwendung GmbH (Frankfurt am Main, Germany).

2.1.3. Statistical analysis

All values are given as arithmetic means ± standard deviation (sd). To determine the significant differences a two-tailed t-test with $\alpha=0.95$ was performed using the statistics add-on in Windows® Excel 2007. A value of $P<0.05$ was considered to be significant.

2.2. Methods

2.2.1. Autoradiographic experiments

Human and rat brain tissues were quick-frozen in isopentane at -45°C in order to block further biological processes including protein degradation and tissue hardening and stored at –80°C. The night before cutting, tissues were transferred to a –20°C freezer. Frozen samples were sectioned in a micro-cryotome into 10µm thick tissue slices for all brain regions and thaw-mounted onto superfrost slides, dried and then stored at –40°C until processing. Autoradiographic experiments

were conducted on frozen human post-mortem brain slices derived from hippocampus, hypothalamus, thalamus and cerebellum, as well as on coronal rat brain slices.

The experimental set-up was conducted according to Able et al. (2009). Briefly, tissue slices were pre-incubated for 15 minutes at room temperature with an assay buffer solution (pH 7.4) containing 25mM HEPES, 5mM $MgCl_2$, 1mM $CaCl_2$, 0.5% BSA, 1mM PMSF, 1µM phosphoramidon, 10µM captopril and air dried. Subsequently, the slices were directly incubated with the TRIS HCl buffer solution containing one of the two commercially available MCHR1 radioligands ([^{125}I]-MCH (0.5nM); [^{125}I]-S36057 (0.05nM)) and one of the competitors (PMC-3886, SNAP-7941 and FE@SNAP) at concentrations ranging from 18-1000nM (equivalent to 100-fold of the K_d value of SNAP-7941 (0.18nM) up to 1µM, Table 1).

Following, slides were washed with 50mM Tris HCl buffer solution (pH 7.4) after incubation, rinsed with ice-cold water, and dried. Thereafter, samples were placed on Phosphor Imager plates for exposure for 6-11 days in dedicated lead shielded cassettes. Autoradiographic images were analyzed with a Cyclone Phosphor Imager and data analysis was performed with OptiQuant® data processing software Version 5.0 and Microsoft Excel® 2007.

2.2.2. Immunohistochemical staining

Immunohistochemical staining experiments were performed on rat and human brain tissues, vicinal to the tissues used for autoradiographic experiments. The staining procedure was a modification of a general protocol (Hofmann, 2002). In detail, the slices were incubated with 0.3% hydrogen peroxide (H_2O_2) for 30min to block endogenous peroxidase activity and were subsequently incubated with an appropriate blocking serum for 30min to prevent unspecific binding. Incubation with the 1:100 diluted primary antibody (MCH-1R (C-17):sc-5534) was performed for 12 hours at 4°C. The biotinylated secondary antibody and the Avidin-Biotin-Complex were prepared according to manufacturer's instructions and incubated for 30min. Finally, the slices were incubated with the freshly prepared AEC solution. The peroxidation reaction was monitored via reflected-light microscope equipped with a camera to determine the ideal point of terminating the reaction (ranging between 25min). The slices were washed twice with PBS buffer for 5min in between

all steps, except after the incubation with the blocking serum. To achieve permanent staining, slices were covered with an aqueous mounting medium and stored in a fridge at 4°C.

3. Results

Regions of interest (ROIs) were drawn around each tissue of each experiment; data were processed by OptiQuant® data software leading to digital light units per square millimetre (DLU/mm^2). DLU/mm^2 values were normalized into percentage values to enable comparison of data of the different experiments: Baseline (total binding) values were set to 100%, and competition was expressed relatively to this value. To compare the potency of the three dedicated MCHR1 ligands, % remaining activity (unspecific and unselective binding) after blocking of MCHR1 was determined, to receive specific amounts of MCHR1 competition (Δx) as shown in Fig. 2. Thus, Δx reflects specific binding blockable through competition.

3.1. Autoradiographic experiments

A general overview of Δx on human and rat brain tissues is shown in Table 2. All values are given in % as mean of quadruplet analyses from ≥2 different experiments each (n≥8).

3.1.1. Rat

Mean Δx (arithmetic mean of all three competitors) in coronal rat brain was found to be 36±10% (24.9% for PMC-3886, 40.6% for SNAP-7941 and 43.4% for FE@SNAP, Table 2).

3.1.1.1 Comparison of differences between radioligands

Comparing [^{125}I]-MCH (0.5nM) and [^{125}I]-S36057 (0.05nM), we observed no significant differences in competition behaviour of the investigated compounds. Therefore, values evinced from both radioligands were considered comparable.

3.1.1.2. Comparison of competitor concentrations

In rat tissue, different concentrations of competitors (18nM-1μM) did not reveal significant differences in Δx for PMC-3886, SNAP-7941 and FE@SNAP.

3.1.2. Human

A typical representative [^{125}I]-MCH competition image in human hypothalamus and thalamus under baseline and blocking conditions is shown in Fig. 3.

PMC-3886 evinced no competition in hippocampus, Δx of 10.2% in hypothalamus, Δx of 3.3% in thalamus and Δx of 10.2% in cerebellum. SNAP-7941 evinced Δx of 16.6% in hippocampus, Δx of 33.0% in hypothalamus, Δx of 16.0% in thalamus and Δx of 12.8% in cerebellum. FE@SNAP evinced Δx of 20.0% in hippocampus, Δx of 10.3% in hypothalamus, Δx of 9.3% in thalamus and Δx of 10.0% in cerebellum (see Table 2).

3.2. Immunohistochemical staining

IHC staining in rat brain evinced high amounts of MCHR1, especially around the area of the third ventricle (Fig. 4A). Human brain region with the highest stained MCHR1 antibody density was hypothalamus and thalamus, medium density was found in hippocampus and medium to low density was found in cerebellum (Fig. 4B-E).

4. Discussion

General

The MCHR1 is an interesting pharmacological and pharmaceutical target, due to its involvement in a variety of pathologies, as diabetes, gut inflammation and adiposity. To understand the mechanisms involved in pathophysiological conditions of this receptor in more detail, non-invasive *in vivo* monitoring of the MCHR1 with PET would be of high value. Therefore, we developed two different potential PET tracers, [^{11}C]SNAP-7941 and [^{18}F]FE@SNAP. Both tracers have been synthesized in a reliable and successful manner (Philippe et al., 2012a, 2012b). Aim of the present study was a comparative autoradiographic *in vitro* investigation using two agonist

radioligands [^{125}I]-MCH and [^{125}I]-S36057 and three specific MCHR1 ligands (PMC-3886 (agonist), SNAP-7941 and FE@SNAP (antagonists)) in rat brain and 4 different human brain regions. Considering that the two radioligands, [^{125}I]-MCH and [^{125}I]-S36057, are both iodine-125 radiolabeled peptides, and are referred to undergo "decay catastrophe" (Doyle et al., 1984; Schmidt, 1984), we wanted to evaluate any differences. No significant differences between baseline binding of these two radioligands and in competition with the three MCHR1 ligands were observed. Additional immunohistochemical staining of the MCHR1 in vicinal human and rat brain regions supported the autoradiographic findings.

Data Analysis

Generally, ROIs were drawn around each tissue of each experiment for normalization of DLU/mm^2 values into percentage values as described in the results part. Focus in this study was the comparison of the potency of the three MCHR1 ligands to compete with commercially available MCHR1 radioligands. Through specific blocking, % remaining activity (unspecific and unselective binding) was received and subsequently specific amounts of MCHR1 competition (Δx) were obtained (Fig. 2). We want to point out, that these values do not necessarily reflect density and absolute quantitative values of MCHR1 in the investigated tissues. Nevertheless, density of MCHR1 derived from immunohistochemical staining was visually ranked and the resulting order was correlated with the ranking of Δx from our autoradiographic experiments. Furthermore, all values were compared with findings from literature (Saito et al., 1999; Sone et al., 2000).

Rat

We evaluated different concentrations ranging from 18nM to 1μM of competitors (PMC-3886, SNAP-7941 and FE@SNAP) to compare their potency. All three competitors lead to a decrease of binding with 100-fold of K_d (18nM for SNAP-7941 and FE@SNAP, 29nM for PMC-3886); interestingly, higher concentrations did not lead to further significant blocking.

Complementary to the high specific amounts of MCHR1 competition found in rat brain tissues by autoradiography (mean Δx 36±10%) IHC evinced high staining of MCHR1-antibody, especially in the dedicated region of the 3rd ventricle.

Human

Keeping the partly significant differences in competition behavior of the three competitors in mind, mean Δx (arithmetic mean over all competitors) for each tissue was calculated for comparison reasons with rat tissues and to gain an overall ranking of competition in the different tissue origins. Therefore, highest amount of mean Δx was found in hypothalamus with 18±13%, followed with 12±11% in hippocampus, 11±2% in cerebellum and 10±6% in thalamus (Table 2). Comparing rat and human Δx, we found higher amounts of mean Δx in rat brain tissues (36±10%) than in summed human brain regions (13±8%) (Table 2).

In detail, SNAP-7941 showed the highest competition potency, leading to significant displacement of the radioligand in hypothalamus compared to PMC-3886 and FE@SNAP and to significant displacement in thalamus in comparison to PMC-3886 (Fig. 5). In hippocampus competition potency of SNAP-7941 and FE@SNAP were comparable; interestingly PMC-3886 evinced no competition. In cerebellum all three competitors showed similar competition potency (Table 2). These differences between the three MCHR1 ligands may be explained from a chemical point of view: PMC-3886 is a peptide (Figure 1 (2)), in contrast to the small molecules SNAP-7941 and FE@SNAP (Figure 1 (3a & b)). From a biochemical point of view, differences could also be caused by well known different binding properties and characteristics of agonists (PMC-3886) and antagonists (SNAP-7941 and FE@SNAP). Differences in the values between the two antagonists SNAP-7941 and FE@SNAP may be explained by potential differences in affinity. (For direct comparison reasons in the autoradiographic experiments, the two antagonists were applied with the same affinity of 0.18nM (Borowsky et al. 2002).)

A ranking order of mean Δx distribution was found as following: hypothalamus>hippocampus>cerebellum>thalamus (Table 2). SNAP-7941 by itself revealed a ranking of Δx distribution in the order of hypothalamus>thalamus>hippocampus> cerebellum, which was in accordance with the distribution described by Sone et al. (2000).

Furthermore, IHC staining revealed the same order as SNAP-7941 and compliments these findings (Fig. 4). Nevertheless, in all autoradiographic rankings, the hypothalamus is the brain tissue with the highest Δx value (Table 2).

Furthermore, it is noteworthy that SNAP-7941 and FE@SNAP were obtained in their racemic form whereas Borowsky et al. described the enantiomerically pure (+)-SNAP-7941 compound. Therefore, absolute amounts of MCHR1 protein are expected to be even higher than determined in this work.

In summary, comparing rat and human specific amounts of MCHR1 competition (Δx), we found higher amounts of mean Δx in rat brain tissues (36±10%) than in summed human brain regions (13±8%) (Table 2). This finding may be explained by the fact that in humans there is a second MCH receptor subtype, namely MCHR2, which does not occur in rodents. The MCHR2 was identified two years after MCHR1 and has a similar distribution in the brain (An et al., 2001; Hill et al., 2001; Sailer et al., 2001; Wang et al., 2001), yet its distinct functions are still to be discovered. Since both radioligands display high affinity towards the MCHR1 and the MCHR2, differences in binding behavior in the two different origins (human and rat) were expected. The examined MCHR1 ligands are considered to be highly selective compounds (Table 1) and therefore higher competition rates in rats are legitimate.

5. Conclusions

Specific amounts of MCHR1 competition (Δx) were found in all investigated brain tissues, whereat hypothalamus was the region with highest Δx. SNAP-7941 revealed a ranking of Δx distribution in the order of hypothalamus>thalamus>hippocampus> cerebellum, which was in accordance with literature (Sone et al., 2000). IHC staining complemented the outcome of the autoradiographic experiments.

The comparative evaluation of PMC-3886 with SNAP-7941 and FE@SNAP revealed highest competition potency for SNAP-7941, followed by FE@SNAP and PMC-3886. Thus, both novel MCHR1 antagonists qualify for further preclinical evaluation as potential MCHR1 PET-tracers.

Acknowledgements

This research is part of an ongoing study, funded by the Austrian Science Fund (FWF P20977-B09; P.I.: M. Mitterhauser). The authors thank Adelheid Wöhrer for providing human tissues from the neurobiobank of the Medical University of Vienna.

References

Able, S.L., Ivarsson, M., Fish, R.L., Clarke, T.L., McCourt, C., Duckworth, J.M., Napier, C., Katugampola, S.D., 2009. Localisation of melanin-concentrating hormone receptor 1 in rat brain and evince that sleep parameters are not altered despite high central receptor occupancy. Eur. J. Pharmacol. 616, 101-106.

An, S., Cutler, G., Zhao, J.J., Huang, S.G., Tian, H., Li, W., Liang, L., Rich, M., Bakleh, A., Du, J., Chen, J.L., Dai, K., 2001. Identification and characterization of a melanin-concentrating hormone receptor. Proc. Natl. Acad. Sci. USA 98, 7576-7581.

Audinot, V., Beauverger, P., Lahaye, C., Suply, T., Rodriguez, M., Ouvry, C., Lamamy, V., Imbert, J., Rique, H., Nahon, J.L., Galizzi, J.-P., Canet, E., Levens, N., Fauchère, J.-L., Boutin, J.A., 2001a. Structure activity relationship studies of MCH-related peptide ligands at SLC-1, the human melanin-concentrating hormone receptor. J. Biol. Chem. 276, 13554-13562.

Audinot, V., Lahaye, C., Suply, T., Beauverger, P., Rodriguez, M., Galizzi, J.-P., Fauchère, J.-L., Boutin, J.A., 2001b. [^{125}I]-S36057 : a new and highly potent radioligand for the melanin-concentrating hormone receptor. Br. J. Pharmacol. 133, 371-378.

Bednarek, M.A., Tan, C., Hreniuk, D.L., Palyha, O.C., MacNeil, D.J., Van der Ploeg, L.H.Y., Howard, A.D., Feighner, S.D., 2002. Synthesis and biological evaluation in vitro of a selective, high potency petide agonist of human melanin-concentrating hormone action at human melanin-conenctrating hormone receptor 1. J. Biol. Chem. 277, 13821-13826.

Bittencourt, J.C., Presse, F., Arias, C., Peto, C., Vaughan, J., Nahon, J.L., Vale, W., Sawchenko, P.E., 1992. The melanin-concentrating hormone system of the rat brain: An immuno- and hybridization histochemical characterization. J. Comp. Neurol. 319, 218-245.

Borowsky, B., Durkin, M.M., Ogozalek, K., Marzabadi, M.R., DeLeon, J., Lagu, B., Heurich, R., Lichtblau, H., Shaposhnik, Z., Daniewska, I., Blackburn, T.P., Branchek, T.A., Gerald, C., Vaysse, P.J., Forray, C., 2002. Antidepressant, anxiolytic and anorectic effects of a melanin-concentrating hormone-1 receptor antagonist. Nat. Med. 8, 825-830.

Bradley, R.L., Kokkotou, E.G., Maratos-Flier, E., Cheatham, B., 2000. Melanin-concentrating hormone regulates leptin synthesis and secretion in rat adipocytes. Diabetes 49, 1073-1077.

Bradley, R.L., Mansfield, J.P., Maratos-Flier, E., Cheatham, B., 2002. Melanin-concentrating hormone activates signaling pathways in 3T3-L1 adipocytes. Am. J. Physiol. Endocrinol. Metab. 283, E584-E592.

Casatti, C.A., Elias, C.F., Sita, L.V., Frigo, L., Furlani, V.C.G., Bauer, J.A., Bittencourt, J.C., 2002. Distribution of melanin-concentrating hormone neurons projecting to the medial mammillary nucleus. Neuroscience 115, 899-915.

Chambers, J., Ames, R.S., Bergsma, D., Muir, A., Fitzgerald, L.R., Hervieu, G., Dytko, G.M., Foley, J.J., Martin, J., Liu, W.S., Park, J., Ellis, C., Ganguly, S., Konchar, S., Cluderay, J., Leslie, R., Wilson, S., Sarau, H.M., 1999. Melanin-concentrating hormone

is the cognate ligand for the orphan G-protein-coupled receptor SLC-1. Nature 400, 261-265.

Doyle, V.M., Buhler, F.R., Burgisser, E., 1984. Inappropriate correction for radioactive decay in fully iodinated adrenergic radioligands. Eur. J. Pharm. 99, 353-356.

Hervieu, G.J., Cluderay, J.E., Harrison, D., Meakin, J., Maycox, P., Nasit, S., Leslie, R.A., 2000. The distribiution of the mRNA and protein products of the melanin-concentrating hormone (MCH) receptor gene, slc-1, in the central nervous system of the rat. Eur. J. Neurosci. 12, 1194-1216.

Hill, J., Duckworth, M., Murdock, P., Rennie, G., Sabido-David, C., Ames, R. S., Szekeres, P., Wilson, S., Bergsma, D.J., Gloger, I.S., Levy, D.S., Chamber; J.K., Muir, A.I., 2001. Molecular cloning and functional characterization of MCH2, a novel human MCH receptor. J. Biol. Chem. 276, 20125-20129.

Hofman, F., 2002. Immunohistochemistry. Curr. Protocols Immun. Suppl 49, 21.4.1-21.4.23.

Ito, M., Gomori, A., Ishihara, A., Oda, Z., Mashiko, S., Matsushita, H., Yumoto, M., Ito, M., Sano, H., Tokita, S., Moriya, M., Iwaasa, H., Kanatani, A., 2003. Characterization of MCH-mediated obesity in mice. Am. J. Physiol. Endocrinol. Metab., 284, E940-E945.

Kokkotou, E., Moss, A.C., Torres, D., Karagiannides, I., Cheifetz, A., Liu, S., O'Brian, M., Maratos-Flier, E., Pothoulakis, C., 2008. Melanin-concentrating hormone as a mediator of intestinal inflammation. Proc. Natl. Acad. Sci. USA 105, 10613-10618.

Lagos, P., Torterolo, P., Jantos, H., Chase, M.H., Monti, J.M., 2009. Effects on sleep of melanin-concentrating hormone (MCH) microinjections into the dorsal raphe nucleus. Brain Res. 1265, 103-110.

Lembo, P.M.C., Grazzini, E., Cao, J., Hubatsch, D.A., Pelletier, M., Hoffert, C., St-Onge, S., Pou, C., Labreque, J., Groblewski, T., O'Donnell, D., Payza, K., Ahmad, S., Walker, P., 1999. The receptor for the orexigenic peptide melanin-concentrating hormone is a G-protein-coupled receptor. Nat. Cell. Biol. 1, 267-271.

Luthin, D.R., 2007. Anti-obesity effects of small molecule melanin-concentrating hormone receptor1 (MCHR1) antagonists. Life Sciences 81, 423-440.

Marsh, D.J., Weingarth, D.T., Novi, D.E., Chen, H.Y., Turmbauer, M.E., Chen, A.S., Guan, X.M., Jiang, M.M., Feng, Y., Camacho, R.E., Shen, Z., Frazier, E.G., Yu, H., Metzger, J.M., Kuca, S.J., Shearman, L.P., Gopal-Truter, S., MacNeil, D.J., Strack, A.M., MacIntyre, D.E., Van der Ploeg, L.H.T., Qian, S., 2002. Melanin-concentrating hormone 1 receptor-deficient mice are lean, hyperactive, and hyperphagic and have altered metabolism. Proc. Natl. Acad. Sci. USA 99, 3240-3245.

Philippe, C., Schirmer, E., Mitterhauser, M., Shanab, K., Lanzenberger, R., Karanikas, G., Spreitzer, H., Viernstein, H., Wadsak, W., 2012a. Radiosynthesis of [^{11}C]SNAP-7941 – the first PET-tracer for the melanin concentrationg hormone receptor 1 (MCHR1). Appl. Radiat. Isot. 616, 101-106.

Philippe, C., Ungersboeck, J., Schirmer, E., Zdravkovic, M., Nics, L., Zeilinger, M., Shanab, K., Lanzenberger, R., Karanikas, G., Spreitzer, H., Viernstein, H., Mitterhauser, M., Wadsak, W., 2012b. [^{18}F]FE@SNAP - A new PET tracer for the melanin concentrating hormone receptor 1 (MCHR1): microfluidic and vessel-based approaches. Bioorg. Med. Chem. 20, 5936-5940.

Pissios, P., Maratos-Flier, E., 2003. Melanin-concentrating hormone: from fish skin to skinny mammals. Trends Endocrinol. Metab. 14, 243-248.

Roy, M., David, N., Cueva, M., Giorgetti, M., 2007. A study of the involvement of melanin-concentrating hormone receptor 1 (MCHR1) in murine models of depression. Biol. Psychiatry 61, 174-180.

Sailer, A.W., Sano, H., Zeng, Z., McDonald, T.P., Pan, J., Pong, S.S., Feighner, S.D., Tan, C.P., Fukami, T., Iwaasa, H., Hreniuk, D.L., Morin, N.R., Sadowski, S.J., Ito, M., Ito, M., Bansal, A., Ky, B., Figueroa, D.J., Jiang, Q., Austin, C.P., MacNeil, D.J., Ishihara, A., Ihara, M., Kanatani, A., Van der Ploeg, L.H.T., Howard A.D., Liu, Q., 2001. Identification and characterization of a second melanin-concentrating hormone receptor, MCH-2R. Proc. Natl. Acad. Sci. USA 98, 7564-7569.

Saito, Y., Nothacker, H.P., Wang, Z., Lin, S.H., Leslie, F., Civelli, O., 1999. Molecular characterization of the melanin-concentrating-hormone receptor. Nature 400, 265-269.

Saito, Y., Cheng, M., Leslie, F.M., Civelli, O., 2001. Expression of the melanin-concentrating hormone (MCH) receptor mRNA in the rat brain. J. Comp. Neurol. 435, 26-40.

Schmidt, J., 1984. The impact of radiodecay on 125-Tyr-54-α-bungarotoxin. J. Biol. Chem. 256, 1160-1166.

Shimomura, Y., Mori, M., Sugo, T., Ishibashi, Y., Abe, M., Kurokawa, T., Onda, H., Nishimura, O., Sumino, Y., Fujino, M., 1999. Isolation and identification of melanin-concentrating hormone as the endogenous ligand of the SLC-1 receptor. Biochem. Biophys. Res. Commun. 261, 622-626.

Sone, M., Takahashi, K., Murakami, O., Totsune, K., Arihara, Z., Satoh, F., Sasano, H., Ito, H., Mouri, T., 2000. Binding sites for melanin-concentrating hormone in the human brain. Peptides 21, 245-250.

Tadayyon, M., Welters, H.J., Haynes, A.C., Cluderay, J.E., Hervieu, G., 2002. Expression of melanin-concentrating hormone in insulin-producing cells: MCH stimulates insulin release in RINm5F and CRI-G1 cell-lines. Biochem. Biophys. Res. Commun. 275, 709-712.

Wang, S., Behan, J., O'Neill, K., Weig, B., Fried, S., Laz, T., Bayne, M., Gustafson, E., Hawes, B.E., 2001. Identification and pharmacological characterization of a novel human melanin-concentrating hormone receptor, MCH-R2. J. Biol. Chem. 276, 34664-34670.

Captions

Fig. 1: Chemical structure of the investigated MCHR1 ligands:
1) Radioligand peptides: a) [^{125}I]-MCH, b) [^{125}I]-S36057,
2) Competitor peptide: PMC-3886,
3) Small molecule competitors: a) SNAP-7941, b) FE@SNAP.

Fig. 2: Analysis scheme of comparative autoradiographic experiments.
BL=baseline/total binding of radioligand
NB=non-specific binding/remaining activity after blocking with the MCHR1 selective compounds
Δx= specific amounts of MCHR1 competition = BL – NB
Thus, Δx reflects specific binding blockable through competition.

Fig.3: Typical representative [^{125}I]-MCH competition image in human hypothalamus and human thalamus (red colours indicate highest uptake of radioligand, white/grey colours indicate no uptake or full competition; Δx values are given in Table 2):
(a) baseline
(b) blocking with PMC-3886
(c) blocking with FE@SNAP
(d) blocking with SNAP-7941

Fig. 4: Typical immunohistochemical staining pictures of the MCHR1 on **coronal rat brain (A)** and ***human post mortem (B-E) brain*** regions (10-fold):
A) coronal rat brain (3V, third ventricle)
B) human hippocampus
C) human hypothalamus
D) human thalamus
E) human cerebellum.

Fig. 5: Comparison of competition of [^{125}I]-MCH or [^{125}I]-S36057 in 4 different human brain regions (hippocampus, hypothalamus, thalamus and cerebellum) by

the MCHR1 agonist PMC-3886, and antagonists SNAP-7941 and FE@SNAP. Significant differences are shown as * (P<0.05, values given in %, mean of quadruplet analyses from ≥2 different experiments each (n≥8)).

Table 1: Selection of the selective and commercially available radioligands for the MCHR1, and the investigated agonist (PMC-3886) and antagonists (SNAP-7941 and FE@SNAP); with an overview over autoradiographic and experimental relevant properties of these compounds as ligand type (agonist, antagonist), affinity and selectivity -as far as known from literature (nd= no data).

Table 2: Overview of MCHR1 appearance (Δx) in relation to the specific blocking efficiency of the MCHR1 ligands PMC-3886, SNAP-7941 and FE@SNAP; competing [^{125}I]-MCH or [^{125}I]-S36057 on rat and human tissue origin (values given in %, mean of quadruplet analyses from ≥2 different experiments each (n≥8)). Significant differences are shown as * (P<0.05). (Ar.mean Δx represents arithmetic mean of all three competitors.)

1) a: Asp-Phe-Asp-Met-Leu-Arg-Cys-Met-Leu-Gly-Arg-Val-[^{125}I]Tyr-Arg-Pro-Cys-Trp-Gln-Val

b: [^{125}I]Tyr-ADO-Arg-Cys-Met-Leu-Gly-Arg-Val-Phe-Arg-Pro-Cys-Trp-OH

2) Ac-D-Arg-Cys-Met-Leu-Asn-Arg-Val-Tyr-Arg-Pro-Cys-NH_2

3)

a: R=CH_3
b: R=$(CH_2)_2F$

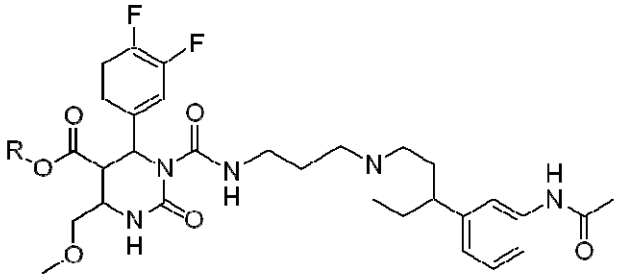

Fig. 1: Chemical structure of the investigated MCHR1 ligands:

1) Radioligand peptides: a) [^{125}I]-MCH, b) [^{125}I]-S36057,

2) Competitor peptide: PMC-3886,

3) Small molecule competitors: a) SNAP-7941, b) FE@SNAP.

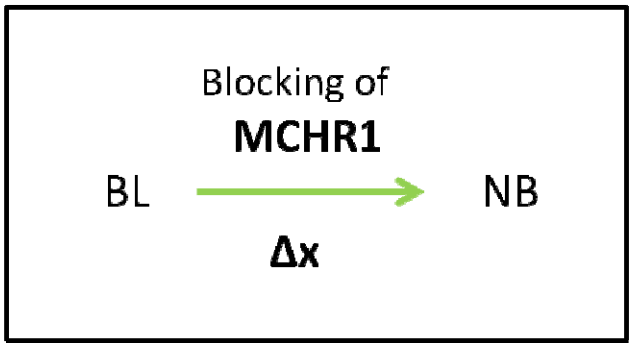

Fig. 2: Analysis scheme of comparative autoradiographic experiments.

BL=baseline/total binding of radioligand

NB=non-specific binding/remaining activity after blocking with the MCHR1 selective compounds

Δx= specific amounts of MCHR1 competition = BL – NB

Thus, Δx reflects specific binding blockable through competition.

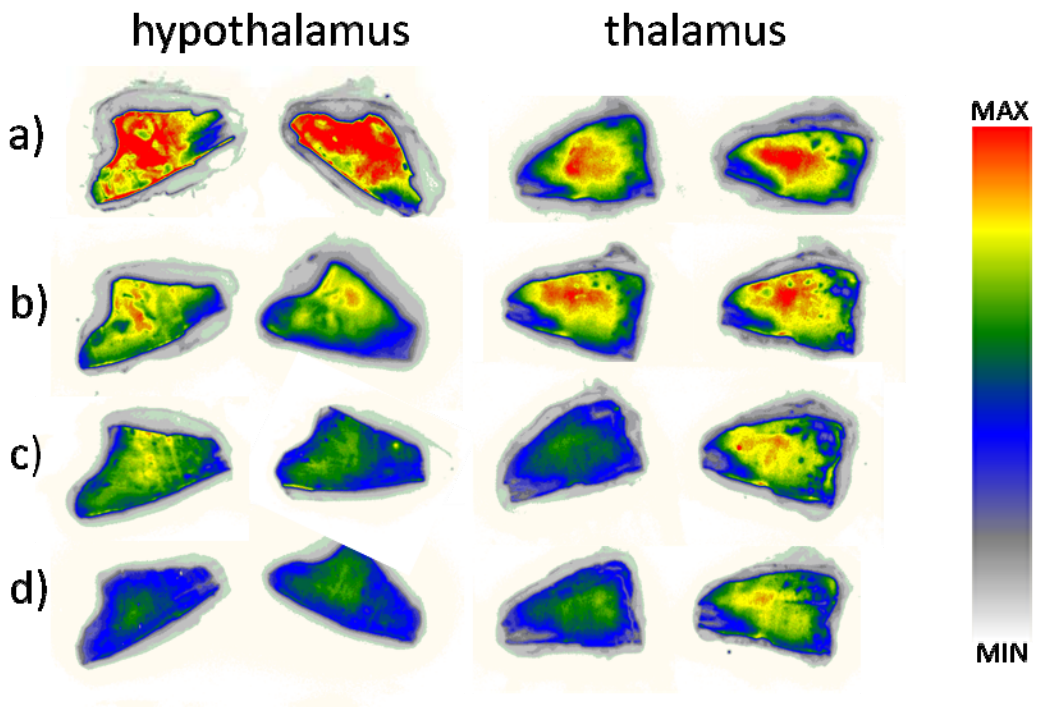

Fig.3: Typical representative [^{125}I]-MCH competition image in human hypothalamus and human thalamus (red colours indicate highest uptake of radioligand, white/grey colours indicate no uptake or full competition; Δx values are given in Table 2):

(a) baseline

(b) blocking with PMC-3886

(c) blocking with FE@SNAP

(d) blocking with SNAP-7941

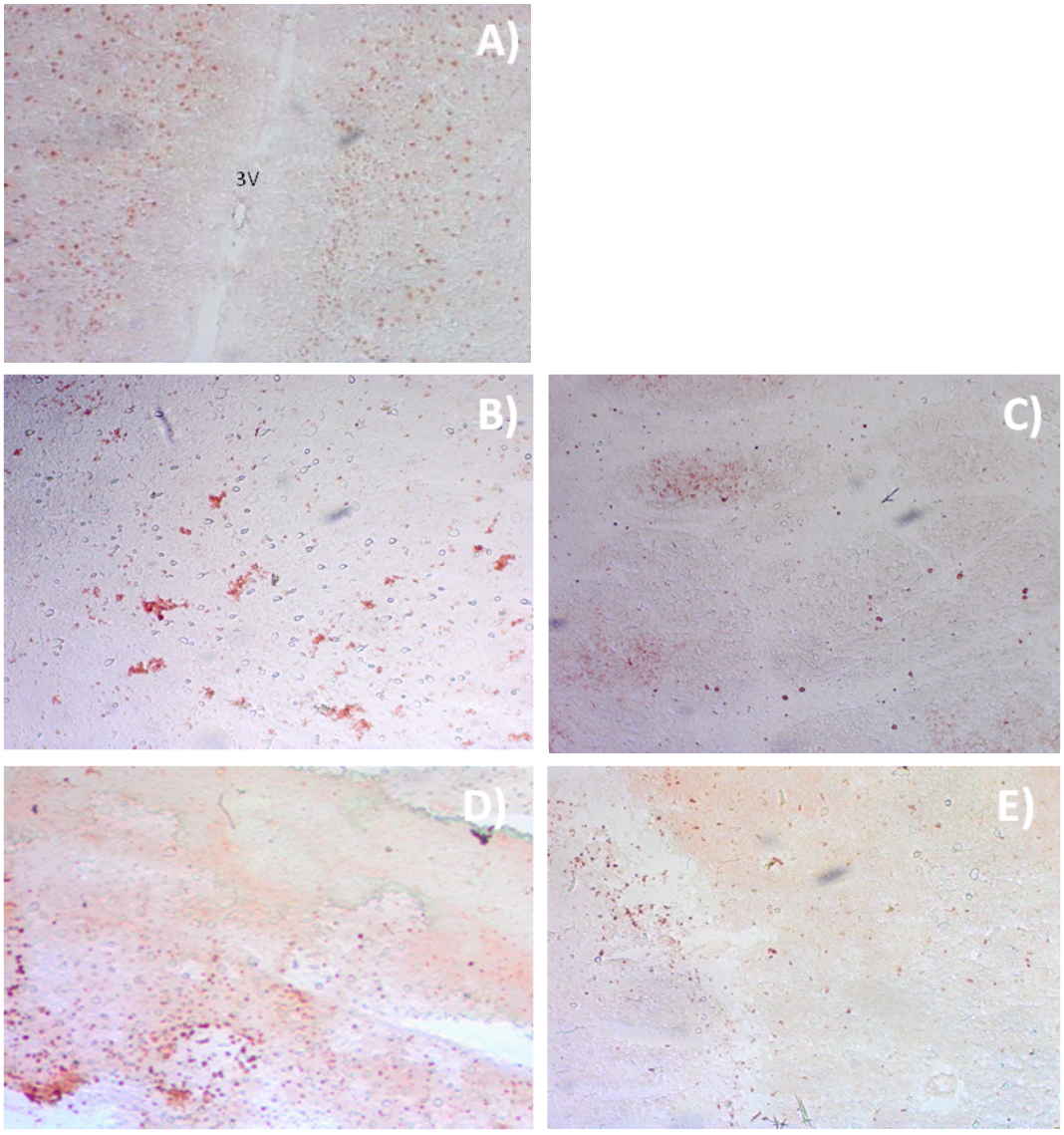

Fig. 4: Typical immunohistochemical staining pictures of the MCHR1 on **coronal rat brain (A)** and ***human post mortem (B-E) brain*** regions (10-fold):

A) coronal rat brain (3V, third ventricle)

B) human hippocampus

C) human hypothalamus

D) human thalamus

E) human cerebellum.

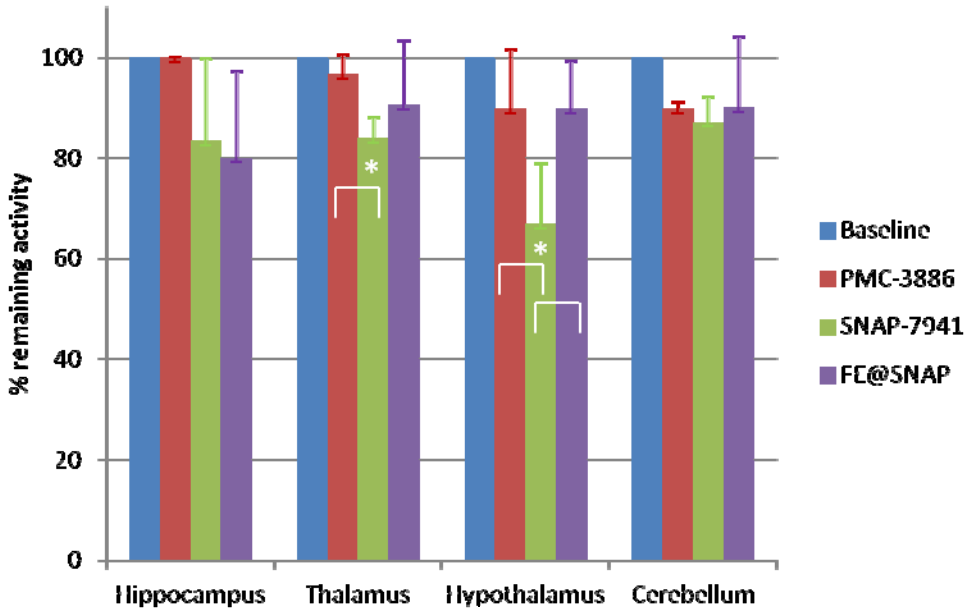

Fig. 5: Comparison of competition of [^{125}I]-MCH or [^{125}I]-S36057 in 4 different human brain regions (hippocampus, hypothalamus, thalamus and cerebellum) by the MCHR1 agonist PMC-3886, and antagonists SNAP-7941 and FE@SNAP. Significant differences are shown as * (P<0.05, values given in %, mean of quadruplet analyses from ≥2 different experiments each (n≥8)).

Ligand	*Compound*	*Receptor*	*Affinity [nM]*	*Selectivity vs MCHR2*	*Reference*
Agonist	[^{125}I]-MCH	MCHR1, MCHR2	0.5	nd	Audinot et al., 2001a
	[^{125}I]-S36057	MCHR1, MCHR2	0.05	nd	Audinot et al., 2001b
	PMC-3886	MCHR1	0.29	6600-fold	Bednarek et al., 2002
Antagonist	SNAP-7941	MCHR1	0.18	>1000-fold	Borowsky at al., 2002
	FE@SNAP	MCHR1	nd	nd	

Table 1: Selection of the selective and commercially available radioligands for the MCHR1, and the investigated agonist (PMC-3886) and antagonists (SNAP-7941 and FE@SNAP); with an overview over autoradiographic and experimental relevant properties of these compounds as ligand type (agonist, antagonist), affinity and selectivity -as far as known from literature (nd= no data).

rat	*radioligand*	*PMC-3886 Δx*	*SNAP-7941 Δx*	*FE@SNAP Δx*	*ar.mean Δx*	*sd*
whole brain	[^{125}I]-S36057	24.9	40.6	43.4	36.3	10.0
human	*radioligand*	*PMC-3886 Δx*	*SNAP-7941 Δx*	*FE@SNAP Δx*	*ar.mean Δx*	*sd*
hippocampus	[^{125}I]-MCH	0.0	16.6	20.0	12.2	10.7
thalamus	[^{125}I]-MCH	3.3	16.0*	9.3	9.5	6.4
hypothalamus	[^{125}I]-MCH	10.2	33.0*	10.3	17.8	13.2
cerebellum	[^{125}I]-S36057	10.2	12.8	10.0	11.0	1.6

Table 2: Overview of MCHR1 appearance (Δx) in relation to the specific blocking efficiency of the MCHR1 ligands PMC-3886, SNAP-7941 and FE@SNAP; competing [^{125}I]-MCH or [^{125}I]-S36057 on rat and human tissue origin (values given in %, mean of quadruplet analyses from ≥2 different experiments each (n≥8)). Significant differences are shown as * (P<0.05). (Ar.mean Δx represents arithmetic mean of all three competitors.)

3. SUMMARY AND DISCUSSION

To be useful as an *in vivo* imaging agent, a PET-tracer has to fulfill a number of prerequisites:

- high binding affinity and selectivity to the target of interest
- low non-specific binding in order to achieve a high target to background ratio
- low plasma protein binding since only the free fraction of the radioligand is available for diffusion out of the vascular space
- sufficient metabolic stability to assure enough intact tracer for imaging of the target of interest
- reliable radiosynthesis method to guarantee enough yield
- high specific radioactivity for imaging the target of interest

Additional prerequisites for CNS PET-tracers:

- reasonable lipophilicity to expect BBB penetration
- potential radiometabolites should not pass the BBB

Within this PhD-thesis, the first and so far only PET-tracers for the MCHR1, [^{11}C]SNAP-7941 and [^{18}F]FE@SNAP, were developed and precilinically evaluated.

[^{11}C]SNAP-7941

The radiosynthesis, consisting of the [^{11}C]methylation of the precursor molecule SNAP-acid (Figure 9), was successful, yielding in 2.9 ± 1.6GBq [^{11}C]SNAP-7941. During the establishment of the radiosynthesis, different reaction solvents, reaction temperatures, reaction times, precursor concentrations and even methylation agents ([^{11}C]CH_3OH and [^{11}C]CH_3OTf) were tested. The optimal reaction conditions were found to be 2min reaction time in acetonitrile at ≤ 25°C reaction temperature using 2mg/ml precursor and [^{11}C]CH_3OTf as methylation agent. The specific radioactivity for the *in vivo* evaluation was acceptable: 108.2 ± 56GBq/μmol at the end of synthesis (EOS). The full radiosynthesis, purification procedure and physiological formulation could be automated to guarantee a safe and reliable

production. All quality control parameters were in accordance with the standards for human application.

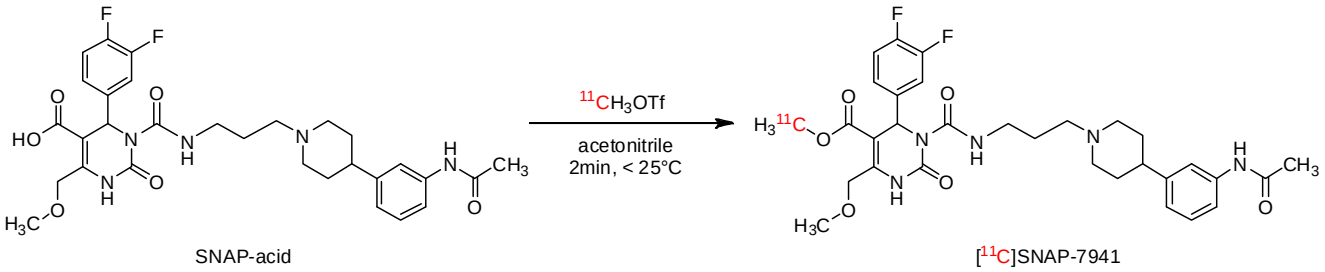

Figure 9: Reaction scheme of the radiosynthesis of [^{11}C]SNAP-7941.

In contrast to the originally described, non-radioactive parent compound, SNAP-7941 [58], which is the (+)-enantiomer, the presented radioactive counterpart [^{11}C]SNAP-7941 is the racemate. However, the binding affinity and selectivity to the MCHR1 were still high: K_i=4.52 ± 0.7nM for the MCHR1; K_i>1000nM for the MCHR2.

The metabolic stability of [^{11}C]SNAP-7941 in plasma and against liver microsomes and carboxylesterases was very high: no degradation in human plasma over 60min; < 10% degradation by liver microsomes (human and rat) over 60min and no decomposition by porcine carboxylesterases (therefore, no MMK could be calculated). Interestingly, in rat plasma, [^{11}C]SNAP-7941 was metabolized considerably: 50.4 ± 1% of intact compound were found after 60min. The formation of a hydrophilic metabolite was observed.

The plasma free fraction was found to be sufficient for imaging: f_1=21.0 ± 1% in human plasma and even 32.4 ± 1% in rat plasma.

The lipophilicity was in a range, where a passive diffusion through the BBB would be expectable: log$D_{7.4}$=3.29, P_m = 0.79.

However, in the *in vivo* experiments in healthy rats, [^{11}C]SNAP-7941 evinced to be a P-gp substrate, since after blocking with the P-gp inhibitor Tariquidar (TQD), the SUV in the brain raised 3-5 times. Borowsky et al. [58] observed a significant reduction in food intake and body weight in rats after ip application of (+)-SNAP-7941. Knowing that drugs have to cross the BBB to reduce body weight [66], our findings were quite surprising.

Nevertheless, no metabolite was found in the brains of the baseline and TQD-pretreatment group.

The biodistribution experiments showed both, uptake in kidneys and intestines. On the basis of the conducted experiments, a specification of the major way of excretion was not possible. Uptake in MCHR1 expressing organs (adrenals, pancreas, eyes, muscle and ovary; Table 1, p. 20) could be observed. Low uptake was found in peripheral fat tissue of the healthy rats. The extend of increase of MCHR1 expression in obese rats is unkown.

[^{18}F]FE@SNAP

Due to the advantage of the longer half-life of fluorine-18 (110min) compared to carbon-11 (20min), [^{18}F]FE@SNAP, a [^{18}F]fluoroethylated derivative of SNAP-7941 was developed. Its radiosynthesis was challenging; no vessel-based approached succeeded. Only the preparation within the microfluidic device was successful, consisting of the direct [^{18}F]fluorination of the tosylated precursor (Tos@SNAP) (Figure 10). Harsh reaction conditions had to be applied: high reaction temperature of 170°C and a short reaction time using an overall flow rate of 150µl/min. Since the microfluidic device was not equipped for purification steps, the crude reaction mixture was purified in a conventional synthesis module. The radiosynthesis (Advion NanoTek®) as well as the purification and physiological formulation (Nuclear Interface®) were automated to guarantee safe and reliable production. The radiochemical yield ranged between 100-650 MBq, which was sufficient for every subsequent preclinical experiment. Specific radioactivity was 24.8 ± 12GBq/µmol EOS.

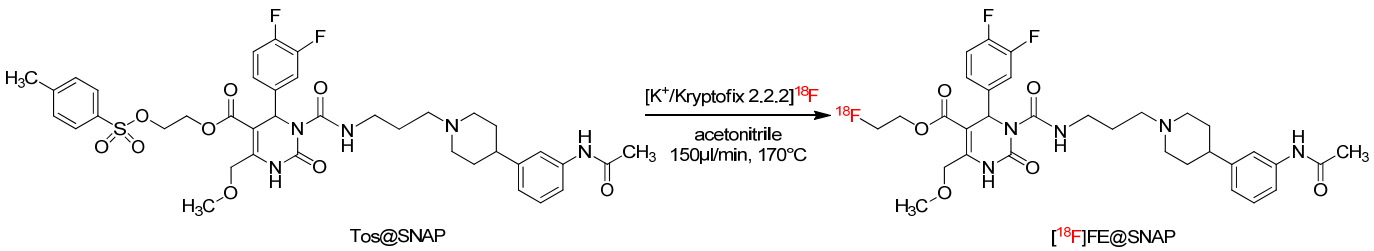

Figure 10: Reaction scheme of the radiosynthesis of [^{18}F]FE@SNAP.

For the development of the radiosynthesis, the discovery mode of the microfluidic device was used. In future, higher radiochemical yields and in consequence higher specific radioactivities can be expected using the sequence mode of the device.
All quality control parameters were in accordance with the standards for human application.
[^{18}F]FE@SNAP evinced high binding affinity and selectivity to the MCHR1: K_d=2.9 ± 2.5nM for the MCHR1; K_i>1000nM for the MCHR2.
Like [^{11}C]SNAP-7941, it is highly stable in human plasma (only 3.9 ± 4% metabolism after 120min), against liver microsomes (< 10% metabolism after 60 min) and porcine carboxylesterases (K_m=347.3μM) and rapidly metabolized in rat plasma (completely after 120min).
The plasma free fraction was lower (f_1=12.6 ± 0.2%) than for [^{11}C]SNAP-7941, but can still be considered high enough for imaging.
Compared to SNAP-7941, the lipophilicity was slightly higher ($\log D_{7.4}$=3.83), but the result of the IAM chromatography (P_m=0.51) was situated in the range of known BBB penetrating compounds.

Comparative in vitro autoradiography of SNAP-7941 and FE@SNAP

To prove the suitability of the two developed PET-tracers, a comparative *in vitro* autoradiographic investigation of the MCHR1 ligands (SNAP-7941, FE@SNAP and the commercially available PMC-3886) was conducted. Rat brain slices and four dedicated human brain tissue slices (hypothalamus, thalamus, hippocampus and cerebellum) were incubated with the MCHR1 radioligands [^{125}I]-MCH and [^{125}I]-S36057, respectively, in the presence of one of the three competitors. SNAP-7941 showed highest competition potency, followed by FE@SNAP and PMC-3886. The specific competition amounts of MCHR1 were 36.3 ± 10% in rat brain and 12.6 ± 8% in summed human brain regions. The higher competition amounts in rat brain can be explained due to the single presence of MCHR1 (whereas in human brain MCHR2 is present too). MCHR1 was found in all brain regions with a ranking of hypothalamus, hippocampus, cerebellum and thalamus. The additionally conducted immunohistochemical staining completed the outcome.

4. CONCLUSION AND OUTLOOK

In this PhD-thesis, the first potential PET-tracers for the MCHR1, [^{11}C]SNAP-7941 and [^{18}F]FE@SNAP, were developed. These two PET-tracers will provide deeper information of MCHR1's role in physiological processes and may lead to the discovery of additional functions of MCH signaling.

The radiosynthesis of both molecules was successful and radiochemical yields were sufficient for subsequent preclinical studies. Both compounds showed high binding affinity, selectivity and metabolic stability. The plasma free fraction was considered high enough for imaging and the lipophilicity suggests passive diffusion through the BBB. Autoradiography supported their potency as MCHR1 ligands.

Due to the lack of facilities and precursor availability, the preclinical evaluation of [^{18}F]FE@SNAP ended with the *in vitro* experiments within this thesis. Further *in vivo* experiments are planned for the future when a new batch of precursor will be available.

The biodistribution experiments of [^{11}C]SNAP-7941 in healthy rats showed uptake in organs expressing the MCHR1 (pancreas, adrenals, eyes, muscle and ovary). Suprisingly, low uptake was found in peripheral fat tissue. Fortunately, no brain metabolite could be detected during the *ex vivo* metabolic stability testing.
Nevertheless, in the small-animal PET experiments, [^{11}C]SNAP-7941 evinced to be a P-gp substrate. However, the P-gp expression in the BBB is more pronounced in rodents than in humans [97]. Species differences in the uptake of P-gp substrates were reported for several tracers, e.g. [^{11}C]WAY-100635 or [^{18}F]altanserin. These radioligands are P-gp substrates in rodents, but serve as routine brain tracers in human applications [95, 96].
To prove the tracer's ability for the *in vivo* imaging of the MCHR1 in the CNS of rats, an i.c.v. injection is planned followed by an *ex vivo* autoradiography. The i.c.v. injection permits to circumvent the BBB.

However, on the basis of the small-animal PET experiments with healthy rats, the suitability of [^{11}C]SNAP-7941 for the visualisation of central and peripheral MCHR1 remains speculative. Further experiments in obese and diabetic rats will show the applicability of the MCHR1 concept.

Furthermore, the synthesis of the enantiomerically enriched precursor SNAP-acid is planned in order to be able to produce (+)-[^{11}C]SNAP-7941. Maybe this (+)-enantiomer will exhibit even better properties than the racemate.

Recently, we discovered specific uptake of [^{11}C]SNAP-7941 in brown adipose tissue (BAT). Since the activation mechanism of BAT is a hot topic of investigation, [^{11}C]SNAP-7941 could be a useful tool for this research area.

5. REFERENCES

[1] Enami M. Melanophore-concentrating hormone (MCH) of possible hypothalamic origin in the catfish, Parasilurus. Science 1955;121:36-7.

[2] Hogben LT and Slome D. The pigmentary effector system VI. The dual character of endocrine coordination in amphibian colour change. Proc R Soc London Biol Sci 1931;108:10-53.

[3] Kawauchi H, Kawazoe I, Tsubokawa M, Kishida M, Baker BI. Characterization of melanin-concentrating hormone in chum salmon pituitaries. Nature 1983;305,321-3.

[4] Barber LD, Baker BI, Penny JC, Eberle AN. Melanin concentrating hormone inhibits the release of αMSH from teleost pituitary glands. Gen Comp Endocrinol 1987;65:79-86.

[5] Rogers SL, Tint IS, Fanapour PC, Gelfand VI. Regulating bidirectional motility of melanophore pigment granules along microtubules in vitro. Proc Natl Acad Sci USA 1997;94:3720-5.

[6] Vaughan JM, Fischer WH, Hoeger C, Rivier J, Vale W. Characterization of melanin-concentrating hormone from rat hypothalamus. Endocrinology 1989;125:1660-5.

[7] Presse F, Nahon JL, Fischer WH, Vale W. Structure of the human melanin concentrating hormone mRNA. Mol Endocrinol 1990;4:632-7.

[8] Griffond B and Baker BJ. Cell and molecular cell biology of melanin-concentrating hormone. Int Rev Cytol 200;213:233-77.

[9] Bittencourt JC, Presse F, Arias C, Peto C, Vaughan JM, Nahon JL, et al. The melanin-concentrating hormone system of the rat brain: an immuno- and hybridization histochemical characterization. J Comp Neurol 1992;319:218-45.

[10] Casatti CA, Elias CF, Sita LV, Frigo L, Furlani VCG, Bauer JA, et al. Distribution of melanin-concentrating hormone neurons projecting to the medial mammillary nucleus. Neuroscience 2002;115:899-915.

[11] Kokkotou E, Moss AC, Torres D, Karagiannides I, Cheifetz A, Liu S. Melanin-concentrating hormone as a mediator of intestinal inflammation. Natl Acad Sci USA 2008;105:10613-8.

[12] Bradley RL, Kokkotou E, Maratos-Flier E, Cheatham B. Melanin-concentrating hormone regulates leptin synthesis and secretion in rat adipocytes. Diabetes 2000;49:1073-7.

[13] Pissios P, Ozcan U, Kokkotou E, Okada T, Liew CW, Liu S, et al. Melanin concentrating hormone is a novel regulator of islet function and growth. Diabetes 2007;56:311-9.

[14] Saito Y, Wang Z, Hagino-Yamagishi K, Civelli O, Kawashima S, Maruyama K, et al. Endogenous melanin-concentrating hormone receptor SLC-1 in human melanoma SK-MEL-37 cells. Biochem Biophys Res Commun 2001;289:44-50.

[15] Marsh DJ, Weingarth DT, Novi DE, Chen HY, Turmbauer ME, Chen AS, et al. Melanin-concentrating hormone 1 receptor-deficient mice are lean, hyperactive, and hyperphagic and have altered metabolism. Proc Natl Acad Sci USA 2002;99:3240-5.

[16] Ito M, Gomori A, Ishihara A, Oda Z, Mashiko S, Yumoto M, et al. Characterization of MCH-mediated obesity in mice. Am J Physiol Endocrinol Metab 2003;284:E940-5.

[17] Drozdz R, Siegrist W, Baker BI, Chluba-de Tapia J, Eberle AN. Melanin-concentrating hormone binding to mouse melanoma cells in vitro. FEBS Lett 1995;359:199-202.

[18] Drozdz R and Eberle AN. Binding sites for melanin-concentrating hormone (MCH) in brain synaptosomes and membranes from peripheral tissues identified with highly titrated MCH. J Recept Sigmal Transduct Res 1995;15:487-502.

[19] Kolakowski Jr LF, Jung BP, Nguyen T, Johnson MP, Lynch KR, Cheng R, et al. Characterization of a human gene related to genes encoding somatostatin receptors. FEBS Lett 1996;398:253-8.

[20] Bachner D, Kreienkamp H, Weise C, Buck F, Richter D. Identification of melanin concentrating hormone (MCH) as the natural ligand for the orphan somatostatin-like receptor 1 (SLC-1). FEBS Lett 1999;457:522-4.

[21] Chambers J, Ames RS, Bergsma D, Muir A, Fitzgerald LR, Hervieu G, et al. Melanin-concentrating hormone ist he cognate ligand for the orphan G-protein-coupled receptor SLC-1. Nature 1999;400:261-5.

[22] Lembo PM, Grazzini E, Cao J, Hubatsch DA, Pelletier M, Hoffert C, et al. The receptor for the orexigenic peptide melanin-concentrating hormone is a G-protein-coupled receptor. Nat Cell Biol 1999;1:267-71.

[23] Saito Y, Nothacker HP, Wang Z, Lin SH, Leslie F, Civelli O. Molecular characterization of the melanin-concentrating-hormone receptor. Nature 1999;400:265-9.

[24] Shimomura Y, Mori M, Sugo T, Ishibashi Y, Abe M, Kurokawa T, et al. Isolation and identification of melanin-concentrating hormone as the endogenous ligand of the SLC-1 receptor. Biochem Biophys Res Commun 1999;261:622-6.

[25] Lakaye B, Minet A, Zorzi W, Grisar T. Cloning of the rat brain cDNA encoding for the SLC-1 G protein-coupled receptor reveals the presence of an intron in the gene. Biochim Biophys Acta 1998;1401:216-20.

[26] Kokkotou E, Tritos NA, Mastaitis JW, Slieker L, Maratos-Flier E. Melanin-concentrating hormone receptor is a target of leptin action in the mouse brain. Endocrinology 2001;142:680-6.

[27] Hawes BE, Kil E, Green B, O'Neill K, Fried S, Graziano MP. The melanin-concentrating hormone receptor couples to multiple G proteins to activate diverse intracellular signaling pathways. Endocrinology 2000;141:4524-32.

[28] Curtis J and Finkbeiner S. Sending signals from the synapse to the nucleus: possible roles for CaMK, Ras/ERK, and SAPK pathways in the regulation of synaptic plasticity and neuronal growth. J Neurisci Res 1999;56:88-95.

[29] Dolphin AC. Mechanisms of modulation of voltage-dependent calcium channels by G proteins. J Physiol 1998;506:3-11.

[30] Yamada M, Inanobe A, Kurachi Y. G protein regulation of potassium ion channels. Pharmacol Rev 1998;50:723-60.

[31] Pissios P and Maratos-Flier E. Melanin-concentrating hormone : from fish skin to skinny mammals. Trends Endocrinol Metab 2003;14:243-7.

[32] Sone M, Takahashi K, Murakami O, Totsune K, Arihara Z, Satoh R, et al. Binding sites for the melanin-concentrating hormone in the human brain. Peptides 2000;21:245-250.

[33] Hervieu GJ, Cluderay JE, Harrison D, Meakin J, Maycox P, Nasir S, et al. The distribution of the mRNA and protein products of the melanin-concentrating hormone (MCH) receptor gene, slc-1, in the central nervous system of the rat. Eur J Neurosci 2000;12:1194-216.

[34] Takahashi K, Totsune K, Murakami O, Sone M, Satho F, Kitamuro T, et al. Expression of the melanin-concentrating hormone receptor messenger ribonucleic acid in tumor tissues of pheochromocytoma, ganglioneuroblastoma, and neuroblastoma. J Clin Endocrinol Metab 2001;86:369-74.

[35] Mori M, Harada M, Terao Y, Sugo T, Watanabe T, Shimomura Y, et al. Cloning of a novel G protein-coupled receptor, SLT, a subtype of the melanin-concentrating hormone receptor. Biochem Biophys Res Commun 2001;283:1013-8.

[36] Hill J, Duckworth M, Murdock P, Rennie G, Sabido-David C, Ames RS, et al. Molecular cloning and functional characterization of MCH2, a novel human MCH receptor. J Biol Chem 2001;276:20125-9.

[37] Saito Y, Cheng M, Leslie FM, Civelli O. Expression of the melanin-concentrating hormone (MCH) receptor mRNA in the rat brain. J Comp Neurol 2001;435:26-40.

[38] Saito Y, Nothacker HP, Civelli O. Melanin-concentrating hormone receptor: an orphan receptor fits the key. TEM 2000;11:299-303.

[39] Suply T, Della Zuana O, Audinot V, Rodriguez M, Beauverger P, Duhault J, et al. SLC-1 receptor mediates effect of melanin-concentrating hormone on feeding behavior in rat: a structure-activity study. J Pharmacol Exp Ther 2001;299:369-74.

[40] Tadayyon M, Welters HJ, Haynes AC, Cluderay JE, Hervieu G. Expression on melanin concentrating hormone receptors in insulin-producing cells: MCH

stimulates insulin release in RINm5F and CRI-G1 cell-lines. Biochem Biophys Res Commun 2000;275:709-12.

[41] An S, Cutler G, Zhao JJ, Huang SG, Tian H, Li W, et al. Identification and characterization of a melanin-concentrating hormone receptor. Proc Natl Acad Sci USA 2001;98:7576-81.

[42] Sailer AW, Sano H, Zeng Z, McDonald TP, Pan J, Pong SS, et al. Identification and characterization of a second melanin-concentrating hormone receptor, MCH-2R. Proc Natl Acad Sci USA 2001;98:7564-9.

[43] Wang S, Behan J, O'Neill K, Weig B, Fried S, Laz T, et al. Identification and pharmacological characterization of a novel human melanin-concentrating hormone receptor, MCH-R2. J Biol Chem 2001;276:34664-34670.

[44] Tan CP, Sano H, Iwaasa H, Pan J, Sailer AW, Hreniuk DL, et al. Melanin-concentrating hormone receptor subtypes 1 and 2: species-specific gene expression. Genomics 2002;79:785-92.

[45] Shimada M, Tritos NA, Lowell BB, Flier JS, Maratos-Flier E. Mice lacking melanin-concentrating hormone are hypophagic and lean. Nature 1998;396:670-4.

[46] Ludwig DS, Tritos NA, Mastaitis JW, Kulkarni R, Kokkotou E, Elmquist J, et al. Melanin-concentrating hormone overexpression in transgenic mice leads to obesity and insulin resistance. J Clin Invest 2001;107:379-86.

[47] Considine RV, Sinha MK, Heiman ML, Kriauciunas A, Stephens TW, Nyce MR, et al. Serum immunoreactive-leptin concentrations in normal-weight and obese humans. N Engl J Med 1996;334:292-5.

[48] Qu D, Ludwig DS, Gammeltoft S, Piper M, Pelleymounter MA, Cullen MJ, et al. A role for melanin-concentrating hormone in the central regulation of feeding behavior. Nature, 1996;380:243-7.

[49] Segal-Lieberman G, Bradley RL, Kokkotou E, Carlson M, Trombly DJ, et al. Melanin-concentrating hormone is a critical mediator of the leptin-deficient phenotype. Proc Natl Acad Sci USA 2003;100:10085-90.

[50] Bjursell M, Gerdin AK, Ploj K, Svensson D, Svensson L, Oscarsson J, et al. Melanin-concentrating hormone receptor 1 deficiency increases insulin sensitivity in obese leptin-deficient mice without affecting body weight. Diabetes 2006;55:725-33.

[51] Schwartz MW and Gelling RW. Rats lighten up with MCH antagonist. Nat Med 2002;8:779-81.

[52] Jeon JY, Bradley RL, Kokkotou EG, Marino FE, Wang X, Pissios P, et al. MCH-/- mice are resistant to aging-associated increase in body weight and insulin resistance. Diabetes 2006;55:428-34.

[53] Verlaet M, Adamantidis A, Coumans B, Chanas G, Zorzi W, Heinen E, et al. Human immune cells express ppMCH mRNA and functional MCHR1 receptor. FEBS Lett 2002;527:205-10.

[54] Sandig H, McDonald J, Gilmour J, Arno M, Lee TH, Cousins DJ. Human Th2 cells selectively express the orexigenic peptide, pro-melanin-concentrating hormone. Proc Natl Acad Sci USA 2007;104:12440-4.

[55] Macdonald D, Murgolo N, Zhang R, Durkin JP, Yao X, Strader CD, et al. Molecular characterization of the melanin-concentrating hormone/receptor complex: identification of critical residues involved in binding and activation. Mol Pharmacol 2000;58:217-25.

[56] Bednarek MA, Hreniuk DL, Tan C, Palyha OC, MacNeil DJ, Van der Ploeg LH, et al. Synthesis and biological evaluation in vitro of selective, high affinity peptide antagonists of human melanin-concentrating hormone action at human melanin-concentrating hormone receptor 1. Biochemistry 2002;41:6383-90.

[57] Takekawa S, Asami A, Ishihara Y, Terauchi J, Kato K, Shimomura Y, et al. T-226296: a novel, orally active and selective melanin-concentrating hormone receptor antagonist. Eur J Pharmacol 2002;438:129-35.

[58] Borowsky B, Durkin MM, Ogozalek K, Marzabadi MR, DeLeon J, Lagu B, et al. Antidepressant, anxiolytic and anorectic effects of a melanin-concentrating hormone-1 receptor antagonist. Nat Med 2002;8:825-30.

[59] Basso AM, Bratcher NA, Gallagher KB, Cowart MD, Zhao C, Sun M, et al. Lack of efficacy of melanin-concentrating hormone-1 receptor antagonists in models of depression and anxiety. Eur J Pharmacol 2006;540:115-20.

[60] Kanuma K, Omodera K, Nishiguchi M, Funakoshi T, Chaki S, Semple G, et al. Discovery of 4-(dimethylamino)quinazolines as potent and selective antagonists for the melanin-concentrating hormone receptor 1. Bioorg Med Chem Lett 2005;15:2565-9.

[61] Kanuma K, Omodera K, Nishiguchi M, Funakoshi T, Chaki S, Semple G, et al. Lead optimization of 4-(dimethylamino)quinazolines, potent and selective antagonists for the melanin-concentrating hormone receptor 1. Bioorg Med Chem Lett 2005;15:3853-6.

[62] Carpenter AJ and Hertzog DL. Melanin concentrating hormone receptor antagonists as potential antiobesity agents. Expert Opin Ther Patents 2002;12:1693-46.

[63] David DJ, Klemenhagen KC, Holick KA, Saxe MD, Mendez I, Santarelli DA, et al. Efficacy of the MCHR1 antagonist N-[3-(1-{[4-(3,4-difluorophenoxy)phenyl]methyl}[4-piperidyl))-4-methylphenyl]-2-methylpropanamide (SNAP 94847) in mouse models of anxiety and depression following acute and chronic administration is independent of hippocampal neurogenesis. J Pharmacol Exp Ther 2007;321:237-48.

[64] Andersen D, Storz T, Liu P, Wang X, Li L, Fan P, et al. Stereoselective synthesis of a MCHr1 antagonist. J Org Chem 2007;72:9648-55.

[65] Rokosz LL. Discovery and development of melanin-concentrating hormone receptor 1 antagonists for the treatment of obesity. Expert Opin Drug Discovery 2007;2:1301-27.

[66] Hu XE, Wos JA, Dowty ME, Suchanek PM, Ji E, Chambers JB, et al. Small-molecule melanin-concentrating hormone-1 receptor antagonists require brain penetration for inhibition of food intake and reduction in body weight. J Pharmacol Exp Ther 2008;324:206-13.

[67] Gattrell WT, Sambrook Smith CP, Smith AJ. An example of designed multiple ligands spanning protein classes: dual MCH-1R antagonists/DPPIV inhibitors. Bioorg Med Chem Lett 2012;22:2464-9.

[68] Méndez-Andino JL and Wos JA. MCH-R1 antagonists: what is keeping most research programs away from the clinic? Drug Discovery Today 2007;12:972-9.

[69] Valentino MA, Lin JE, Waldman SA. Central and peripheral molecular targets for antiobesity pharmacotherapy. Clin Pharmacol Ther 2010;87:652.

[70] Högberg T, Frimurer TM, Sasmal PK. Melanin concentrating hormone receptor 1 (MCHR1) antagonists – still a viable approach for obesity treatment? Bioorg Med Chem Lett 2012;22:6039-47.

[71] Hicks RJ, Dorow D, Roselt P. PET tracer development – a tale of mice and men. Cancer Imaging 2006;6:S102-6.

[72] Ametamey SM, Honer M, Schubiger PA. Molecular imaging with PET. Chem Rev 2008;108:1501-16.

[73] http://vefir.mh.is/emjul/efni/nemverk/nemverkv09/SPG/eldsneyti.htm (19.3.2013)

[74] Wadsak W. and Mitterhauser M. Basics and principles of radiopharmaceuticals for PET/CT. Eur J Radiol 2010;73:461-9.

[75] Vallabhajosula S. Molecular Imaging. Radiopharmaceuticals for PET and SPECT. Springer-Verlag Berlin Heidlberg 2009.

[76] Wester HJ. Pharmaceutical Radiochemistry (I). Munich Molecular Imaging Handbook Series. SCINTOMICS Print Media and Publishing Fürstenfeldbruck Germany 2010.

[77] Langstrom B and Lundqvist H. The preparation of 11C-methyl iodide and its use in the synthesis of 11C-methyl-L-methionine. Int J Appl Radiat Isotop 1976;27:357-63.

[78] Larsen P, Ulin J, Dahlstrom K, Jensen M. Synthesis of [11C]iodomethane by iodination of [11C]methane. Appl Radiat Isotop 1997;48:153-7.

[79] Jewett DM. A simple synthesis of [11C]methyl triflate. Int J Radiat Appl Instrum Appl Radiat Isot 1992;43:1383-5.

[80] Ido T, Wan CN, Casella V, Fowler JS, Wolf AP, Reivich M, et al. Labeled 2-deoxy-D-glucose analogs: 18F-labeled 2-deoxy-2-fluoro-D-glucose, 2-deoxy-2-fluoro-D-mannose and 14C-2-deoxy-2-fluoro-D-glucose. J Labeled Compounds Radiopharm 1978;24:174–83.

[81] Vallabhajosula S. 18F-Labeled Positron emission tomographic radiopharmaceuticals in oncology: an overview of radiochemistry and mechanisms of tumor localization. Sem Nucl Med 2007;37:400-19.

[82] http://www3.gehealthcare.com/~/media/Downloads/us/Product/Product-Categories/PET-Radiopharmacy/TracerCenter/Tracer-Lab/GEHC-TRACERlab-FX-C-Pro-ProductSpec.pdf?Parent={82CA10FF-D453-4696-868B-88477503913A} (7.4.2013)

[83] Schubiger PA, Lehmann L, Friebe M. PET Chemistry. The Driving Force in Molecular Imaging. Springer-Verlag Berlin Heidlberg 2007.

[84] Radiopharmaceutica, 7.0/0125. In: European Pharmacopeia, official Austrian version, 7th edition, Verlag Österreich GmbH, Vienna, 2011. pp. 1067-1075.

[85] Lappin G and Temple S. Radiotracers in Drug Development. CRC Press Florida USA 2006.

[86] Osman S, Lundkvist C, Pike VW, Halldin C, McCarron JA, Swahn CG, et al. Characterization of the radioactive metabolites of the 5-HT1A receptor radioligand, [O-methyl-11C]WAY-100635, in monkey and human plasma by HPLC: comparison of the behavior of an identified radioactive metabolite with parent radioligand in monkey using PET. Nucl Med Biol 1996;23:627-34.

[87] Osman S, Lundkvist C, Pike VW, Halldin C, McCarron JA, Swahn CG, et al. Characterization of the appearance of radioactive metabolites in monkey and human plasma from the 5-HT1A receptor radioligand, [carbonyl-11C]WAY-100635 – explenation of high signal contrast in PET and aid to biomathematical modeling. Nucl Med Biol 1998;25:215-23.

[88] Pike VW. PET radiotracers: crossing the blood brain barrier and surviving metabolism. Trends Pharmacol Sci 2009;30:431-40.

[89] Menten L and Michaelis MI. Die kinetik der invertinwirkung. Biochem Z 1913;49: 333-69.

[90] Clark DE. In silico prediction of blood-brain barrier permeation. Drug Discovery Today 2003;8:927-33.

[91] Naik P and Cucullo L. In vitro blood-brain barrier models: Current and perspective technologies. J Pharm Sci 2012;101:1337-54.

[92] Ong S, Liu H, Qiu X, Bhat G, Pidgeon C. Membrane partition coefficients chromatographically measured using immobilized artificial membrane surfaces. Anal Chem 1995;67:755-62.

[93] Terasaki T, Ohtsuki S, Hori S, Takanaga H, Nakashima E, Hosoya K. New approaches to in vitro models of blood-brain barrier drug transport. Drug Discovery Today 2003;8:944-54.

[94] Didziapertis R, Japertas P, Avdeef A, Petrauskas A. Classification analysis of P-glycoprotein substrate specificity. J Drug Target 2003;11:391-406.

[95] Elsinga P, Hendrikse NH, Bart J, van Waarde A, Vaalburg W. Positron emission tomography studies on binding of central nervous system drugs and P-glycoprotein function in the rodent brain. Mol Imaging Biol 2005;7:37-40.

[96] Syvänen S, Lindhe Ö, Palner M, Kornum BR, Rahman O, Langström B, et al. Species differences in blood-brain barrier transport of three positron emission tomography radioligands with emphasis on P-glycoprotein transport. Drug Metab Dispos 2009;37:635-43.

[97] Uchida Y, Othsuki S, Katsukura Y, Ikeda C, Suzuki T, Kamiie J, et al. Quantitative targeted absolute proteomics of human blood-brain-barrier transporters and receptors. J Neurochem 2011; doi: 10.1111/j.1471-4159.2011.07208.x

[98] Wharton J and Polak JM. Receptor Autoradiography. Principles and Practice. Oxford University Press, New York, USA 1993.

[99] Yao R, Lecomte R, Crawford ES. Small-animal PET: what is it, and why do we need it? J Nucl Med Technol 2012;40:157-65.

6.1. Curriculum vitae

Mag. pharm. Cécile Philippe

Education

2009 - 2013	PhD. studies at the Departement of Pharmaceutical Technology and Biopharmaceutics, University of Vienna, Austria Scientific work at the Department of Nuclear Medicine, Medical University of Vienna, Austria
04/2009	Graduation as Magistra Pharmaciae
2008	Diploma thesis in radiopharmaceutical technology at the Department of Nuclear Medicine, Medical University of Vienna, Austria Title of the diploma thesis: "Radiopharmazeutisch-technologische Aspekte in der Arzneiformenentwicklung" (Supervisor: o. Univ. Prof. Mag. Dr. Helmut Viernstein)
2002 - 2009	Diploma study of Pharmacy at the University of Vienna, Austria
06/2002	University-entrance diploma
1994 - 2002	Grammar school at the „Höhere Internatsschule des Bundes Schloss Traunsee", Gmunden, Austria
1990 - 1994	Elementary school in Kremsmünster, Austria

Scientific experience

Since 09/2010	Teaching assistant at the Department of Pharmaceutical Technology and Biopharmaceutics, University of Vienna, Austria
11/2012	EANM Learning Course on Trends in PET-Methodologies, Vienna, Austria
09/2010	CIMST Summer School on Biomedical Imaging at ETH Zurich, Switzerland
07/2008	Internship at the „Adler-Pharmacy", Wels, Austria
09/2006	Internship at the Hospital Pharmacy of the General Hospital of Vienna, Austria

Languages

Native speaker in German and French. English fluently.

6.2. Scientific publications

Peer reviewed research articles

Preparation and first preclinical evaluation of [^{18}F]FE@SNAP: a potential PET tracer for the melanin concentrating hormone receptor 1 (MCHR1)
Philippe C, Nics L, Zeilinger M, Schirmer E, Spreitzer H, Karanikas G, Lanzenberger R, Viernstein H, Wadsak W, Mitterhauser M.
Scientia Pharmaceutica (2013), in press (doi:10.3797/scipharm.1306-02).

Preclinical *in vitro* & *in vivo* evaluation of [^{11}C]SNAP-7941 - the first PET tracer for the melanin concentrating hormone receptor 1
Philippe C, Nics L, Zeilinger M, Kuntner C, Wanek T, Mairinger S, Shanab K, Spreitzer H, Viernstein H, Wadsak W, Mitterhauser M.
Nuclear Medicine and Biology (2013), in press (doi:10.1016/j.nucmedbio.2013.05.010).

Interaction of ^{11}C-Tariquidar and ^{11}C-Elacridar with P-glycoprotein and breast cancer resistance protein at the human blood-brain barrier
Bauer M, Karch R, Zeitlinger M, Stanek J, Philippe C, Wadsak W, Mitterhauser M, Jäger W, Haslacher H, Müller M, Langer O.
Journal of Nuclear Medicine (2013), in press.

Cerebral serotonin transporter asymmetry in males and male-to-female transsexuals: a PET study with [^{11}C]DASB
Kranz GS, Hahn A, Baldinger P, Häusler D, Philippe C, Kaufmann U, Wadsak W, Savli M, Höflich A, Kraus C, Vanicek T, Mitterhauser M, Kasper S, Lanzenberger R.
Brain Structure and Function (2012), doi:10.1007/s00429-012-0492-4

[^{18}F]FE@SNAP - A new PET tracer for the melanin concentrating hormone receptor 1 (MCHR1): Microfluidic and vessel-based approaches
Philippe C, Ungersboeck J, Schirmer E, Zdravkovic M, Nics L, Zeilinger M, Shanab K, Lanzenberger R, Karanikas G, Spreitzer H, Viernstein H, Mitterhauser M, Wadsak W.
Bioorganic & Medicinal Chemistry (2012) 20:5936-5940.

Optimization of [^{11}C]DASB-synthesis: Vessel-based and flow-through microreactor methods
Ungersboeck J, Philippe C, Haeusler D, Mitterhauser M, Lanzenberger R, Dudczak R, Wadsak W.
Applied Radiation and Isotopes (2012) 70:2615-2620.

Radiosynthesis of [^{11}C]SNAP-7941 – the first PET-tracer for the melanin concentrating hormone receptor 1 (MCHR1)
Philippe C, Schirmer E, Mitterhauser M, Shanab K, Lanzenberger R, Karanikas G, Spreitzer H, Viernstein H, Wadsak W.
Applied Radiation and Isotopes (2012) 70:2287-2294.

Prediction of SSRI treatment response in major depression based on serotonin transporter interplay between median raphe nucleus and projection areas
Lanzenberger R, Kranz GS, Häusler D, Akimova E, Savli M, Hahn A, Wadsak W, Spindelegger C, Philippe C, Fink M, Mitterhauser M, Kasper S.
Neuroimage (2012) 63:874-881.

Differential modulation of self-referential processing in the default mode network via serotonin-1A receptors
Hahn A, Wadsak W, Windischberger C, Baldinger P, Höflich AS, Losak J, Nics L, Philippe C, Kranz GS, Kraus C, Mitterhauser M, Karanikas G, Kasper S, Lanzenberger R.
Proceedings of the National Academy of Sciences (2012) 109(7):2619-2624.

Optimization of the radiosynthesis of the Alzheimer tracer 2-(4-N [^{11}C]methylaminophenyl)-6-hydroxybenzothiazole ([^{11}C]PIB)
Philippe C, Haeusler D, Mitterhauser M, Ungersboeck J, Viernstein H, Dudczak R, Wadsak W.
Applied Radiation and Isotopes (2011) 69:1212-1217.

Microfluidic preparation of [^{18}F]FE@SUPPY and [^{18}F]FE@SUPPY:2 – comparison with conventional radiosyntheses
Ungersboeck J, Philippe C, Mien LK, Haeusler D, Shanab K, Lanzenberger R, Spreitzer H, Keppler B, Dudczak R, Kletter K, Mitterhauser M, Wadsak W.
Nuclear Medicine and Biology (2011) 38:427-437.

„Label and go"– A fast and easy radiolabelling method for pellets
Philippe C, Mien LK, Salar-Behzadi S, Knäusl B, Wadsak W, Dudczak R, Kletter K, Viernstein H, Mitterhauser M.
Applied Radiation and Isotopes (2010) 68:399-403.

Simple and rapid preparation of [^{11}C]DASB with high quality and reliability for routine applications
Haeusler D, Mien LK, Nics L, Ungersboeck J, Philippe C, Lanzenberger R, Kletter K, Dudczak R, Mitterhauser M, Wadsak W.
Applied Radiation and Isotopes (2009) 67:1654-1660.

Meeting abstracts

Oral presentations:

"En route" for [^{18}F]FE@SNAP: A potential PETtracer for obesity via the MCHR1
Philippe C, Ungersböck J, Schirmer E, Spreitzer H, Viernstein H, Wadsak W, Mitterhauser M.
Nuklearmedizin (2011) 50:A160.
Radioactive Isotopes in Clinical Medicine and Research - 30th International Symposium, January 11-14, 2012, Bad Hofgastein, Austria.

[^{11}C]SNAP-7941 & [^{18}F]FE@SNAP – die ersten potentiellen PET-Tracer für den MCHR1: erste Ergebnisse
Philippe C, Ungersböck J, Haeusler D, Nics L, Schirmer E, Spreitzer H, Dudczak R, Viernstein H, Wadsak W, Mitterhauser M.
19. Jahrestagung der Arbeitsgemeinschaft Radiochemie/Radiopharmazie; September 15-17, 2011; Ochsenfurt, Germany

Radiosynthesis of [^{11}C]SNAP-7941: the first potential PET-ligand for the MCHR1
Philippe C, Nics N, Hartmann S, Schirmer E, Kletter K, Dudczak R, Viernstein H, Wadsak W, Mitterhauser M.
European Journal of Nuclear Medicine & Molecular Imaging (2010) 37:S206.
EANM'10 - Annual Congress of the European Association of Nuclear Medicine, October 9-13, 2010, Vienna, Austria.

Poster presentations:

[^{11}C]SNAP-7941, the first Tracer for the Melanin Concentrating Hormone Receptor 1: Biodistribution and small animal PET
Philippe C, Kuntner C, Wanek T, Mairinger S, Schirmer E, Spreitzer H, Viernstein H, Wadsak W, Mitterhauser M.
Journal of Labelled Compounds and Radiopharmaceuticals (2013) 56:S419.
ISRS'13 - The 20th International Symposium on Radiopharmaceutical Sciences, May 12-17, 2013, Jeju, South Korea.

Radiosynthesis & first preclinical evaluation of [^{18}F]FE@SNAP – a potential PET-tracer for the melanin concentrating hormone receptor 1
Philippe C, Nics L, Zeilinger M, Ungersböck J, Haeusler D, Hendl M, Heissenberger T, Schirmer E, Spreitzer H, Dudczak R, Viernstein H, Wadsak W, Mitterhauser M.
European Journal of Nuclear Medicine & Molecular Imaging (2012) 39:S534.
EANM'12 - Annual Congress of the European Association of Nuclear Medicine, October 27-31, 2012, Milan, Italy.

[^{11}C]SNAP-7941, the first potential PET-Tracer for the MCHR1: Preparation and Automatisation
Philippe C, Schirmer E, Spreitzer H, Dudczak R, Viernstein H, Wadsak W, Mitterhauser M.
Journal of Labelled Compounds and Radiopharmaceuticals (2011) 54:S106.
ISRS'11 - The 19th International Symposium on Radiopharmaceutical Sciences, August 28-September 2, 2013, Amsterdam, Netherlands.

The "Dril & Fill" Method
Philippe C, Haeusler D, Mien LK, Kletter K, Dudczak R, Wadsak W, Viernstein H, Mitterhauser M.
Scientia Pharmaceutica (2010) 78:650.
CESPT'10 - 8th Central European Symposium on Pharmaceutical Technology, September 16-18, 2010, Graz, Austria.

Rapid radiosynthesis of [^{18}F]FE@SUPPY:2 using a microfluidic device
Philippe C, Ungersböck J, Mien L-K, Kletter K, Dudczak R, Viernstein H, Mitterhauser M, Wadsak W.
Nuklearmedizin (2009) 48:A159-160.
Radioactive Isotopes in Clinical Medicine and Research - 29th International Symposium, January 16-19, 2010, Bad Hofgastein, Austria.

Partikel-Markierung mit [^{18}F]Fluorid für PEPT
Philippe C, Salar-Behzadi S, Raith M, Mien LK, Wadsak W, Viernstein H, Dudczak R, Kletter K, Mitterhauser M.
Nuklearmedizin (2008) 47:A160.
OGN'09 - 7. Jahrestagung der Österreichischen Gesellschaft für Nuklearmedizin, January 22-24, 2009, Salzburg, Austria.

Book chapter

Synthesis of 2-(4-N-[^{11}C]methylaminophenyl)-6-hydroxybenzothiazole ([^{11}C]6-OH-BTA-1; [^{11}C]PIB)
Philippe C, Mitterhauser M, Wadsak W.
In: Radiochemical Syntheses: Volume 1: Radiopharmaceuticals for Positron Emission Tomography. Wiley Series on Radiochemical Syntheses. Scott PJH, Hockley PG, editors. John Wiley & Sons, Inc., New Jersey (2012) 177-189.